BAY OF BISCAY COHERENCE STUDY USING LARGE APERTURE SEISMIC ARRAY

William H. Luehrmann

Seismic Engineering Company

Prepared for:

Advanced Research Projects Agency
Office of Naval Research

31 December 1973

UNCLASSIFIED

SECURITY CLASSIFICATION OF THIS PAGE (When Data Entered)

REPORT DOCUMENTATION PAGE	READ INSTRUCTIONS BEFORE COMPLETING FORM
1. REPORT NUMBER	2. GOVT ACCESSION NO. 3. RECIPIENT'S CATALOG NUMBER AD-782 047
4. TITLE (and Subtitle) Bay of Biscay Coherence Study Using Large Aperture Seismic Array	5. TYPE OF REPORT & PERIOD COVERED FINAL REPORT March-August 1973
	6. PERFORMING ORG. REPORT NUMBER H SECo #73-4
7. AUTHOR(s) William H. Luehrmann	8. CONTRACT OR GRANT NUMBER(s) N00014-73-C-0302
9. PERFORMING ORGANIZATION NAME AND ADDRESS Seismic Engineering Company 3616 W. Alabama Houston, Texas 77027	10. PROGRAM ELEMENT, PROJECT, TASK AREA & WORK UNIT NUMBERS
11. CONTROLLING OFFICE NAME AND ADDRESS Office of Naval Research Department of the Navy Arlington, Va. 22217	12. REPORT DATE December 1973
	13. NUMBER OF PAGES 143
14. MONITORING AGENCY NAME & ADDRESS(if different from Controlling Office) Naval Undersea Center San Diego, Calif. 92132 Code 502	15. SECURITY CLASS. (of this report) UNCLASSIFIED
	15a. DECLASSIFICATION/DOWNGRADING SCHEDULE

16. DISTRIBUTION STATEMENT (of this Report)

17. DISTRIBUTION STATEMENT (of the abstract entered in Block 20, if different from Report)

18. SUPPLEMENTARY NOTES

19. KEY WORDS (Continue on reverse side if necessary and identify by block number)

Seismic Array
Array Coherence
Talpey phase coherence
Talpey Amplitude Coherence
Array Aperture
Sound Power Level Spectrum
Quadrature Sampling

20. ABSTRACT (Continue on reverse side if necessary and identify by block number)

The report covers computer processing and analysis of acoustic data obtained with a long aperture seismic receiving array and a mono frequency acoustic source in the Bay of Biscay.

Twelve sets of "signal plus noise" and "noise only" acoustic data obtained at 4 source-receiver separation distances were processed to evaluate array performance.

DD FORM 1 JAN 73 1473 EDITION OF 1 NOV 65 IS OBSOLETE

UNCLASSIFIED

SECURITY CLASSIFICATION OF THIS PAGE (When Data Entered)

Block 20 contd.

These included 1) coherence vs aperture using a cross correlation technique developed by SECo, and 2) coherence vs aperture for time averaged phase and amplitude products based on a mathematical analysis by T. E. Talpey. Coherence values for both techniques were compared for equivalence or superiority in expressing array performance.

Signal plus coherence values of 80-95% were obtained at apertures of 2250 meters, and at source receiver separations up to 30 miles. At greater separation coherence values decreased due to several factors detailed in the report.

In general, array coherence can be described by either technique. However, where the array is receiving weak, narrow band signals in the presence of high, wide band ambient noise fields the Talpey technique provides higher signal to noise ratios.

FINAL REPORT
Bay of Biscay Coherence Study with Large Aperture Seismic Array

Contract No:
N00014-73-C-0302

ARPA Order No. 2308

Program Code No. 3E20

Scientific Officer:
Manager, LRAPP,
Office of the Chief
of Naval Research,
Office of Naval Research,
Department of the Navy.
800 North Quincy Street
Arlington, Va. 22217

Date of Contract:
01 March 1973

Final report due:
31 December, 1973

Contractor:
SEISMIC ENGINEERING
COMPANY

Amount of Contract:
$58,325.00

Principal Investigator:
W. H. Luehrmann
(713)-621-2611

This research was supported by the ADVANCED RESEARCH PROJECTS AGENCY of the Department of Defense and was monitored by Office of Naval Research under Contract No. N00014-73-C-0302.

TABLE OF CONTENTS

LIST OF ILLUSTRATIONS

SECo Coherence Plots

Talpey Correlation Plots

Tape No's.	S-R Distance	Fig. No's. Amplitude Only	Amplitude Phase
03, 04	15	36	37
05, 06	15	38	39
20, 21	30	40	41
22, 23	30	42	43
24, 25	30	44	45
66, 69	30	46	47
67, 70	30	48	49
32, 33	45	50	51
44, 45, 46	60	52	53
47, 48, 49	60	54	55
50, 51	60	56	57

Data Flow - Power Spectrum	58
Program Flow - Power Spectrum	59
Power Spectrum Plot - f 0.500 Hz	60
Power Spectrum Plot - f 0.0833 Hz	61

B A Y O F B I S C A Y

COHERENCE STUDY USING LARGE APERTURE SEISMIC ARRAY

FINAL REPORT

SUMMARY:

This Seismic Engineering Company (SECo) report covers field acquisition and subsequent coherence analysis of acoustic data obtained with a 2400 meter, 48 element geophysical towed array and 62.5 Hz acoustic source in the Bay of Biscay. The data was acquired using company funds and the analysis supported by the Office of Naval Research under the Sponsorship of the Strategic Technology Office, ARPA.

One SECo vessel transported the receiving array and another the acoustic source. The vessels were positioned at 15, 30, 45, and 60 mile separations. These tests, conducted in May, 1972, were designed to evaluate the signal plus noise and noise only coherence of a large aperture array. Data were recorded on a 60 channel digital magnetic tape recording system and processed on a Control Data series 3200 digital computer.

Analysis included two independent techniques for calculating array element to element coherence vs. separation. One was a development by SECo; the second follows the theory outlined by T. E. Talpey of

BTL. Both techniques yield quantitative information relating to array performance with reasonable consistency achieved between the two methods.

The output level and frequency content of the acoustic source were studied. Source level was found to be at least 20 dB below rated 80 dB output, providing results with signal to noise ratios too low to predict fully array performance.

Nevertheless, the project has produced substantive results in describing two aspects of array coherence:

First, a significant, quantitative set of data was obtained on the noise coherence of long arrays. These data set favorable limits on noise coherence to be expected from arrays with apertures to 2,250 meters.

Second, as signal plus noise coherence was always higher than noise only coherence, the "source-on" data establishes a "floor" under the coherence obtainable in the use of long midwater arrays.

INTRODUCTION:

This report covers computer processing and subsequent coherence analysis of a set of acoustic data acquired by Seismic Engineering Company (SECo) in early 1972. These data, covering a series of acoustic transmission tests in deep water in the Bay of Biscay, were obtained to evaluate the spatial coherence properties of the deep sound channel using a large aperture seismic array (a SECo geophysical streamer).

A preliminary array coherence study was made by SECo which was both interesting and encouraging. Results of the study, submitted to the Office of Naval Research (ONR) as part of an unsolicited proposal, requested funds to enter into a more exhaustive study of the available data.

The proposal requested funding to complete the following work objectives:

A. A detailed coherence analysis of 25 field tapes. These tapes comprise all Bay of Biscay tow tests with the array essentially "broadside" to the source, and encompass a source-receiver separation from 15 to 60 miles.

B. Investigate the array correlation technique proposed by T. E. Talpey, B.T.L. Inc., - "Array Response in the Presence of Simultaneous Amplitude and Phase Fluctuations", develop suitable algorithms, and computor process the

same 25 previously selected "broadside" tapes for array correlation with this technique.

C. Compare the techniques outlined in tasks 1 and 2 above and evaluate the ability of each technique to express array coherence.

D. Modify present SECo power spectrum program to obtain higher frequency resolution, and test program.

E. Prepare a suitable final report which documents prior SECo work as well as work performed under this contract.

Computer processing was initiated in May 1973, and final processing completed in August 1973.

All project objectives were completed and are presented in detail in the sections which follow.

As far as the author is aware, this has been the first comprehensive study - combined field program and processing analysis - to evaluate spatial coherence over reasonably long acoustic paths with a large aperture geophysical type towed array. Thus, there are no yardsticks available to measure the "goodness" of the final results of this

project. However, study of source intensity level records, power spectrum level programs and the suite of coherence versus aperture plots obtained using both SECo and Talpey processing techniques permitted the following observations:

A. The piezoelectric acoustic source rated at 80 dB (re 1 dyne/cm^2) delivered a maximum level of 62 dB on initial calibration and, after failure during the first set of data acquisition, performed at a substantially lower level throughout the exercise. This resulted in field data which had signal to noise ratios well below unity. In fact, monitor records showed little or no trace of the 62.5 Hz frequency when the source was energized.

B. SECo Coherence Calculations.

1. Spatial coherence in the Bay of Biscay was high for apertures up to 2,300 meters (7,500 feet), considering the array was at shallow depth and the low source intensity.

2. Array coherence (calculated with the SECo designed technique), using element pairs selected to optimize coherence, reached over 95 percent at apertures of 2,000 meters or more, for source receiver separations of 15-30 miles.

3. One minute data sampling provided higher coherence than 3 minute sampling. This is an indication that either the source frequency was changing during this time window or spatial coherence in the Bay of Biscay sound channel is perturbed over 2-3 minute time periods.

4. At distances beyond 30 miles, coherence values decreased significantly. This is possibly due to the effects of multiple path energy causing destructive interference, and local noise combined with lower signal to noise ratios. These very low received signal levels resulted from an acoustic source level 20 to 30 dB below anticipated output.

5. Where "source plus noise" and "noise only" data were obtained in rapid sequence, the SECo coherence values showed a S/N ratio of 2:1 or higher to apertures of 2,000 meters (all cases except one). This indicates spatial perturbations would not limit source indentification at any of the source - receiver distances in the experiment.

C. Talpey Time Averaged Amplitude and Phase Array Correlations.

1. The Talpey correlation curves do not have the same shapes as SECo coherence curves.

2. Talpey signal to noise (S/N) ratios for amplitude product, or amplitude-phase product are higher than SECo coherence S/N ratios at the far source - receiver distances (beyond 30 miles), which implies the Talpey technique provides possibly superior detection of weak narrow band signals in a high level wide band background noise field.

3. Generally, Talpey amplitude-phase product correlations produced higher S/N ratios than amplitude only, indicating that phase may be important at frequencies below 100 Hz.

4. Array coherence for phase data only is quite poor in most cases. This is probably due to the very low signal to noise ratio of the received data, and absence of narrow band filtering prior to Talpey FFT analysis.

D. In essentially all cases both SECo coherence and Talpey amplitude correlations produced data with signal to noise ratios of 2:1 or higher to apertures of 2,000 meters.

E. The SECo standard power spectrum program, modified to increase the frequency resolution from 0.500 Hz to 0.0833 Hz., was tested with one field tape from the Bay of Biscay. The

high resolution spectra show Bay of Biscay data which has a fine line frequency structure totally absent in the 0.500 Hz resolution data. Actual frequency separation appears limited to approximately 0.15-0.2 Hz. At the expense of more computer time, resolution could be further increased,if desired,with only minor changes in the program.

While these observations are of value in analyzing various techniques to express array coherence, it is felt the most significant contributions from this study are:

A. The presentation of quantitative data on expected noise coherence for long arrays, i.e. the ability to establish boundaries on array noise correlations for arrays from 50 to 2,250 meters aperture. These data can then be compared with other sets of data in other environments and array configurations.

B. As signal plus noise coherence was higher than noise only coherence even though the raw data had very low S/N ratio and the source exhibited short term frequency perturbations, the signal plus noise results establish minimum signal levels necessary for detectability over apertures to 2,250 meters. These data will be useful for designing arrays with adequate gains to provide specific detection capabilities.

PRIOR WORK BY SECO

FIELD DATA ACQUISITION

The field data acquisition phase of the Bay of Biscay Project was planned during early 1972. Actual field work began May 4, with mobilization of two SECo vessels, M/V SEISMIC SURVEYOR and M/V SEISMIC EXPLORER in the North Sea port of Den Helder.

Vessels

The two modern vessels are used to provide world wide geophysical services to the petroleum industry. Both are custom designed, and are among the finest operating today. Several pictures are included of side and stern views of the vessels, the streamer and reel, and interior views of the instrument room (see Figures a, b, c).

"M/V SEISMIC SURVEYOR"

Contracted from Stewart & Stevenson Services, Inc., Houston, Texas, and constructed at Mangone Shipbuilding Company, also in Houston. Construction was completed in 1969, and the vessel was registered at the Port of Houston on August 20, 1969.

The following details describe the vessel:

OFFICIAL NUMBER:	522195
SIZE:	165 ft. O.A. x 36 ft. beam x 15 ft. deep
GROSS TONNAGE:	295.69
NET TONNAGE:	201
NORMAL DRAFT:	9 to 11 feet
CRUISING RANGE:	10,000 miles
ACCOMMODATIONS:	Four 4-man and five 2-man Staterooms = 26 men
MAIN ENGINES:	Two V-12 GM 567C
CONTINUOUS BHP, EACH:	1120 @ 720 RPM
SPEED RANGE:	3 to 15 knots
GENERATORS:	Two GM 871, 100 KW each
RADIOS:	(1) 30-channel SSB radiotelephone RF 201M-DN-30 with RF 102 1000 watt linear amplifier. (2) 10 Channel AM radiotelephone Apelco AE-190 CM.
RADIO CALL SIGN:	WY7539
RADAR:	Decca RM 329 with 9 ft. antenna
GYROCOMPASS:	Sperry Mark 227
AUTOPILOT:	Sperry Gyropilot
FATHOMETER:	Two Simrad ES-2C

"M/V SEISMIC EXPLORER"

Contracted from Stewart & Stevenson Services, Inc., Houston, Texas, and constructed at Mangone Shipbuilding Company, also in Houston. Construction was completed in September, 1967. The vessel was registered at the Port of Houston on October 24, 1967.

The following details describe the vessel:

OFFICIAL NUMBER	511366
SIZE:	165 ft. O.A. 36 ft. beam x 15 ft. deep
GROSS TONNAGE:	291.25
NET TONNAGE:	198
NORMAL DRAFT:	9 to 11 ft.
CRUISING RANGE:	10,000 miles
ACCOMMODATIONS:	Five 4-man and three 2-man Staterooms = 26 men
MAIN ENGINES:	Two V-12 GM 567C
CONTINUOUS BHP, EACH:	1120 @ 720 RPM
SPEED RANGE:	3 to 15 knots
GENERATORS:	Two GM 871, 100 KW each
AUXILIARY ENGINES: (For geophysical use)	Five GM 371
AUTO PILOT:	Sperry Gyropilot
GYROCOMPASS:	Sperry Mark 14 Model 1
RADAR:	Decca RM 329 with 9 ft. antenna

RADIO: 23 channel Northern N539L

RADIO CALL SIGN: WR-8350

FATHOMETERS: Two Simrad 512 - 15 WL

Recording Instruments

All streamer data were recorded with a Texas Instruments Model DFS III digital recording system which employs binary-gain amplifiers. The instrumentation block is illustrated in Figure 1. These instruments are custom installed in shock-mounted computer cabinets in the instrument room along with the cameras, controllers, monitors, and other peripheral equipment.

The following special features are included:

(1) 48 Recording channels.

(2) Dual ten-inch reel tape decks.

(3) Read-after-write which allows data to be monitored in real time.

(4) The 9-track, ½ inch tape is recorded in SEG-EPR Format "A". See attached 2 byte format, Figure 2.

(5) Custom equipment controller which controls both monitor camera and marks the fathometer and cross-section camera.

In addition the following monitors are also included:

(1) 32-trace SIE Model ER-6 electrostatic camera which provides wiggle-trace records at selected intervals. (Of the 48 seismic traces that were recorded on tape, odd traces were photographed alternately with even traces.)

(2) Six cable depth readouts.

The seismic amplifier passband was 27-124 Hz, with a slope of 18 dB/octave on the low frequency cutoff and 72 dB/octave on the high frequency cutoff. Instrument amplitude and phase response plots are shown in Figures 3 & 4. The response is from amplifier input terminals to recording tape. The curves were obtained by applying a single input pulse and calculating the curves on a computer using the output data read from the tape recording.

Navigation

Decca Main Chain positioning service was used to position the SEISMIC EXPLORER. Position location accuracy from this chain is about $\pm$ 0.5 miles during daylight hours and $\pm$ 2.5 miles at night.

The SEISMIC EXPLORER was anchored with a twenty eight (28) foot parachute sea anchor. Continuous winds of 10 to 20 knots caused substantial drift of the vessel, and the position of the recording vessel was subject to changes in direction to compensate for this drift.

The SEISMIC SURVEYOR has on board a Satellite-Doppler Sonar Navigation System containing the following sub-systems:

(1) Magnavox Model MX-702 satellite receiver

(2) Hewlett-Packard Model 2115 digital computer

(3) Marquardt Model MRA-2015A Doppler-Sonar

(4) NUS Model TR-3 velocimeter

(5) Houston Instrument Model 6655 omnigraphic plotter

(6) Sperry Mark 227 gyro-compass

(7) Custom integration hardware

(8) Custom software

The custom hardware and software furnish the capacity of completely integrating the above systems. A series of up-down counters in the Doppler-Sonar collect both on-course and off-course distances and velocities. These data are buffered to the computer on its command which allows the computation of ship's position at any time in both x - y distance and geographical coordinates (latitude and longitude). These continuous velocity data are also used in computing a more accurate satellite fix during a satellite pass. The time instant of a satellite fix is event-marked on the plotter by the computer. The ship's position at the time of a satellite fix based on the Doppler-Sonar data extended from the last accepted fix is compared with the ship's position computed from the new fix by a special computer program.

There are three factors which influence satellite position fix accuracy. They are: 1) accuracy of expressing ship's motion, 2) accuracy of antenna height, which is derived by reference to a geoidal height map, and 3) adequacy of the satellite navigation equipment and fix program. The overall accuracy of the total system varies between 200 and 600 feet based on measurements in the field.

The navigation satellites are in circular polar orbits, about 600 nautical miles high. Each point on the revolving earth passes under every satellite orbit twice in 24 hours. Because the satellites circle the

earth in only 1-3/4 hours, they pass within the line of sight of an earth observer at least twice each time he is near an orbit. Therefore, each satellite will provide at least four navigation fixes per 24-hour day. With the five satellites being maintained operational today, one can expect no less than 20 passes per day, averaging 1.2 hours between fixes.

The Marquardt Doppler-Sonar's operating range is 1,000 nautical miles with a display accuracy of .2%. The velocity range of the Doppler-Sonar is 0-25 knots with an accuracy of .01 knots. The heading accuracy of the gyro-compass and therefore of the Doppler-Sonar is $\pm$ .75 degrees.

Whenever the water depth exceeds 600 feet, as was the case in the Bay of Biscay, the bottom return is lost, which necessitates switching to tracking the water mass rather than the water bottom. When the Doppler - Sonar switched to water track, the accuracy of its readings was dependent on local currents. Generally, continuous positional accuracy was at least 1000-1500 feet between satellite passes for all tracks computed for this project.

Towed Array

The seismic streamer configuration used in this test is shown in Fig. 5. It is one from a series of marine streamers engineered and fabricated by SECo for petroleum exploration. It contains SECo's patented Multidyne ™ acceleration cancelling hydrophone elements which contribute

to a superior signal to noise ratio in the seismic pass band. Over 100,000 Multidyne hydrophone elements are now in streamers being used for oil exploration. Special deep water elements have recently been built for streamers on several classified Navy projects.

The streamer as used in the Bay of Biscay test consisted of a "faired" lead-in cable and 200 meters of elastic "decoupler" section to reduce towing noise. Four cable depth controllers (birds) were utilized. These depth controllers were remotely controlled from the instrument room to regulate tow depth at 33 meters. Six strategically located depth transducers provided a monitor of cable depth. A strain gauge load-cell monitored the streamer tension from both the instrument room and the wheelhouse.

Details on the configuration used in the field include:

a) Offset distance of 375 meters to first group

b) 48 groups

c) 50 meter group intervals

d) Thirty (30) hydrophones each active group, linear spacing

e) 2400 meter active length, end to end

Frequency response and sensitivity of a typical group are shown in Figure 6. The directional response of a typical section is shown in Figure 7; the curve is plotted such that the 90° response would be that to a "broadside" wave front.

Acoustic Source

A large piezoelectric projector was placed on the source vessel, M/V SEISMIC EXPLORER. This source was powered from a separate, nominal 60 Hz, 240 volt A.C. motor-generator. The motor-generator set was adjusted in speed to provide a frequency several Hz above the 60 Hz supply on the receiving vessel so that the acoustic source frequency would not overlap any 60 Hz electrical pick-up. Source depth was 66 meters. Calculation of actual radiated power level is discussed in the section on Data Reduction.

General Test Parameters

All field data were acquired in the Bay of Biscay area. The general location is identified in Figure 8.

A series of streamer runs were made at source-receiver distances of approximately 15, 30 and 60 miles, with several array orientations - broadside, end on, 15 degrees and 45 degrees to the axis. A detailed map identifying these lines is shown in Fig. 9.

At each location, and on each line, the source was turned on for a period of six minutes (one tape reel length), off for a period of six minutes, and this process was repeated once or twice in most cases. Table "1" contains a listing of all data acquired. This technique provided six minutes of "source plus noise" data closely followed by six minutes

of "noise only" data hopefully of similar frequency content and amplitude as that obtained during the "source-on" data acquisition.

T A B L E " 1 "

LISTING OF FIELD DATA TAPES

SOURCE-RECEIVER DISTANCE	SOURCE-ON		SOURCE-OFF	
	F.T. No.	Orientation	F.T. No.	Orientation
10 miles	2	End On	1	End On
15 miles	3, 5	Broadside	4, 6	Broadside
20 miles	7	End On	8	End On
30 miles	13,14,15	End On	9,10,11,12	End On
30 miles	16, 18	45°)	17, 19	45°)
30 miles	20,22,24	Broadside	21,23,25	Broadside
30 miles	66,67,68	Broadside	69,70,71	Broadside
30 miles	26, 28	15°)	27, 29	15°)
38 miles	30	End On	31	End On
45 miles	32	Broadside	33, 24	Broadside
50 miles	35	End On	36	End On
60 miles	37,39,41	End On	38,40,42,43	End On
	44,47,50	Broadside	45,46,48,49,51	Broadside
	52,55,57	15°)	53,54,56,58	15°)
	59,62,64	45°)	60,61,63,65	45°)

Selection of the three approximate ranges, 15 miles, 30 miles and 60 miles were based on theoretical acoustic ray path data. This data is shown in Fig. 10. The ray paths were predicted for known water depths in the Bay of Biscay area chosen, and on anticipated temperatures for the area during the spring of the year.

To further establish that reasonable signal levels would be received for these distances, two propagation loss charts were prepared. The two cases studied were: 1) total absorption of energy reaching the water bottom, and 2) total reflection of bottom bounce energy. The propagation loss charts are shown in Figure 11. Attenuation values were reasonable for the acoustic level anticipated from the crystal source array and our receiver array sensitivity.

Tests were conducted during May 9-12, 1972, and all tapes were shipped to Houston, Texas, for analysis by SECo.

DATA REDUCTION AND ANALYSIS

Field data reduction was performed at the Houston, Texas computer facility of Geophysical Data Processing Center, Inc. (GDPC), a Whitehall Electronics subsidiary.

Processing equipment at GDPC includes a large scale CDC 3200 series computer with SPAM high speed algorithm module, 7 and 9 track tape transports, and Calcomp pen plotter. The computer system is complemented by a highly versatile, unique off-line computer with 7, 9 and 21 track tape transport capability for reformatting almost any tape for computer input.

Acoustic Source Intensity Level

The piezoelectric projector utilized in the experimental program was rated at 80 dB (re 1 dyne/cm^2). To verify this source level, prior to beginning the series of tow runs a calibrated hydrophone was suspended three feet from the projector and the hydrophone output recorded on the DFS III digital recording system on the SEISMIC EXPLORER. From the digital data and hydrophone calibration value, the source intensity was computed to be 62 dB (re 1 dyne/cm^2). This undoubtedly was the maximum level observed from the source, as it failed during the first immersion shortly after the experimental work began, and after repair operated at reduced output throughout data acquisition. It

is likely the level was 48-56 dB during much of this work. Unfortunately, no further calibrations were taken.

Early computer output of raw data from several traces shown in Fig. 12 confirmed that the signal plus noise and noise only waveforms were substantially identical, indicating a S/N ratio of much less than unity. While the low source level was not totally disastrous, it did make the correlation studies more difficult. A signal level at least 20 dB above Bay of Biscay background sea noise had been anticipated, and is likely required to provide unquestionable coherence values for large aperture arrays operating in tow mode.

Selection of Traces to be Analyzed

R. J. Urick in "Principles of Underwater Sound for Engineers", page 53, Fig. 3.12 (refer Figure 13), illustrates a theoretical example of signal and noise coherence along a three element array. Both signal and noise exhibit a general "bell shaped" curve. Although the SECo array was not three element and was in a very noisy medium, the same type of curves were expected from the computer analysis.

To provide spacing intervals which would adequately describe this type of curve, and yet not consume a prohibitive amount of computer time, the following series of distance intervals along the streamer were chosen:

Trace Numbers	Spacing (Separation between center of groups)
46-47	50 meters
45-47	100 meters
41-45	200 meters
40-47	350 meters
32-47	750 meters
28-47	950 meters
9-47	1900 meters
2-47	2250 meters

These traces were used for both source-on and source-off data reduction and analysis.

Computer Processes - Description

The data recorded on the DFS III digital field recorder is recorded at 800 bpi on one-half inch magnetic tape, 2400 feet in length. A total of 48 seismic traces or "curves" are recorded simultaneously for a time of six (6) minutes. These 48 data curves are digitized prior to being written on the tape, and are written in a time-sequenced standard digital format (Figure 2) along the 2400 feet of tape.

Several processes are required to prepare and process each data trace. These steps are diagrammed in Fig. 14. A short explanation of each step follows below. It should be noted that these programs were designed for rapid processing of standard geophysical data and one should expect to make some modifications for optimum processing of other types of data such as the Bay of Biscay work.

1. Off-line reformat

A special off-line computer first processed the original field tapes. This specialized equipment was designed to transform original field tape with extremely long record lengths into copy tapes consisting of a series of short blocks of data which are readily input into the main computer.

2. Demultiplex (SUBEDIT)

This program reads the "small block" copy tapes and separates the 48 sequential or side-by-side curves into 48 continuous and sepa-

rate traces. This is an essential step in the processing because the computer programs require that individual traces be isolated.

3. Filter (SUBFIL)

The filter program reads the isolated curves from the edit program and bandpasses the data one trace at a time. The bandpass technique which is employed involves the detection of the recorded signal by cross-correlation with a known signal. This technique is ideal for poor signal-to-noise ratio data, the phase relationship of the data is preserved and the technique works well when the signal to be detected is contained in a wideband of noise. (See Section 6.2 in "Correlation Techniques", Dr.-Ing. Habil, F.H. Lange, London ICIFFE Books Ltd.)

For our work the known signal was constructed by the following equation:

$$\text{Known signal (t)} = \sum_{\omega = x}^{\omega = y} \sum_{t=0}^{t=6} A \cdot \text{Cos}\,(\omega t)$$

The known signal is constructed for a 6 second period using the band of angular frequencies from x to y. The bandwidth of this technique can be extremely small. The "A" term is used to control the amplitude of the known signal. The 0.1 bandwidth was selected to straddle the known signal frequency.

4. Cross-Correlation (XCORBIG)

The cross-correlation program can process either filtered or unfiltered data. This same program will do both cross-correlations and auto-correlations. The equation which performs these processes is as follows:

$$F(t) = \frac{\Sigma x \cdot y}{\sqrt{\Sigma x^2 \cdot \Sigma y^2}}$$

x = one curve
y = other curve
x = y for autocorrelation

This equation normalizes the answers to a range of plus one to minus one (+1.0 to -1.0). A (+1) value is the in-phase condition and a (-1) value is the out-of-phase condition. (Again refer to "Correlation Techniques" by Dr.-Ing. Habil, F.H. Lange.)

5. Power Spectra (POWER TT)

The auto-correlation function from the XCORBIG program for a given trace is used as the input. The frequency content of the trace is analyzed by the program and a Calcomp plot tape is the output.

6. Calcomp plot tape (PLOTAUTO)

This program accepts the output from the XCORBIG program and other programs, and creates a tope for off-line pen plotting on the Calcomp plotter.

Analysis of Results

Prior to any filtering or cross-correlation, a series of power spectra of the raw field data for 15, 30 and 60 mile broadside configuration were run in order to evaluate source plus noise data for presence of the source frequency, and compare with noise (source-off) data. Several typical plots are shown in Figure 15. Most of the source plus noise spectra plots exhibited a reasonably well defined 62 Hz source peak, as well as other peaks that appeared to be related to shipping in the area. These other peaks changed with source-receiver separation, and time of acquisition.

The power spectra program used in this analysis had a resolving power of one Hz, and it was not possible to get more quantitative indications of the actual power near the 62.75 Hz source frequency.

The source-on and source-off spectra were encouraging, and it was decided to continue the analysis using 30 mile broadside data. Field tapes 21 (source-off) and 22 (source-on) were selected for further study.

As pointed out earlier, the unfiltered source-on data indicated the source-on to noise (S/N) ratio was probably 1:1 or poorer. To improve the S/N ratio of the signal plus noise data prior to cross-correlating for coherence, several filtering tests were tried including standard geophysical and narrow bandpass filtering programs. The filtered recordings were Calcomp plotted and examined for presence of the source frequency. Results from these programs were not acceptable and we continued to study other techniques.

The correlation filter (SUBFIL) program described above appeared to be a powerful method to extract the source signal from the high noise background, and this was tried next. The end frequencies, x and y, required to construct the "known signal" were determined by cross-correlating signal-on trace #47 with individual sine waves ranging from 62.00 Hz to 63.00 Hz, which were incremented at 0.05 Hz steps. The resultant plot of correlation percent vs frequency is shown in Figure 16. The source frequency band is easily identified, and 62.70 Hz and 62.80 Hz were used to determine end frequencies x and y.

Reproductions of "before" and "after" filtering for several source-on and source-off traces are shown in Figures 12 and 17. The improvement in S/N ratio is startling.

All selected traces in field tapes 21 and 22 were filtered with the "known signal" operator described above, and then trace pairs were cross-correlated as previously indicated in the table on page 19.

Typical cross-correlation Calcomp plots are shown in Figure 18.

Calculations of the angular orientation of the array from true broadside for each correlation plot can be made from the following equation:

$$\sin \theta = \frac{V \Delta T}{ns}$$

θ = angle from true "broadside" (perpendicular)

V = velocity of sound in water

ΔT = time in ms to first (or appropriate peak as read on correlation plot.)

ns = spacing used in correlation

Results are tabulated below:

Spacing	Δt	sin θ	θ
S	6	.175	10^{o} 5'
2S	10	.146	8^{o} 24'
4S	20	.146	8^{o} 24'
7S	30	.125	7^{o} 11'
15S	68	.132	7^{o} 35'
19S	86	.132	7^{o} 35'
38S	192	.149	8^{o} 34'
45S	220	.143	8^{o} 13'

Navigation data taken during the test were plotted and the array angle was measured to be 6^{o} ($\pm$ 2^{o}) to broadside for field tapes 21 and 22. The comparison with calculated angles appears reasonable.

Finally, each cross-correlation plot (both source-on and source-off) was examined for correlation percentage with the array steered to the calculated broadside condition and these percentages plotted as a function of aperture (separation). The coherence plot is shown in Figure 19.

The source-on coherence curve shown in Figure 19 is very similar in general shape to the one shown in Urick, "Principles of Underwater Sound for Engineers", page 53, for a three-element array (this curve has been reproduced in Figure 13.). The correlation is 97 percent at an aperture of 50 meters, and exceeds 95 percent out to an aperture of about 350 meters.

It is important to note the coherence falls to a rather low value at the maximum aperture of 2250 meters. This information may help in evaluating the maximum usable length of long arrays.

The source-off (noise) array coherence curve is less like the theoretical curve of Urick. Data points have considerable scatter, and coherence values tend to exhibit somewhat random properties.

Based on the evidence described above, funds were requested to extend the analysis. Contract N00014-73-C-0302 was awarded, and further computer work begun in May 1973.

WORK COVERED UNDER ONR CONTRACT #N00014-73-C-0302

CONTRACT REQUIREMENTS - SECo contractual obligations are listed below by task:

1. Complete the coherence analysis of 25 broadside oriented Bay of Biscay field tapes using previously evaluated SECo technique to obtain coherence values.

2. Study paper by T. E. Talpey on a method to correlate array response and program algorithms to permit correlation analysis of 25 "broadside" field tapes indicated in item 1.

3. Compare results of Talpey correlation analysis with SECo coherence analysis and determine equivalence of results.

4. Modify SECo sound power spectrum level program to provide higher frequency resolution (to 0.09 Hz) within narrow spectral bands.

5. Prepare final report documenting all results including prior SECo work.

TASK I - COHERENCE STUDIES WITH SECo TECHNIQUE

The 25 field tapes studies were selected broadside oriented tapes taken from the list in Table 1, page 19. They are shown below:

TABLE 2

SOURCE-RECEIVER DISTANCE (MILES)	SOURCE-ON FT NUMBER	SOURCE-OFF FT NUMBER
15	3,5	4,6
30	20,22, 24,66, 67,68	21,23, 69,70
45	32	33,34
60	44,47, 50	45,46, 48,49,51

NOTE: #68 had many parity errors and could not be analyzed.

Standard Pairs Technique

All tapes were prepared for processing and initial coherence vs aperture values obtained using the programs developed during the earlier SECo Bay of Biscay study. These programs are described in detail in the section "Prior Work", pages 10 through 30 inclusive, and will not be discussed again in this section, other than to state that identical procedures were followed in processing the indicated 25 field tapes.

Normalized coherence vs array aperture graphs using this mathematical procedure are shown in Figures 20 through 30 (see curves labeled "standard pairs").

It was evident from the initial results that coherence values were quite variable, even within the bounds of a given source - receiver separation. While the scope of the contract did not require work beyond that already

accomplished, it was decided to continue processing studies to determine, if possible, the parameters which most affect coherence and modify procedures accordingly to provide a second series of coherence vs aperture measurements.

Optimized Pairs Technique

A study was made of the only source monitor tape made during the Bay of Biscay exercise, and it was noted the source had a frequency perturbation which was both random and significant. The Δf was at least $\pm$ 0.1 Hz and the period appeared to be one minute or less. Several field tapes were next studied by examining one channel. A frequency scan was made at eight discrete time locations covering the six minute tape record, and the results were outputted such that individual frequencies could be identified to within 0.06125 Hz. These tests also confirmed perturbation of the signal frequency during the six minute record time, with the fluctuations having a period of around one minute or less. This is what one might one might expect from a governor controlled diesel engine driving a generator source. This does not preclude the possibility that the environment (interference patterns, doppler, traffic noise, etc) controlled the observed frequency pattern. However, with the available field data the two effects cannot be separated.

Next, coherence was studied as a function of the time average used for

correlation. Computer results showed that as the time average was reduced to approximately that of the observed perturbations coherence values increased significantly.

The signal to noise characteristics of each channel in the array was then studied. Power spectra were obtained for all channels on a given field tape, and the S/N ratio judged by examining the 62.7 Hz source frequency peak on the power spectrum curve. Channels were tabulated from high S/N to low S/N, and only channels with good or excellent S/N were included in the suite from which trace pairs were selected for coherence measurements.

Coherence values were calculated with this technique for all source-on tapes except #44, and are indicated on the graphs as the "optimized pairs" curves.

Coherence Analysis

Coherence results for various signal plus noise and noise only conditions are shown in Figures 20 through 34. Results are discussed below:

1. Coherence vs aperture.

   There is a decrease in coherence with increased aperture, although the effect is not marked at source-receiver distances of 30 miles or less. Very good coherence (80% or greater) is seen at apertures to 1000 meters and certain of the "optimized pairs" curves indicate coherence above 80% at apertures of 2000 meters or more.

At forty-five and sixty miles the coherence values are degraded. This is partly due to geometrical divergence of the source energy and possibly to the rather strong probability that significant multiple path interference patterns are present at these distances. The results are also distrubed by the unexpectedly low source energy (which was only 63 dB rather than an anticipated 80-90 dB and probably was even lower during later phases of the data acquisition) and to the receiver array being located very near the surface (100') and subject to a rather high ambient noise field.

2. Coherence versus source-receiver separation.

   A distinct drop in "source-on" coherence is evident at the 45 and 60 mile separations. However, in most instances signal plus noise coherence is still significantly greater than noise only coherence.

3. Spread in array coherence at a given source-receiver separation.

   Figures 31 and 33 indicate the fairly large spread in array coherence at 30 and 60 mile separation, but with data samples taken from several minutes to several days separated in time. It is observed that data samples taken close in time have reasonably similar coherence over the full aperture, while samples separated several days are widely different. It is almost impossible to state whether this variability is due to large-scale fluctuations in the ocean background noise or to source frequency and amplitude changes.

4. Noise only coherence.

Figures 32 and 34 indicate the spread in noise coherence over a several minute to several day period at 30 and 60 mile separations. Again the curves have generally similar shape, no coherence above 60% except for elements separated 50 meters. Record 21 appears anomalous, all other noise data at 30 miles including data widely separated in time, has coherence value of 20-30% over the full aperture.

5. Signal plus noise and noise only coherence sets.

For sets of data where source-on and source-off data were taken without pause except to switch tape transports, all but one set have source-on coherence values substantially (X2 or greater) higher than source-off, to apertures approaching 2000 meters or greater in several cases. These data show that the source was definitely identifiable, and that the identity would be possible with the full array aperture in most instances.

While coherence in the Bay of Biscay area was variable it is believed that the observed variations were only partly temporal and were also a function of experimental limitations.

TASK II - TALPEY CORRELATION TECHNIQUE FOR NARROW BAND DETECTION OF UNDERWATER TARGETS.

General Theory

Numerous studies have been made of array performance. In some cases amplitude fluctuations have been ignored, and degradation of array performance attributed only to lack of phase coherence across the array aperture.

T. E. Talpey (Array Response, Proceedings of 28th Navy Symposium on Underwater Acoustics, November 1970) developed a method which expresses array performance as determined by both amplitude and phase of the detector elements.

Consider the narrow band output e_i of element i, in an array of N elements. Then:

$$e_i = A_i \cos(\omega t + \phi_i) \qquad (1)$$

A_i is the amplitude of the signal

ϕ is the phase of the signal

A_i and ϕ_i are slowly changing random variables.

Talpey shows that the time average array power can be written as:

$$\langle |E|^2 \rangle = \sum_{i=1}^{N} \sum_{j=1}^{N} \langle A_i A_j \rangle \langle \cos(\phi_i - \phi_j) \rangle \qquad (2)$$

Here $\langle\ \rangle$ denotes a time average of the order of several minutes.

A_i, A_j, ϕ_i, ϕ_j, may be obtained by quadrature sampling of the narrow band output from element i and j, or may be determined by FFT analysis of the signals from i and j, as A and ϕ are the modulus and argument of the discrete Fourier transform coefficient at angular frequency ω.

In our case, as the narrow band source signal was deeply buried (perhaps 30 to 40 dB) in a wideband noise field, that is,the field recordings were wideband (8-128 Hz), we used the FFT method to obtain the A's and $\emptyset$'s for the array elements used in the pairs correlation. Eight separate Fourier transforms were calculated for all selected elements over 3 minutes of the field recording, and the eight A_i's and $\emptyset_i$'s were averaged to provide time average values as required in equation (2). As each transform uses 2048 points, with 2 ms data approximately 4 seconds of field record is used in each calculation.

Computer Processes - Description

As stated, the Tolpey correlation procedure involves determining trace averages for both amplitude and phase. These may be calculated by quadrature sampling the narrow band filtered trace data, or from the modulus and argument of FFT calculations restricted to a narrow range of frequencies covering the known source frequency (including its perturbation). The latter technique was selected.

FFT Transform

The FFT transform program, (FOURI), uses the well known Cooley-Tukey transform which materially reduces computer run time. This transform takes the raw trace data recorded in the time domain and transforms it to the frequency domain.

The Bay of Biscay data was field recorded with a 2 millisecond digitizing

interval, thus 500 samples represent one second of time. Our transform used 2048 samples. The 2 ms sampling interval restricts the band width of the frequency transform to an upper limit of 250 Hz. The sampling theorem states that if Δt is the sampling interval, then frequency values $\omega > \frac{\pi}{\Delta t}$ radians/second will alias with those in the range 0, $\frac{\pi}{\Delta t}$ ($\frac{\pi}{\Delta t} = \omega_{Ny}$ the Nyquist frequency). In our case, the field digital recording system has a very sharp anti-alias filter (high-cut filter) which insures that frequencies beyond $\omega = \frac{\pi}{\Delta t}$ are down at least 72 dB. The sampling theorem tells us that for Δt = .002 seconds our maximum frequency with any significant power will be:

$$f_A = \frac{\omega_{Ny}}{2\pi} = \frac{\pi}{\Delta t} = \frac{1}{2\Delta t} = 250 \text{ Hz}$$

The frequency resolution of the transformed data is determined from the Nyquist frequency and the number of samples used in the transform, as shown:

$$\Delta f = \frac{f_{Ny}}{\text{No. of Samples}} = \frac{250}{2048} = 0.12207 \text{ Hz}$$

Note that the output of the transform is limited to those frequencies which are an <u>even multiple</u> of Δf, and fall within the band from 0-250 Hz.

Since the Bay of Biscay source frequency was only approximately 62.5 Hz (it had a slow perturbation of at least 0.2 Hz), it was necessary to determine the phase and amplitude values for several frequencies which surrounded 62.5 Hz. The ten frequencies from 62.011719 Hz to 63.11035 which are even multiples of Δf were calculated and outputted for analysis.

Amplitude and phase were displayed for each frequency, and the frequency which had maximum amplitude was selected as the one which represented the source frequency.

Further, since each transform was limited to 2048 samples (i.e. about 4 seconds of time domain data), a total of eight (8) frequency domain transforms per trace spread over three minutes of data were used. Eight transforms were performed at equal intervals along the trace. In effect, we sampled the frequency at eight separate times over the three minute data sample. These eight amplitudes and phases were then averaged as discussed in the next section describing Talpey program (TALPYL).

However, before proceeding it should be noted that the frequency domain data consists of an amplitude and a phase for each frequency which is an even multiple of the frequency sampling rate (Δf). The FFT transform is an exact transform in that the results are meaningful only for these discrete, even multiple frequencies. It is incorrect to interpolate for frequencies which lie between two transformed frequencies. For example, if a time domain frequency signal is created at 62.45 Hz, and then the trace is transformed to the frequency domain with transformed frequencies of say 62.37 and 62.50, theoretically, interpolation cannot be used to analyze the 62.45 Hz waveform. The implication is that the Fast Fourier transform is truly correct only if the source frequency is constant and the transform is designed to transform that exact frequency. In practice, it appears that if the frequency is close to one of the discrete even

numbered multiples of the frequencies sampling rate, the amplitude and phase values are realistic.

Talpey Program (TALPYL)

This program is used to compute time averages of the amplitude and phase values used to obtain the basic array correlation.

The program reads the frequency domain results from the FFT program (FOURI) for all eight transforms per trace, and calculates a time average amplitude and phase for the trace. The eight phase values are saved and used to evaluate the phase perturbations around zero phase.

Using the Talpey equations, the array correlations (or coherence) for any two selected traces (aperture) is then computed from the following:

$$\text{Coherence} = \langle A_x \rangle \cdot \langle A_y \rangle \cdot \langle \cos (\phi_{xi} - \phi_{yi} - \phi_{xy}) \rangle$$

where

$\langle A_x \rangle$ = Time average of the 8 amplitudes of trace x, (selected frequency)

$$= \frac{\sum_{i=1}^{i=8} A_{xi}}{8}$$

A_y = Time average of the 8 amplitudes of trace y, (selected frequency)

$$= \frac{\sum_{i=1}^{i=8} A_{yi}}{8}$$

$$\phi_{xy} = \langle \phi_x \rangle - \langle \phi_y \rangle$$

$\langle \phi_x \rangle$ = Time average of the phase of trace x (selected frequency)

$$= \frac{\sum_{i=1}^{i=8} \phi_{xi}}{8}$$

$\langle \phi_y \rangle$ = Time average of the phase of trace y (selected frequency)

$$= \frac{\sum_{i=1}^{i=8} \phi_{yi}}{8}$$

ϕ_{xi} = Phase of trace x computed at i·th transform location

ϕ_{yi} = Phase of trace y computed at i·th transform location

A_{xi}, A_{yi} = Amplitude of trace x and y at i·th transform location

The effect of phase perturbations around zero phase on array coherence is included in the term cos (ϕ_{xi} - ϕ_{yi} - ϕ_{xy}). ϕ_{xy} is used to shift the phase of trace y to the phase of trace x. The term (ϕ_{xi}-ϕ_{yi}-ϕ_{xy}) indicates the phase difference between trace x and trace y after the phase of trace y has been shifted by the difference $\langle \phi_y \rangle - \langle \phi_x \rangle$.

TALPEY - DATA FLOW DIAGRAM

Data flow is shown in Figure 35, including program functior and name. The output is a listing of time averaged amplitudes, phase, and correlation products for the selected aperture. These data provide the basic information from which Talpey normalized correlation plots are obtained.

Analysis of Results

Results of the Talpey amplitude and amplitude-phase products correlations are shown in Figures 36 through 57. The even numbered Figures 36 through 56 show coherence as determined by the average of the amplitude

$A_i \cdot A_j$ only. The odd numbered Figures 37 through 57 are plots of coherence as a function of the product of amplitude and phase. These latter curves indicate the effect of phase perturbations on overall array coherence.

Analysis of the plots indicate the following:

1. For a given field tape there is general similarity in magnitude and magnitude plus phase,i.e. in most cases the introduction of phase perturbations did not materially alter the coherence curve shape. This agrees with Talpey's conclusion that phase is most important above 100 Hz.
2. All data shows abnormally low correlation for the 50 meter element pair separation. This would lead one to suspect that one of the two elements making up this pair is noisy, or has some other field problem. Due to the tight computing schedule, a repeat of the 50 meters aperture with different traces was not possible.
3. Amplitude plus phase correlations have higher signal to noise ratios over amplitude only correlations for 6 of the 11 sets of data (20,21; 24,25; 47,48,49; 50,51; 66,69; 67,70). Three sets were essentially equivalent (05,06; 32,33,34; 44,45,46) and two sets (FT 03,04 and FT 22,23) showed slight degradation. The improvement noted in the six sets is strong evidence for the preliminary conclusion that both amplitude and phase factors should be included in real time low frequency signal identification if using Talpey averaging techniques.

4. The improvement indicated in item 3 above is most significant at the greater source-receiver distances, i.e. where S/N ratios are low.

5. Correlations--either amplitude or ampltidue plus phase--have significantly better S/N ratios for small source-receiver distances.

6. At source-receiver separations of 30 miles or less correlations of ≈ 80% were obtained at apertures approaching 2000 meters. These were for standard element pairs, not optimized pairs which should produce higher correlation values.

7. In essentially all cases, signal-on correlation was at least twice the noise only correlation, for apertures approaching the maximum 2,250 meters, i.e. the signal was detectable above ambient noise under all conditions.

The phase plots $\langle \cos |\phi_i - \phi_j| \rangle$ for signal plus noise and noise only are shown in Figures 58 thru 68. These plots indicate relatively low phase coherence, and in most cases the curves are similar for signal plus noise and noise only. This probably reflects the extremely low signal-to-noise ratio for the "source-on" data. Only at short apertures and minimum source-receiver separation does the time average show occasional percentage values well above 50% (the time average value expected for purely random noise where absolute magnitudes are used in obtaining the quantity $\langle \cos |\phi_i - \phi_j| \rangle$)

It should be emphasized that these results are not unexpected when it is understood that the Talpey coherence results were obtained for extremely adverse signal plus noise conditions which included:

1. Signal to noise ratio of recorded data was very low, perhaps -30 dB.
2. The raw signal was not narrow band filtered prior to performing the FFT computations. In the SECo coherence study, the raw data was heavily filtered with a cross-correlation technique greatly improving the signal to noise ratio.
3. The Talpey study was not made on the "optimized pairs" elements, due to time and budget limitations. It is possible the results might have been somewhat improved if computations had been made on these pairs of elements. However, from examination of intermediate data on phase angles during the FFT calculations on individual traces it appeared that phase coherence was still low, even on traces which were "optimized pairs" traces.

TASK III - COMPARISON - SECo COHERENCE TECHNIQUE VS TALPEY CORRELATION

Both the classical determination of coherence with the cross correlation technique (SECo Coherence) and the Talpey correlation based on time averaged amplitude and phase products have merit as methods to discriminate narrow band signals in the presence of wide band noise. However,

the mathematical techniques are different and it may be of some interest to compare the sets of coherence vs aperture curves. Obviously, any conclusions are tentative, and perhaps limited to the set of data taken in the Bay of Biscay. It should also be mentioned that comparisons are for the "standard pairs" elements, not the "optimized pairs". Presumably Talpey "signal-on" correlations would be higher for the "optimized pairs" data.

Visual observation indicates that:

1. The general shape of the SECo coherence vs Talpey correlation curves are different, but both show decreased coherence at large apertures and maximum source-receiver distances.

2. There is no consistent pattern of differences.

3. The signal-on to signal-off ratio S/N would appear to be higher for Talpey phase plus amplitude curves than for SECo coherence curves, especially at large source-receiver distances and large apertures. This effect might be more pronounced with significantly longer time averages for the Talpey calculations. These calculations were not possible with our 6 minute field records and computing format.

4. In the few instances where the SECo coherence for "signal plus noise" was the same or less than for "noise only", i.e. S/N 1 (FT 44,45; 50,51), the Talpey correlation showed approximately a 2:1 signal-on to signal-off ratio. This would indicate the Talpey technique is the superior of the two methods for separating a very low level narrow band signal in the presence of wide band high amplitude noise. This conclusion is,of course, restricted to the parameters of this experiment, and the paucity of data analysis available at this time.

5. Talpey phase coherence plots show low phase coherence across the array. The lack of array phase coherence is probably due to the extremely low signal level of the acoustic source and absense of filtering prior to FFT analysis. A source level at least 20 dB greater would be required to evaluate array phase coherence.

TASK IV - MODIFY SECo SOUND POWER SPECTRUM LEVEL PROGRAM TO PROVIDE FREQUENCY RESOLUTION TO 0.0833 HERTZ

General

The SECo sound power spectrum level program initially had a frequency resolution of 0.5 Hz. Under Task IV funding this program was modified to 0.083 Hz, the maximum resolution possible with the present field tape reformat technique which provides blocks of 6 second data to the computer.

Program modifications included increasing the size of the cosine transform table, processing more auto-correlation (auto-covariance) values and providing increased buffer areas to the limit of the memory availability.

The basic program design was not modified, but the order of some processes was changed to facilitate data handling, etc.

Computer Programs - Power Spectrum

A description of the complete absolute level sound power spectrum is detailed below. Figures 58 & 59 show the sequence of programs in the absolute level power spectrum calculation.

Several functions must be computed to provide an absolute level sound power spectrum. These are discussed separately in the next paragraphs.

1. Normalized Auto-Correlation (Auto-Covariance) Calculation

By definition the auto-correlation function, of X(t) which is a stationery, ergodic, zero mean, stochastic process is:

$$X(\tau) = \lim_{T \to \infty} \frac{1}{2T} \int_{-T}^{+T} X(t) \cdot (t-\tau)\, dt$$

When the function x(t) is a sampled function (eg. digital techniques have been used to record the function) the normalized auto-correlation function may be expressed as:

$$\chi_\tau = \sum_{n=0}^{N} X_n \cdot X_{n-\tau} \Big/ \sum_{n=0}^{N} X_n^2 \quad , \tau = 0, 1, \text{---} K,$$

where X_n values are sampled values of the signal trace used (may be a summed signal). The squared term in the denominator normalizes the auto-correlation function to values between (-1.0) and (+1.0), the lag τ ranges from 0 to K = 3000, i.e. the total lag covers 6 seconds, and N is 9×10^4 samples to cover a 3 minute time window. The K value of 3000 provides a $\Delta f = 0.083$ Hz discussed in the next section.

2. Estimation of Normalized Power Density Spectrum (PS)

A process which has a summable auto-correlation function has a power spectral density which may be expressed as:

$$S(f) = 2 \sum_{\tau=0}^{\tau=\infty} \chi(\tau) \cos(\tau f)$$

in our high resolution case we let τ range over 3000, 2 ms. lags, and

compute the cosine transform, which provides us with our power spectrum.

The series of expressions set up in the program to handle the discrete, finite cosine transform are shown below:

$$PS_0 = \Delta t \left[\chi_0 + 2 \sum_{\tau=1}^{K-1} \chi_\tau + \chi_K \right]$$

$$PS_1 = \Delta t \left[\chi_0 + 2 \sum_{\tau=1}^{K-1} \chi_\tau \cos \frac{\tau \pi}{K} + \chi_K \cos \pi \right]$$

$$PS_2 = \Delta t \left[\chi_0 + 2 \sum_{\tau=1}^{K-1} \chi_\tau \cos \frac{2\tau \pi}{K} + \chi_K \cos 2\pi \right]$$

$$PS = \Delta t \left[\chi_0 + 2 \sum_{\tau=1}^{K-1} \chi_\tau \cos \frac{n\tau \pi}{K} + \chi_K \cos n\pi \right]$$

$$PS_K = \Delta t \left[\chi_0 + 2 \sum_{\tau=1}^{K-1} \chi_K \cos \tau \pi + \chi_K \cos K \pi \right]$$

Where $t = .002$ seconds (1 sample time)

K = maximum lag = 3000 points

$\omega = 2\pi f$

The PS is next convolved with a 0.25 - 0.50 - 0.25 Hanning filter to smooth the PS, as the relatively short sample and lag requires smoothing to remove the effects of truncation.

The Hanning smoothing procedure is shown as follows:

$$U_0 = 1/2 \quad (PS_0 + PS_1)$$

$$U_\tau = 1/4\ PS_{\tau-1} + 1/2\ PS_\tau + 1/2\ PS_{\tau+1}$$

$$U_K = 1/2 \quad (PS_{K-1} + PS_K)$$

$$\tau = 1, 2, - - - -(K - 1)$$

K = Maximum lag, i.e. = 3000

The smoothed power spectrum U (τ) is still a normalized spectrum, as the autocorrelation function (χ) was normalized. To make the PS values relative true amplitude, the normalizing factor computed for the auto-correlation (i.e. χ_o) is now used as a <u>multiplying</u> factor.

Relative true (PS_τ) $= \chi_o \times U_\tau$

Lastly the PS data is converted to decibel form by taking 10 $\log_{10}$ (PS_τ). Each spectral value is now in decibels, although not yet put in absolute level re 1 dyne/cm^2.

Before continuing to the calculations which determine the absolute power spectrum values, a few comments are helpful in determining some limitations inherent in the spectrum values.

The most important parameter in the program is the sampling rate, as it controls the highest frequency component which has meaning. The sampling theorem states that if Δt is the sampling interval, then frequency values $\omega > \frac{\pi}{\Delta t}$ radians/second will alias with those in the range 0, $\frac{\pi}{\Delta t}$ ($\frac{\pi}{\Delta t} = \omega_{NY}$ the Nyquist frequency). In our case, the field digital recording system has a very sharp anti-alias filter (high-cut filter) which insures that frequencies beyond $\omega = \frac{\pi}{\Delta t}$ are down at least 72 dB. This also tells us that for $\Delta t = .002$ seconds our maximum frequency with any significant

power will be:

$$f_A = \frac{1}{2\Delta t} = \frac{1}{.004} = 250 \text{ Hz}$$

In actuality, the high cut filter in the field recording system has its (-3dB) point set at 1/2 f_A = 125 Hz, so that we can use a frequency band with an upper limit of 125 Hz in our spectrum analysis. The low frequency limit is also set by filters in the field system. For the data analyzed in this study, the (-3dB) point was set at 10 Hz, with a 36 dB/octave slope. Effectively, the power spectrum then is computed over the pass-band from 10 - 125 Hz. A correction may be made to indicate true accustic levels below 10 Hz.

The maximum lag (K) determines the resolution of the PS curve. It can be shown that:

$$\Delta f \cong \frac{fNy}{K}$$

thus, in the high resolution analysis where K was set to maximum lag of 3000 samples the frequency resolution is 0.083 Hertz, as:

$$\Delta f \cong \frac{fNy}{K} = \frac{250 \text{ Hz}}{3000} = 0.0833 \text{ Hz}, \quad fNy = \text{Nyquist frequency}$$

To look for greater frequency resolution, one can increase K at the expense of more computer time. This may be compensated for by restricting the frequency band over which the PS is computed.

The accuracy of estimation of the PS calculation is directly dependent on sample size. A larger size will normally yield better estimates. A three

minute sample should have good statistics. Further, the maximum lag at which the autocorrelations are calculated should not be set too close to the sample size. A rule of thumb is $N \gg 5\ K$. In our case:

$$N = 9 \times 10^4$$

$$K = 3000$$

$$N = 30\ K$$

Of course, a primary reason for the long sampling time was to obtain reasonable statistics on ocean acoustics, which require long sampling intervals for the data to have any correlation.

3. Scaling The Power Spectrum in Absolute Units

Several steps are involved in absolutizing the PS values. The procedure is based on equating the root mean square value of the original trace time domain data to the root mean square value of the power spectrum data. The procedure is described as follows:

1. Express the absolute RMS value of the 3 minute data signal - X_{RMSA}

   a) Determine the RMS value in volts of the time series used in the PS analysis. This will be either a three minute sample of a single element or one of the summed outputs. This is calculated as:

$$X_{RMS} \left(= \frac{1}{T} \sum_{i=0}^{T} X_i^2 \right)^{1/2}$$

where $X_i = Y_i \cdot M \cdot G$ = volts

Y_i = sample level in bits

M = MV/bit for digitizer in recording system.

= .250 MV/bit for the system used in Bay of Biscay work.

G = total gain of recording system.
(96 dB = 63.1×10^5 for most Bay of Biscay)

b) $$X_{(RMS)\ Abs} = X_{RMS} / E_s = \text{microbars}$$

E_s = element sensitivity = 3.8 u volts/μ bar for all the SECo sections.

2. Determine the intensity level value of X_{RMSA} for unit frequency bandwidth, expressed in dB re 1 μ bar.

a) $$I_X = X^2_{RMSA}\ (dB) = 10 \log \left(\frac{X_{RMSA}}{1\ \mu\ bar} \right)^2$$

$$= 20 \log X_{RMSA}$$

Now X_{RMSA}^2 is the RMS intensity level over the bandwidth of the recording system, i.e. 10 Hz to 125 Hz. To express over a 1 Hz bandwidth, we can divide by the bandwidth - assuming reasonably flat spectrum data.

b) I_A = Intensity per Hertz = $\frac{Ix}{BW}$

$$I_A = \frac{X_{RMSA}^2}{BW} = \frac{20 \log X_{RMSA}}{10 \log BW}\ (dB)$$

$$I_A = 20 \log X_{RMSA} - 10 \log (125 - 10)$$

Note that intensity per unit frequency has the same units as our power spectrum level, both have units of amplitude

squared per hertz. This provides us a means of using RMS time values to establish an absolute level value for the PS curve, and thus absolutize the ordinate of the power spectrum graph, i.e.

$$I_A = \frac{X_{RMSA}^2}{Hz} = PS_{RMSA}$$

Thus, we compute:

$$PS_{RMS} = \left(\sum_{i=0}^{K} \frac{PS_i^2}{K} \right)^{1/2}$$

This value locates a point on the ordinate which has the value PS_{RMS} and also has the value I_{RMSA} in dB re 1μ bar. This establishes the absolute dB scale for the power spectral density plot.

In the computer program this is implemented by taking the difference between the value of PS_{RMS} and I_A and subtracting from the value of the PS for each frequency domain point, i.e.

$$PS_A(\tau) = PS(\tau) - (PS_{RMS} - I_A)$$

The resultant data is then in a form ready for plotting.

The above procedure is acceptable over a limited bandwidth and where the power spectral density is reasonably flat.

It is felt the data under analysis falls in these bounds.

Once the absolute spectral power density scale has been computed for the Power Spectrum Curve, the final Calcomp plotting tape is created. This tape is plotted using an off-line Calcomp system.

Test Results

Figures 60 and 61 are examples of the SECo 0.5 Hz resolution (Fig. 60) and 0.0833 Hz (Fig. 61) resolution power spectrum plots from one Bay of Biscay field tape.

The high resolution spectrum extends just to 30 Hz, so only this portion of Figure 60 is of concern for comparison purposes.

Several portions of the 30 Hz band have been noted and identified. These clearly indicate the increased resolving power of the modified program, and show the interesting fact that the broad peaks in the 0.5 Hz spectrum actually consist of numerous narrow and separated frequency maxima, as listed in the following tabulation:

	Figure 60 0.5 Hz Δf	Figure 61 0.0833 Hz Δf
Region 1	2 peaks covering 6 Hertz	11 peaks
Region 2	2 peaks covering 4.5 Hz	7 peaks
Region 3	1 peak covering 1.5 Hz	2 peaks
Region 4	1 broad peak coverion 10 Hz	13 or more peaks

It is also seen from Figure 61 that even with increased resolution frequency maxima still have widths of 0.2 Hz or greater from start to end of clearly separated peaks. This indicates that still greater resolution in the power spectrum program (i.e. $N > 3000$ points) would be required to resolve peaks which lie closer together than 0.1-0.2 Hertz. It is possible that a fine line frequency spectrum exists in the Bay of Biscay which is not shown with the resolving power of the present program.

CONCLUSIONS

The preceding sections have indicated that limiting conditions exist relative to the quantitative value of the signal plus noise coherence results due to the low acoustic source level and relatively high ambient noise level existing in the Bay of Biscay. These limits are such that it is unlikely that the signal plus noise coherence plots obtained adequately expresses array coherence vs aperture, especially at the large apertures (in excess of 1,000 meters).

There are, however, two sets of data which present significant contributions resulting from this work. These are:

A. A set of quantitative measurements of noise coherence for array apertures to 2,250 meters. These data place absolute level boundaries on noise coherence which may be compared to other sets of data from the same or other areas to evaluate ambient noise similarities, levels, etc.

B. A set of signal plus noise coherence measurements which establish minimum values necessary for signal detection. As stated earlier, in spite of low source power, high noise levels and source frequency perturbations, array coherence values with the source on were consistently higher than with the source turned off. While these coherence plots are possibly

suspect for predicting actual array coherence fall off with aperture, they do set minimum values for signal buried in noise necessary to permit signal detection. As such they are important in the design of arrays with adequate gain to permit signal detection under specified conditions.

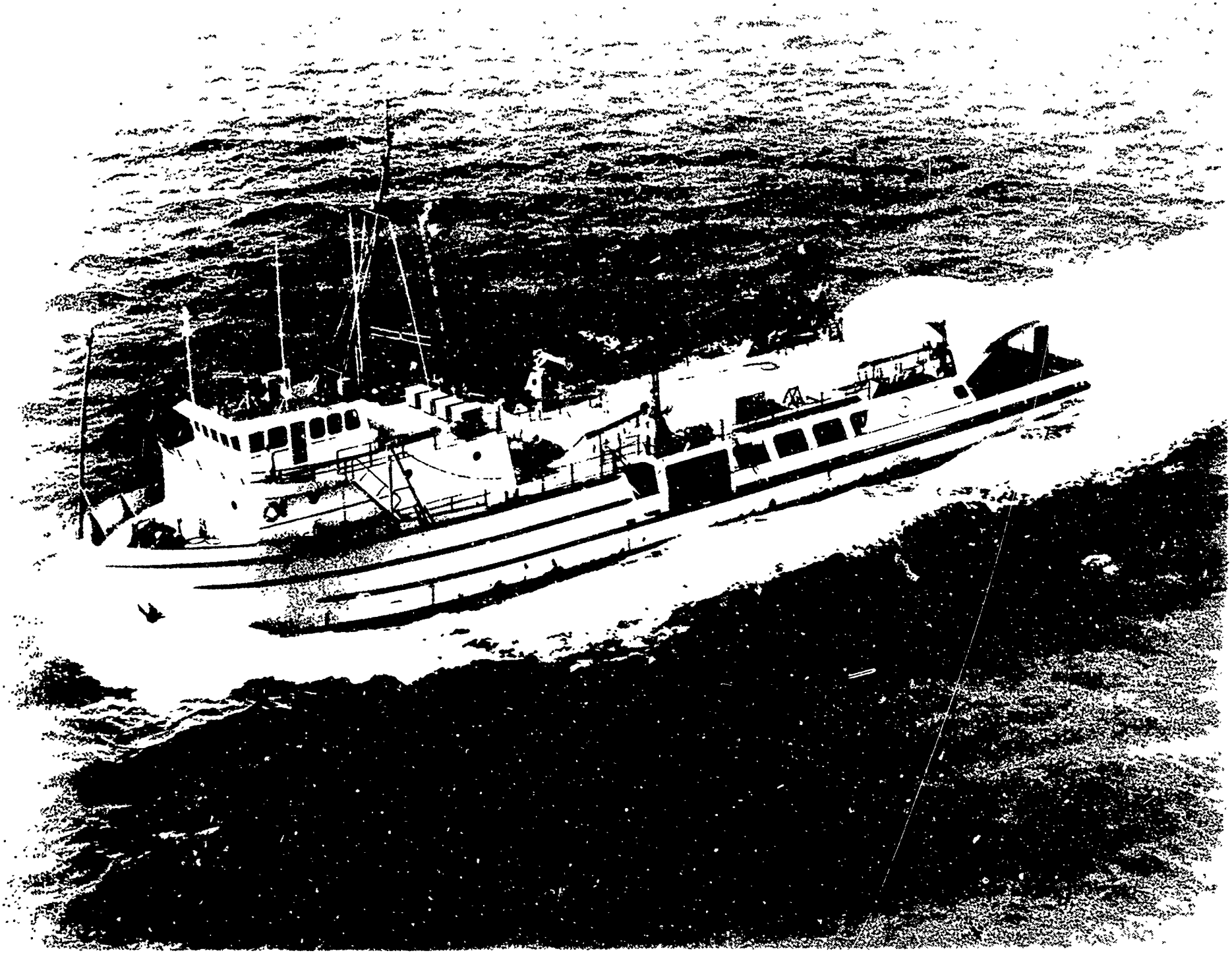

Figure A

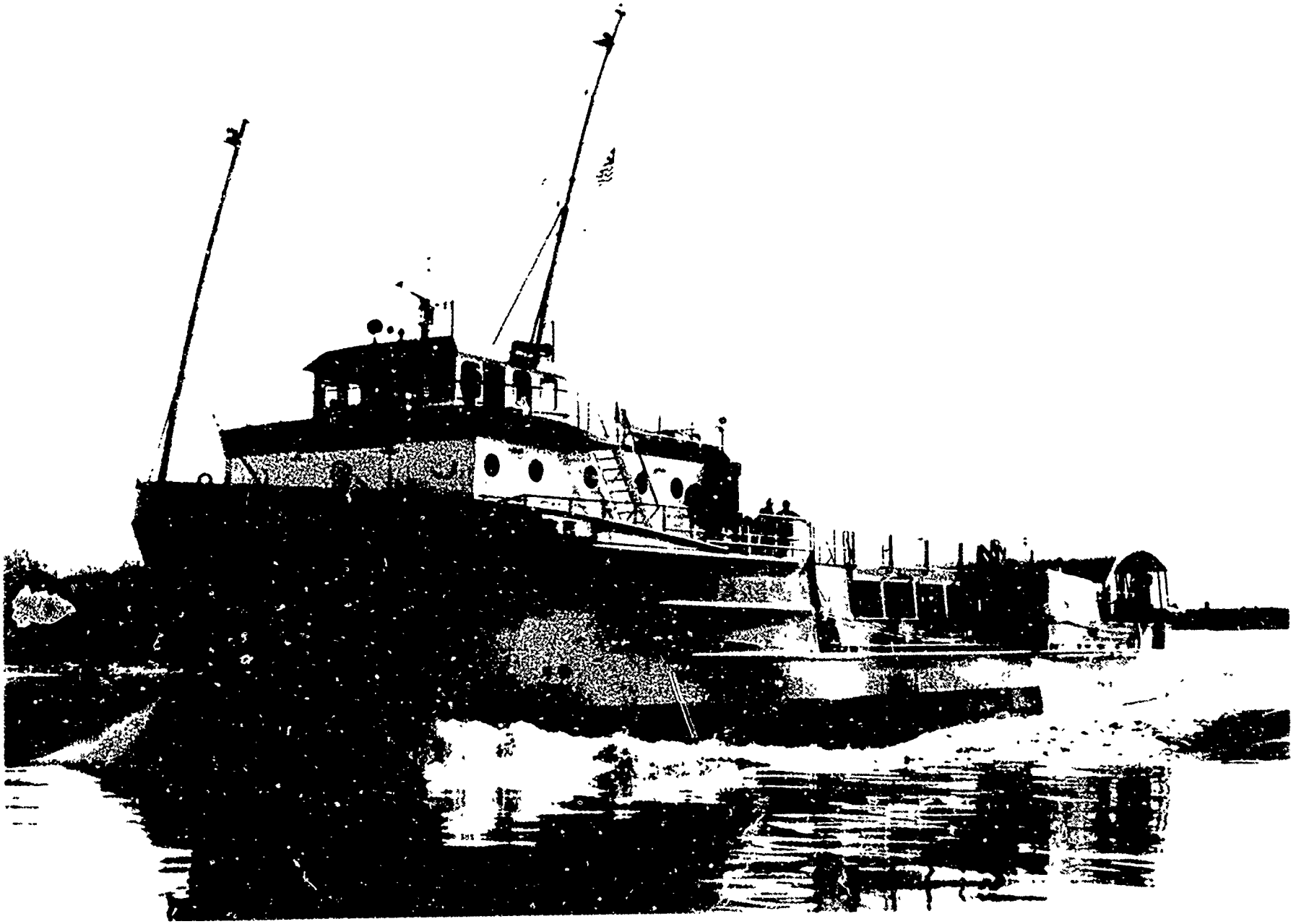

Figure B

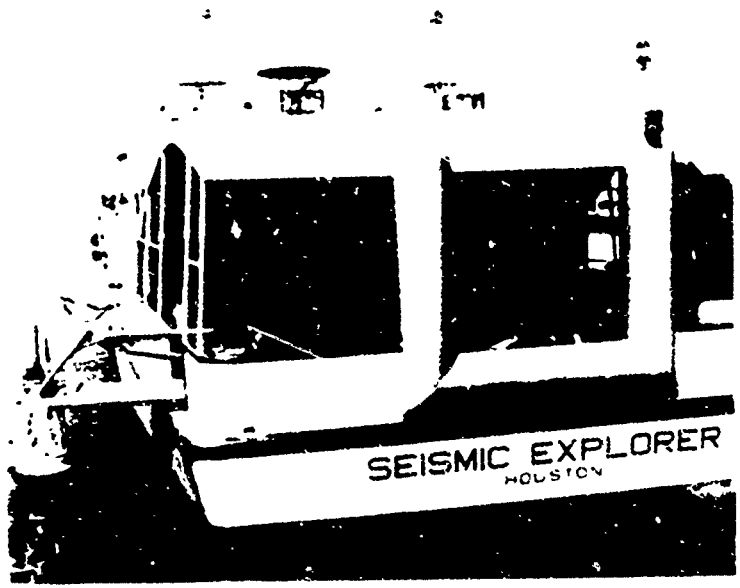

STERN VIEW OF VIBROSEIS

DFS-3 DIGITAL RECORDER

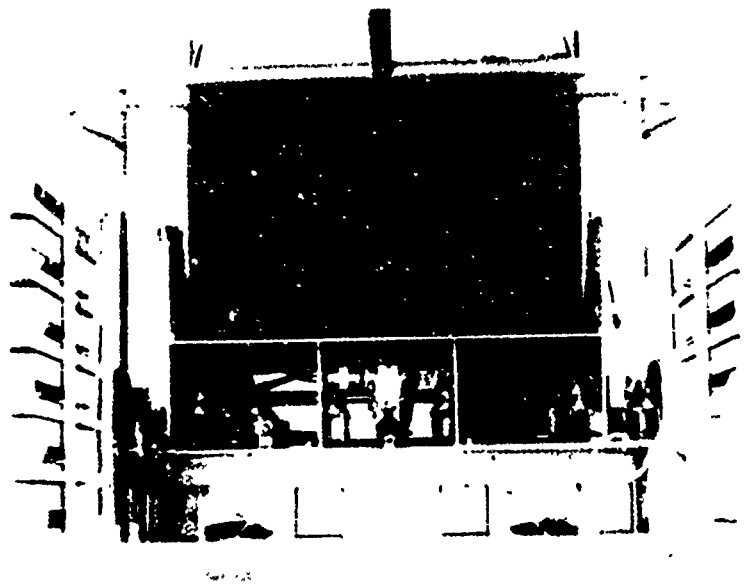

48 CHANNEL SECo STREAMER

SATELLITE-DOPPLER SONAR NAVIGATOR

Figure C

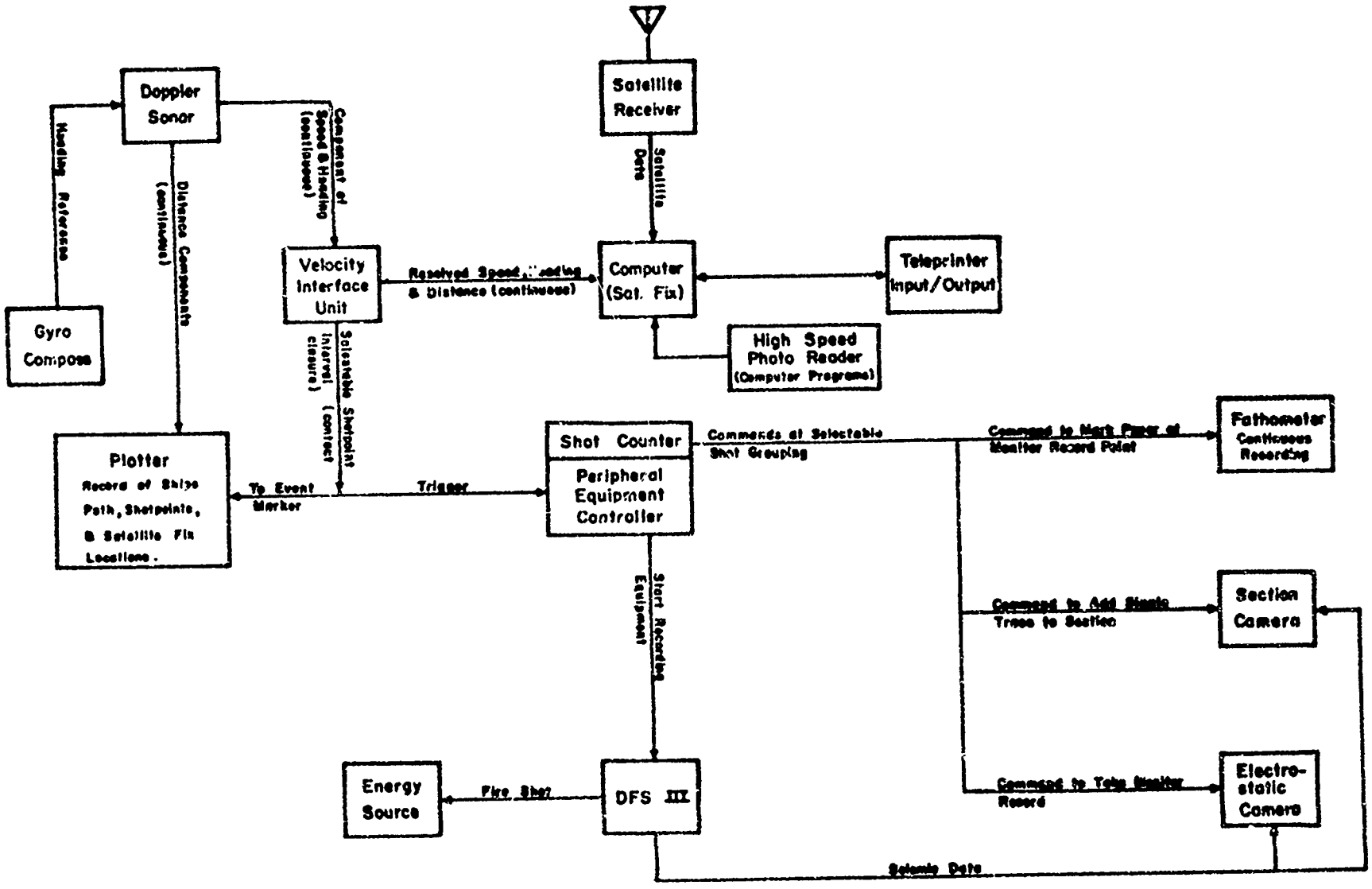
Doppler Sonar
Satellite Receiver
Heading Reference
Distance Components (continuous)
Component of Speed & Heading (continuous)
Satellite Data
Velocity Interface Unit
Resolved Speed & Heading & Distance (continuous)
Computer (Sat. Fix)
Teleprinter Input/Output
Gyro Compass
High Speed Photo Reader (Computer Programs)
Selectable Shotpoint Interval (contact closure)
Plotter
Record of Ships Path, Shotpoints, & Satellite Fix Locations.
To Event Marker
Trigger
Shot Counter
Peripheral Equipment Controller
Commands at Selectable Shot Grouping
Command to Mark Paper at Monitor Record Point
Fathometer Continuous Recording
Start Recording Equipment
Command to Add Blanks Trace to Section
Section Camera
Command to Take Monitor Record
Electro-static Camera
Energy Source
Fire Shot
DFS III
Seismic Data

FIGURE 1

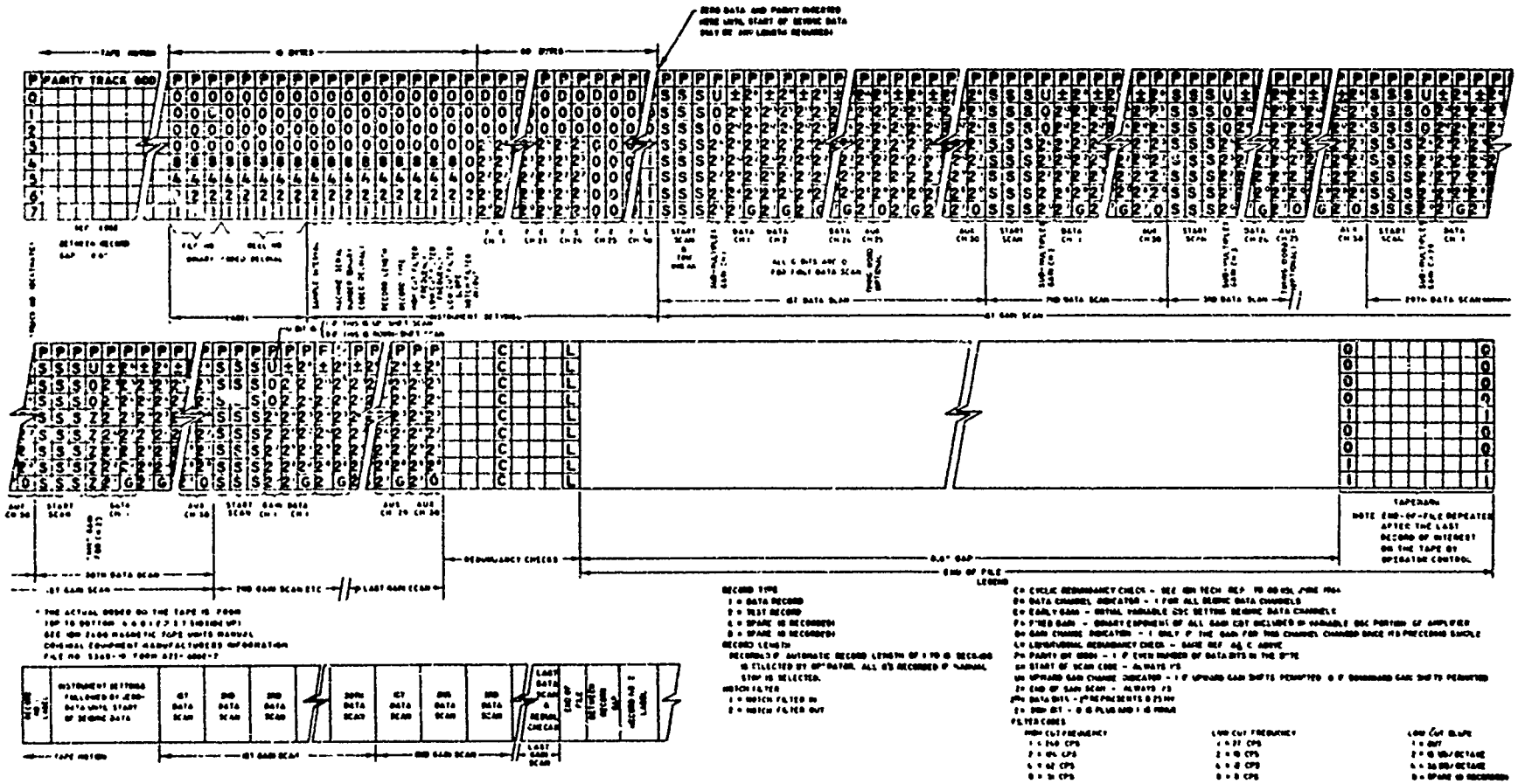

SEG A/EPR

DIGITAL SEISMIC FORMAT

Figure 2

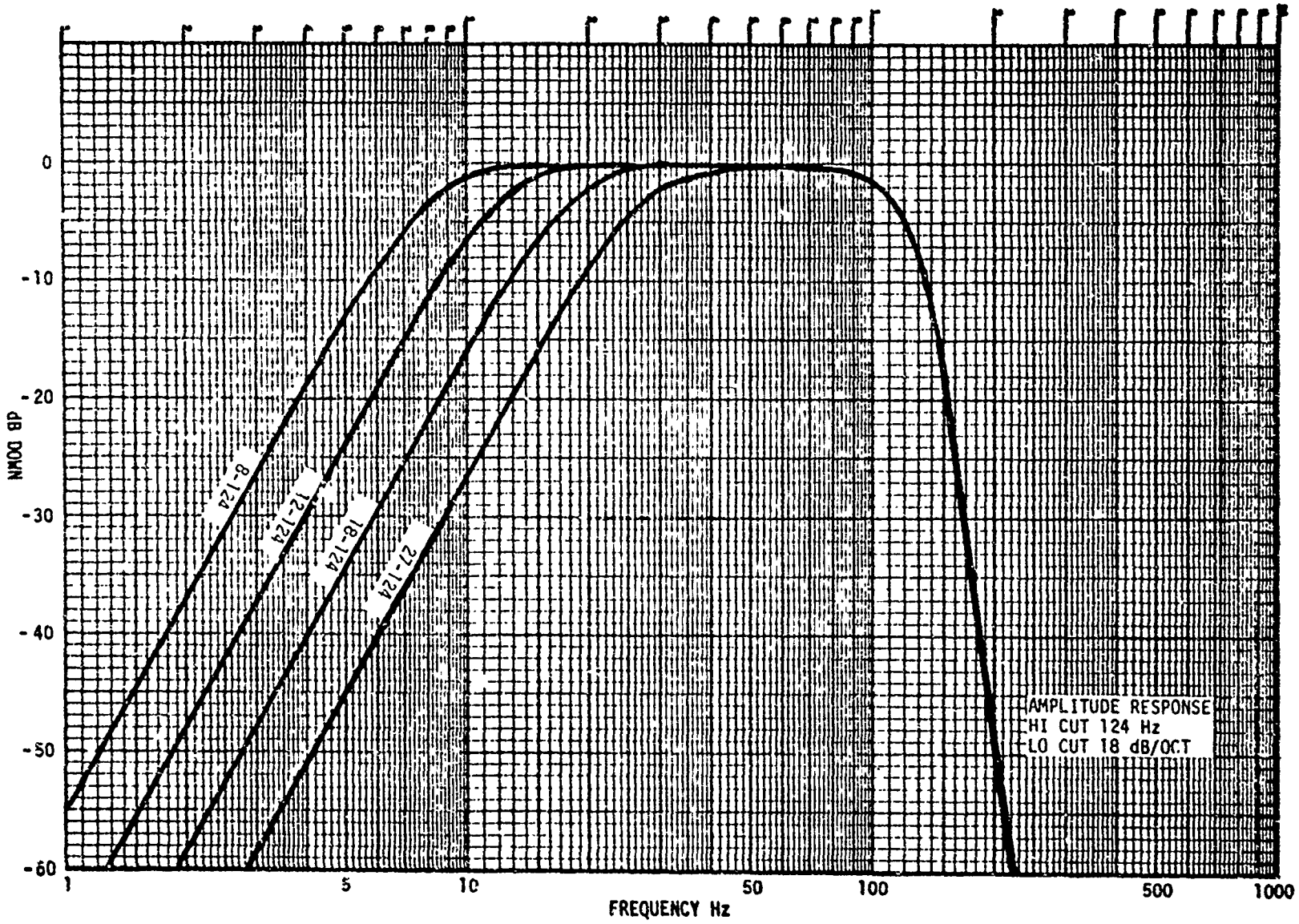

Figure 3 Amplitude Response, 18 dB/Oct., 124 Hz

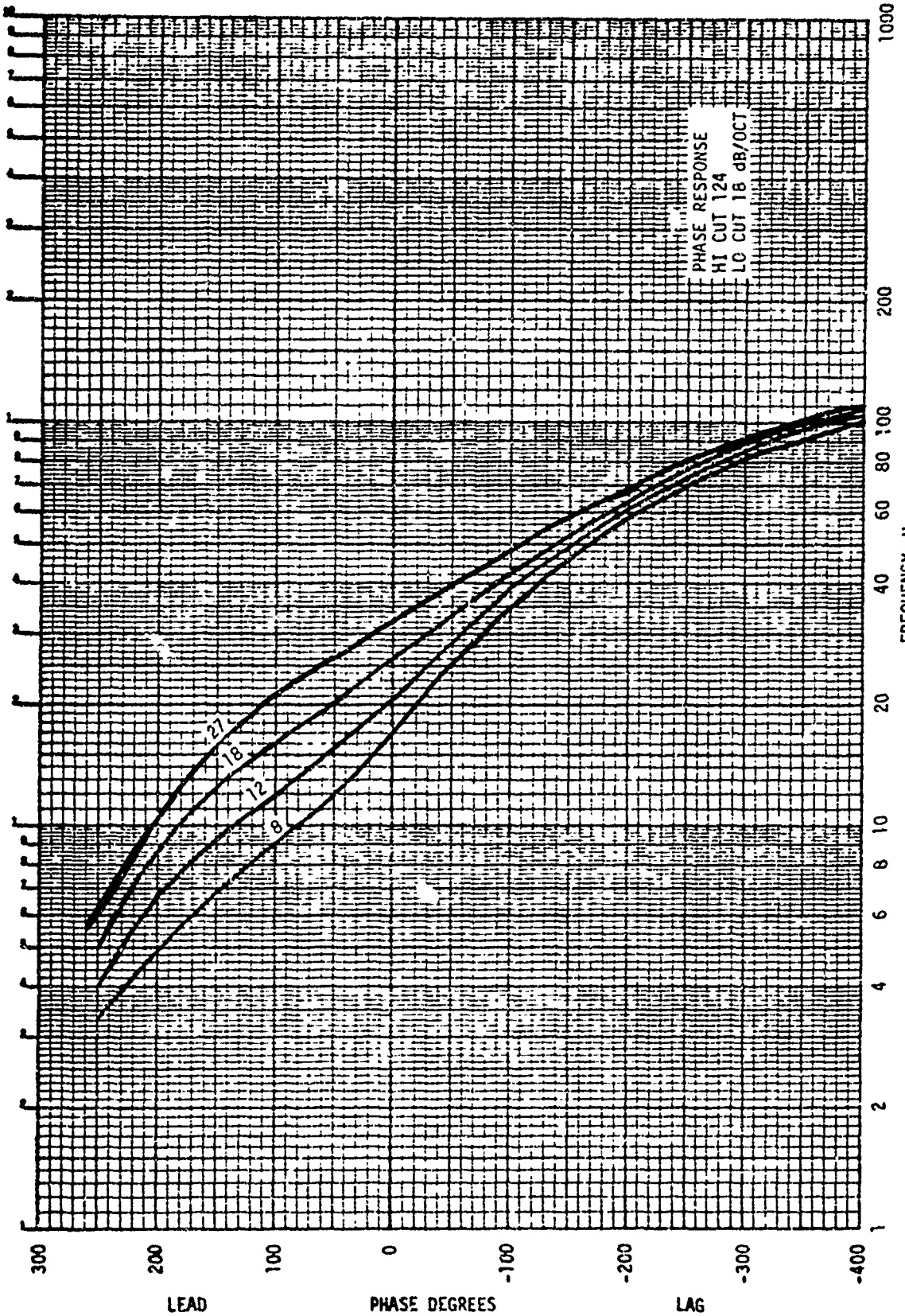

Figure 4 Phase Response, 18 dB/Oct., 124 Hz

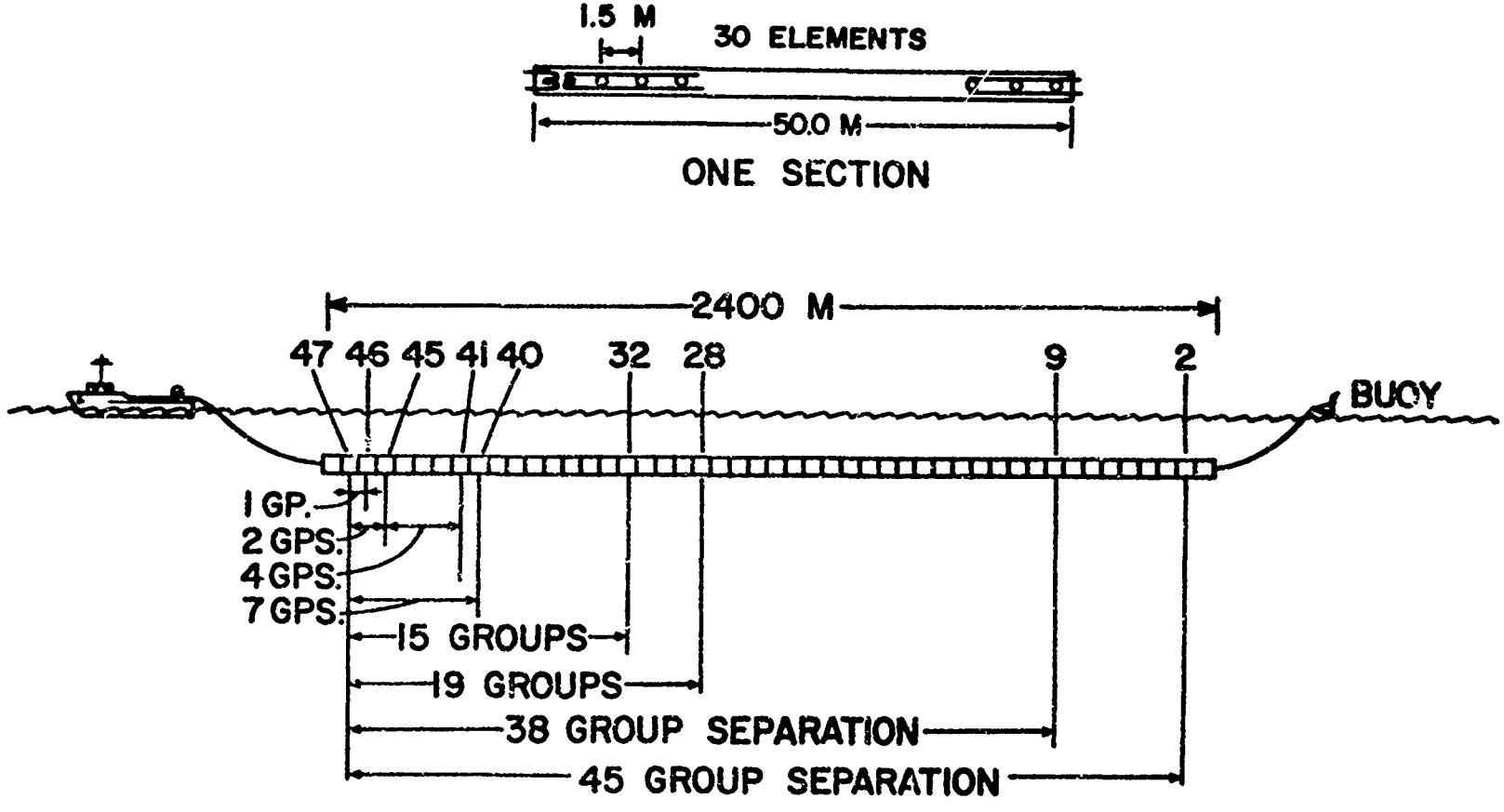

STREAMER DIAGRAM

SHOWING PAIRS USED FOR COHERENCE MEASUREMENTS

SECo COHERENCE TEST

Figure 5

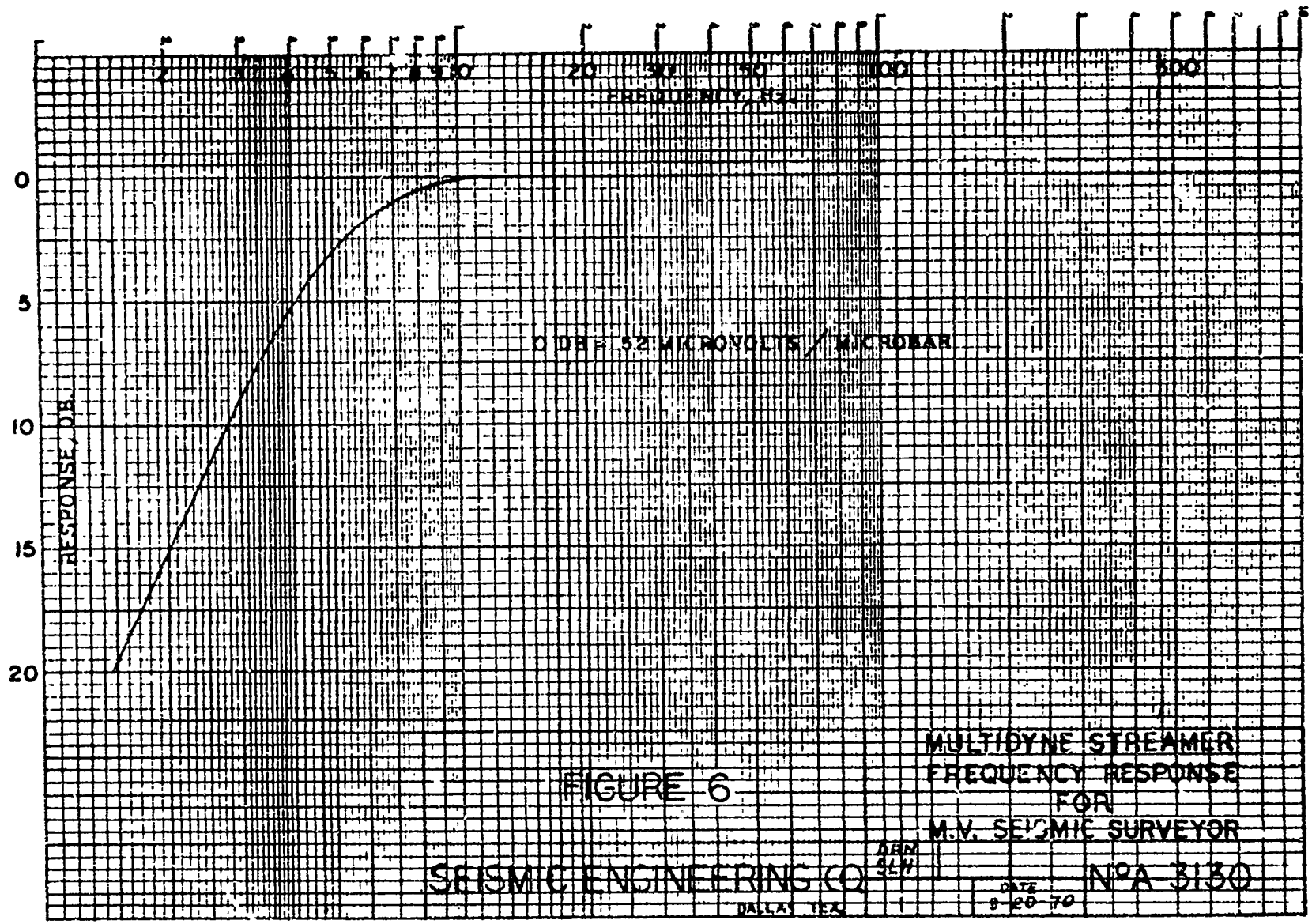

FIGURE 6

MULTIDYNE STREAMER
FREQUENCY RESPONSE
FOR
M.V. SEISMIC SURVEYOR

SEISMIC ENGINEERING CO.
DALLAS, TEXAS

DRN ALH
DATE 8-20-70

NºA 3130

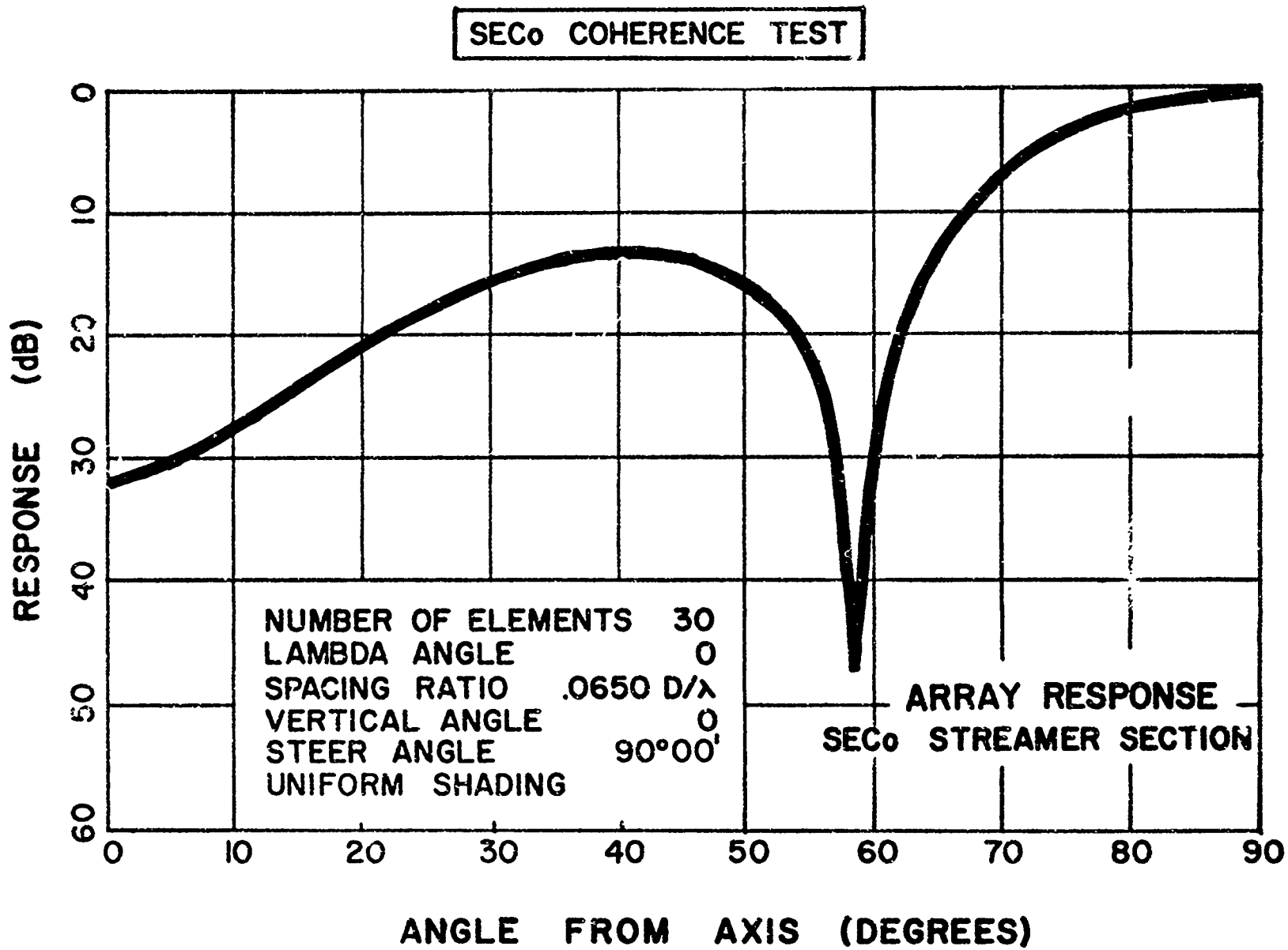
SECo COHERENCE TEST
RESPONSE (dB)
0
10
20
30
40
50
60
NUMBER OF ELEMENTS 30
LAMBDA ANGLE 0
SPACING RATIO .0650 D/λ
VERTICAL ANGLE 0
STEER ANGLE 90°00'
UNIFORM SHADING
ARRAY RESPONSE
SECo STREAMER SECTION
0
10
20
30
40
50
60
70
80
90
ANGLE FROM AXIS (DEGREES)

Figure 7

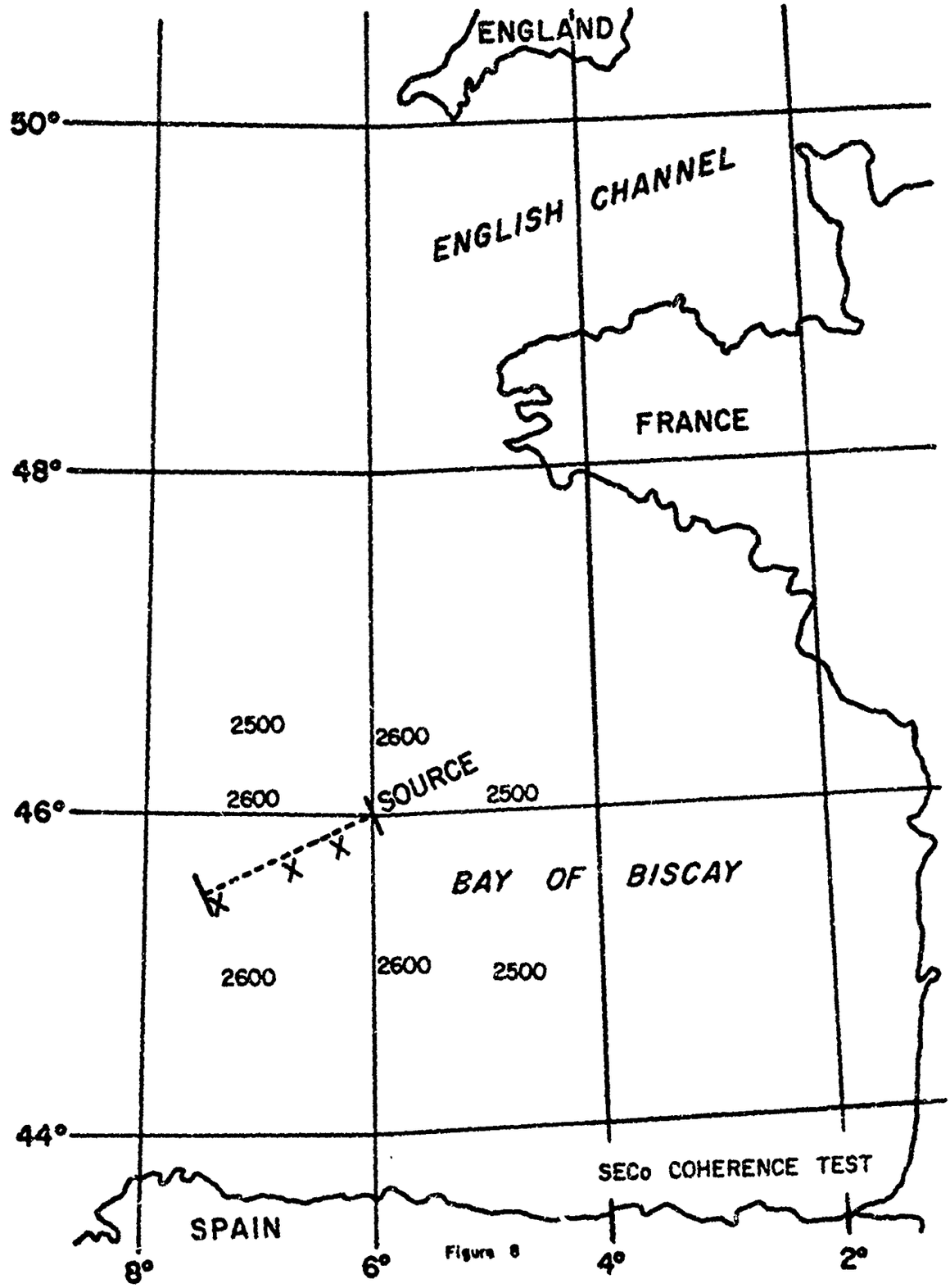
ENGLAND
50°
ENGLISH CHANNEL
FRANCE
48°
2500
2600
2600
SOURCE
2500
46°
BAY OF BISCAY
2600
2600
2500
44°
SECo COHERENCE TEST
SPAIN
8°
6°
4°
2°

Figure 8

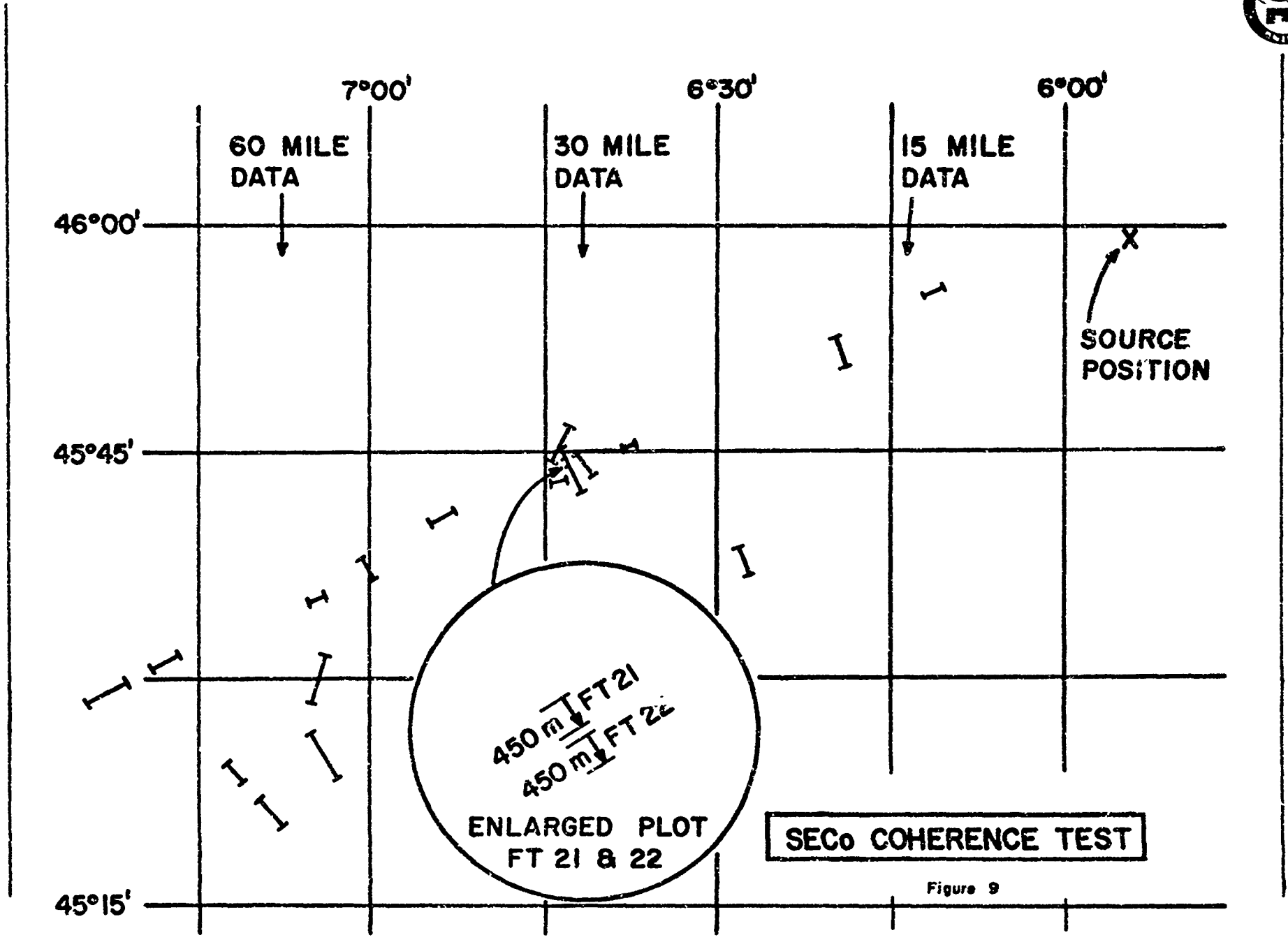
7°00'
6°30'
6°00'
60 MILE DATA
30 MILE DATA
15 MILE DATA
46°00'
45°45'
45°15'
SOURCE POSITION
450 m
FT 21
450 m
FT 22
ENLARGED PLOT
FT 21 & 22
SECo COHERENCE TEST

Figure 9

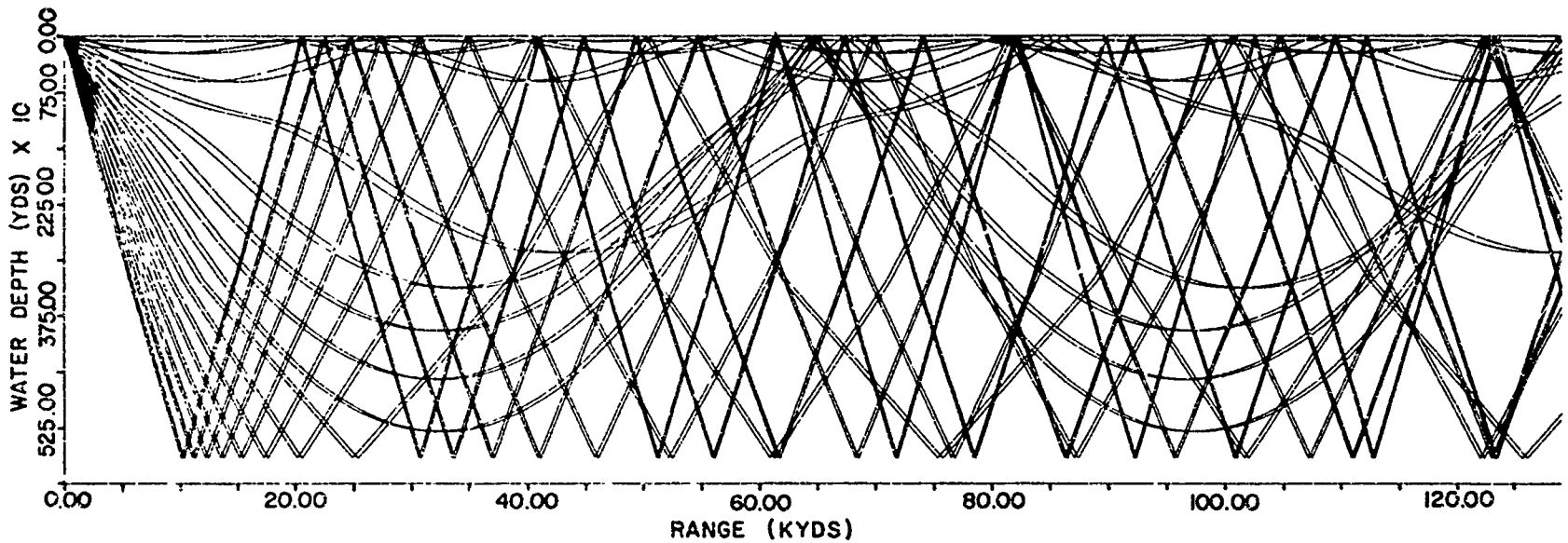

RAY PATH CHART
BAY OF BISCAY
SOURCE DEPTH : 67 YDS

SECo COHERENCE TEST

Figure 10

PROPAGATION LOSS CHARTS

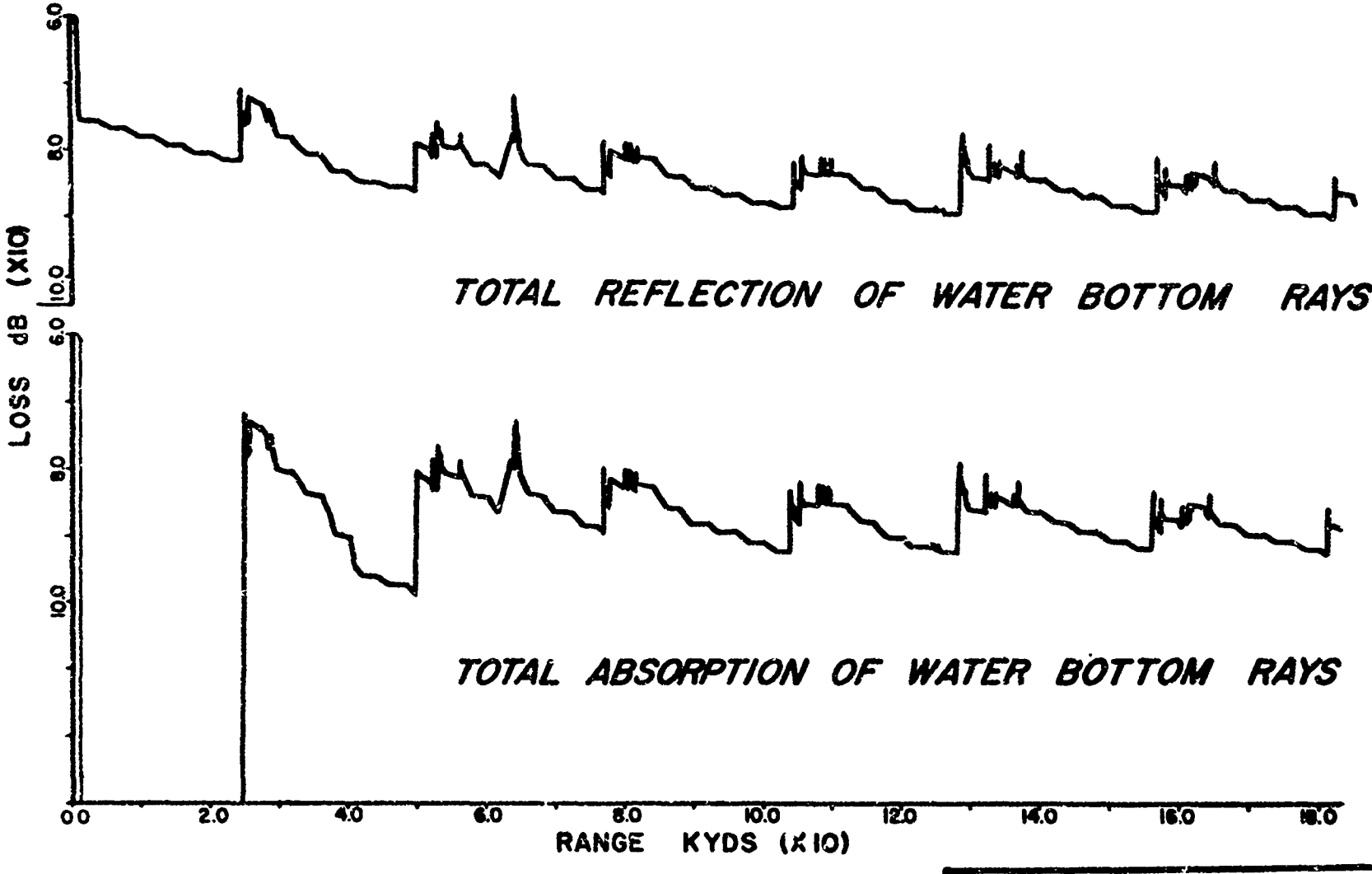

SECo COHERENCE TEST

Figure 11

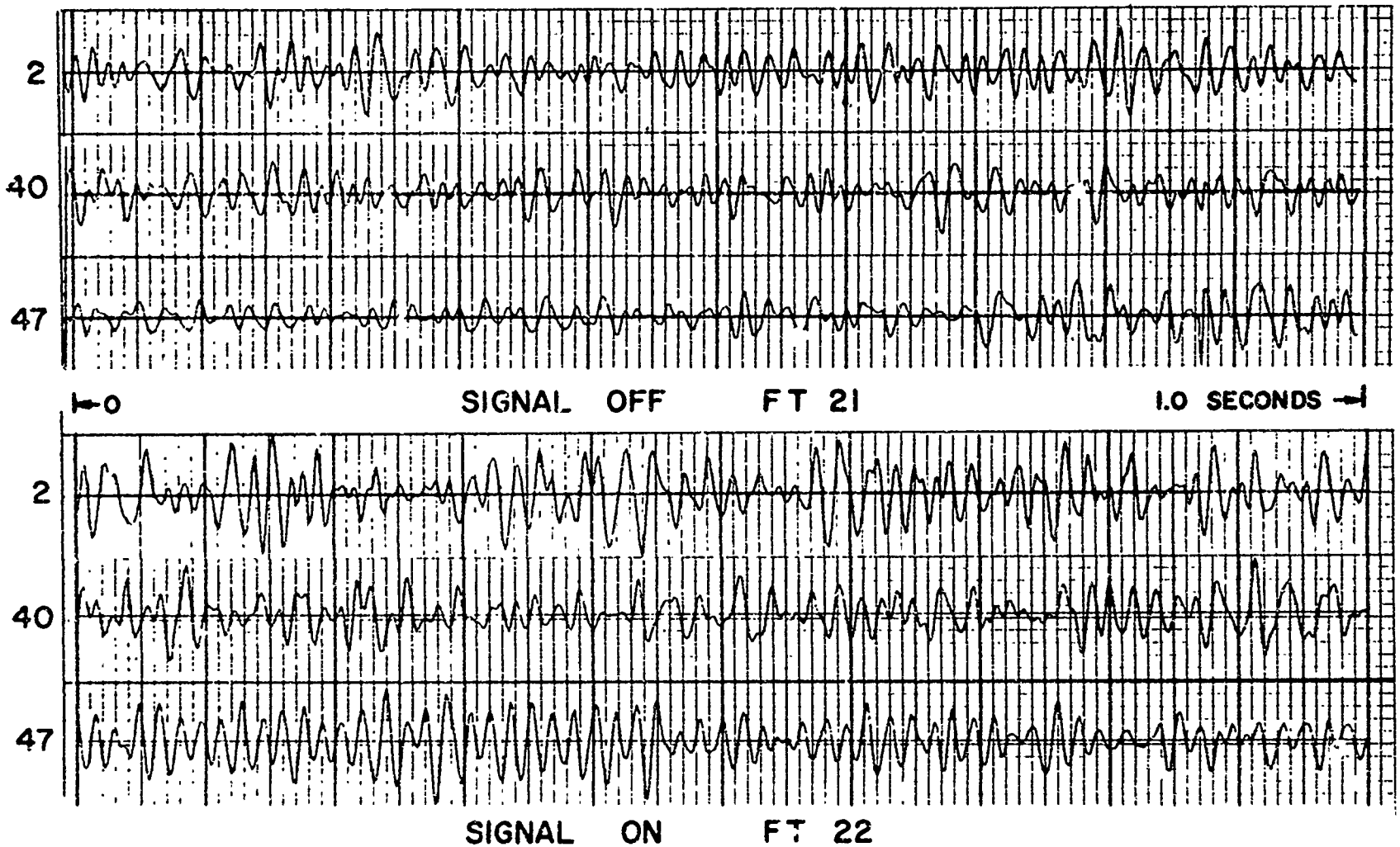

TRACE REPRODUCTIONS - RAW DATA

SECo COHERENCE TEST

Figure 12

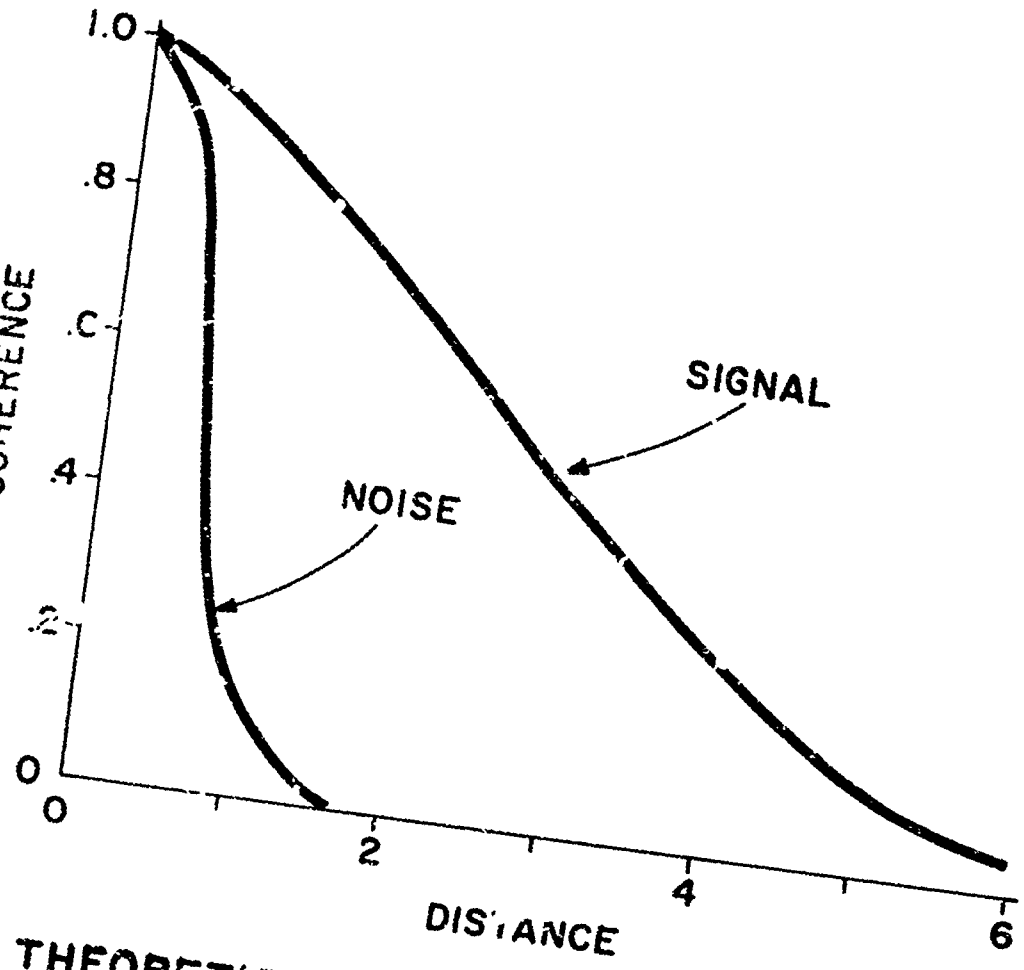

THEORETICAL SIGNAL-NOISE COHERENCE
THREE ELEMENT ARRAY
(AFTER URICK)

Figure 13

G.D.P.C. - COMPUTER PROCESSING DATA FLOW

PROGRAM FUNCTION	*PROGRAM NAME*
REFORMAT/DEMULTIPLEX	SUBEDIT
FILTER; BAND PASS, NARROW BAND, VIBROSEIS, OTHER	SUBFIL
COMPUTE POWER SPECTRUM	POWER TT
CROSS CORRELATE	XCOR
AUTOCORRELATE	XCOR BIG
FORMAT RESULTS FOR CALCOMP PEN PLOT	PLOT AUTO, SUBPLOT

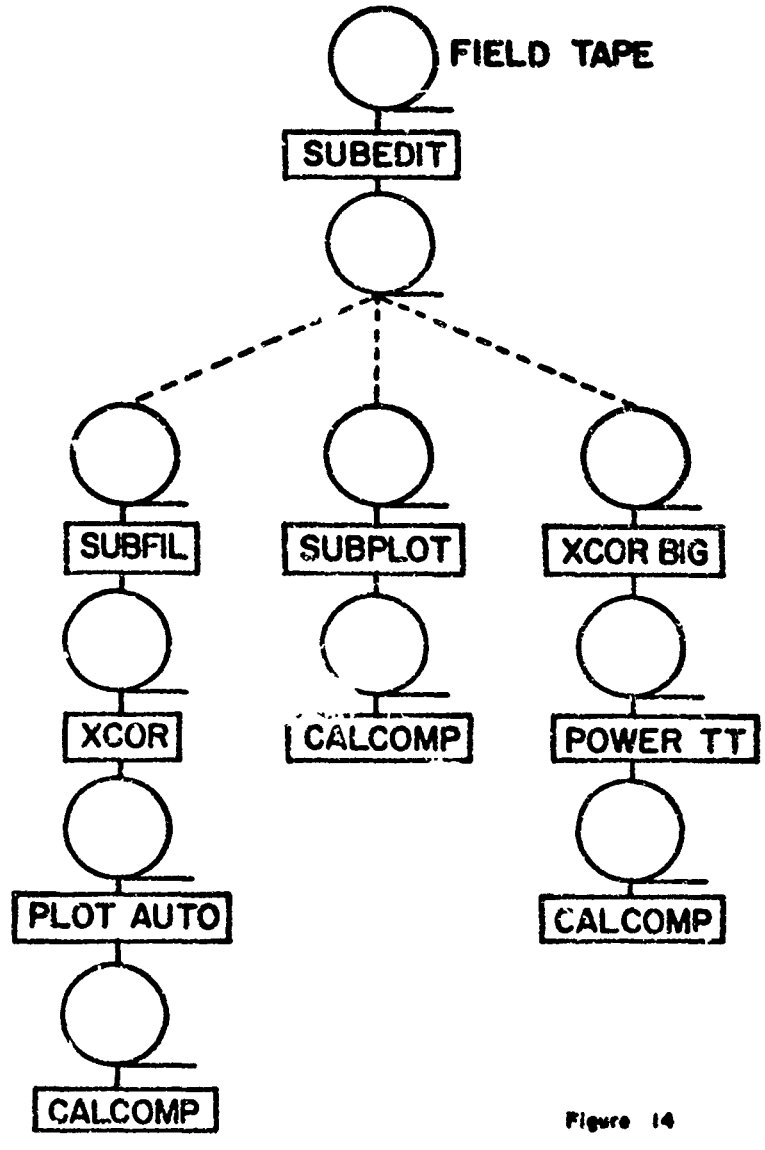

Figure 14

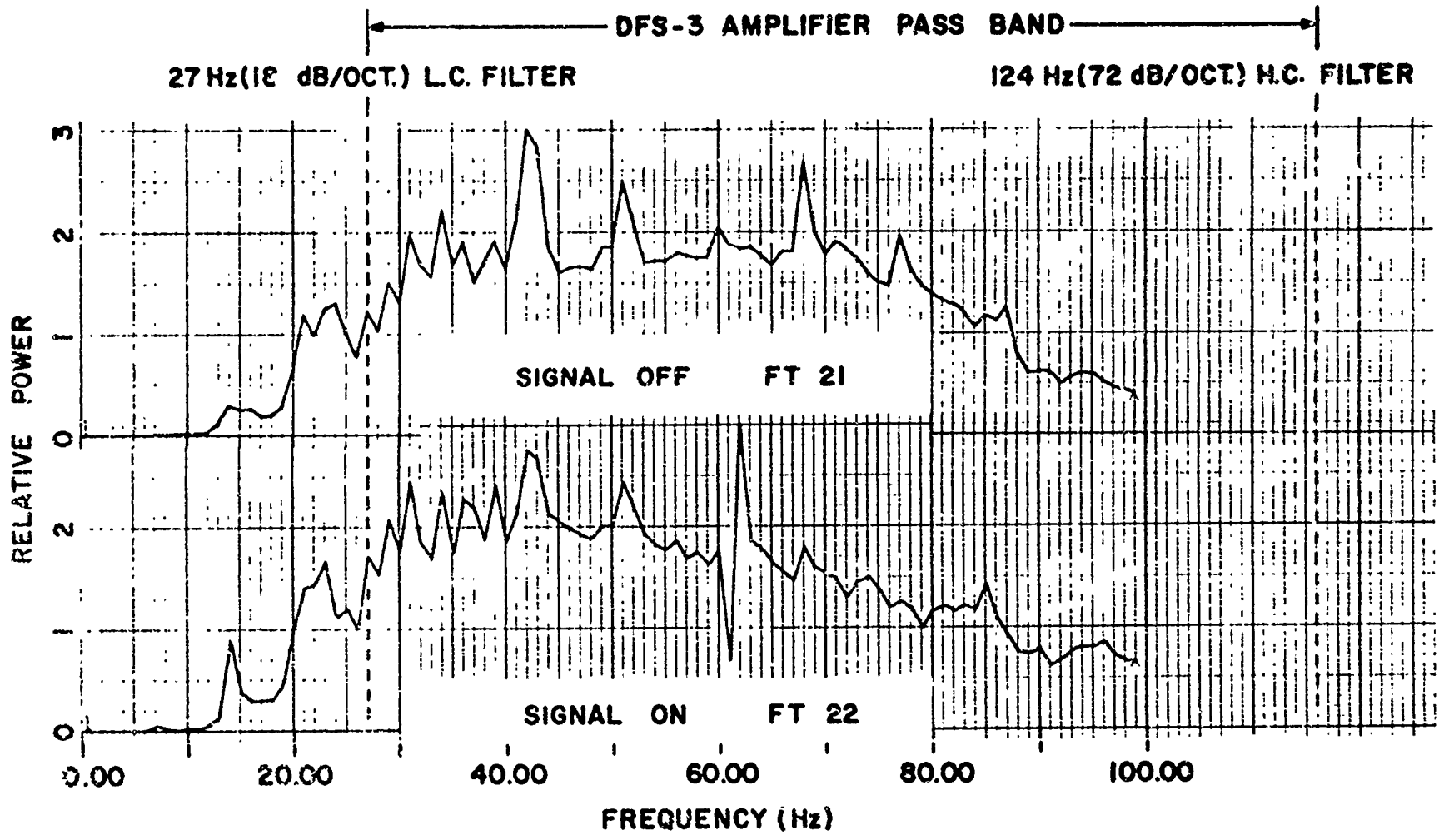

TYPICAL POWER SPECTRA PLOTS

SECo COHERENCE TEST

Figure 15

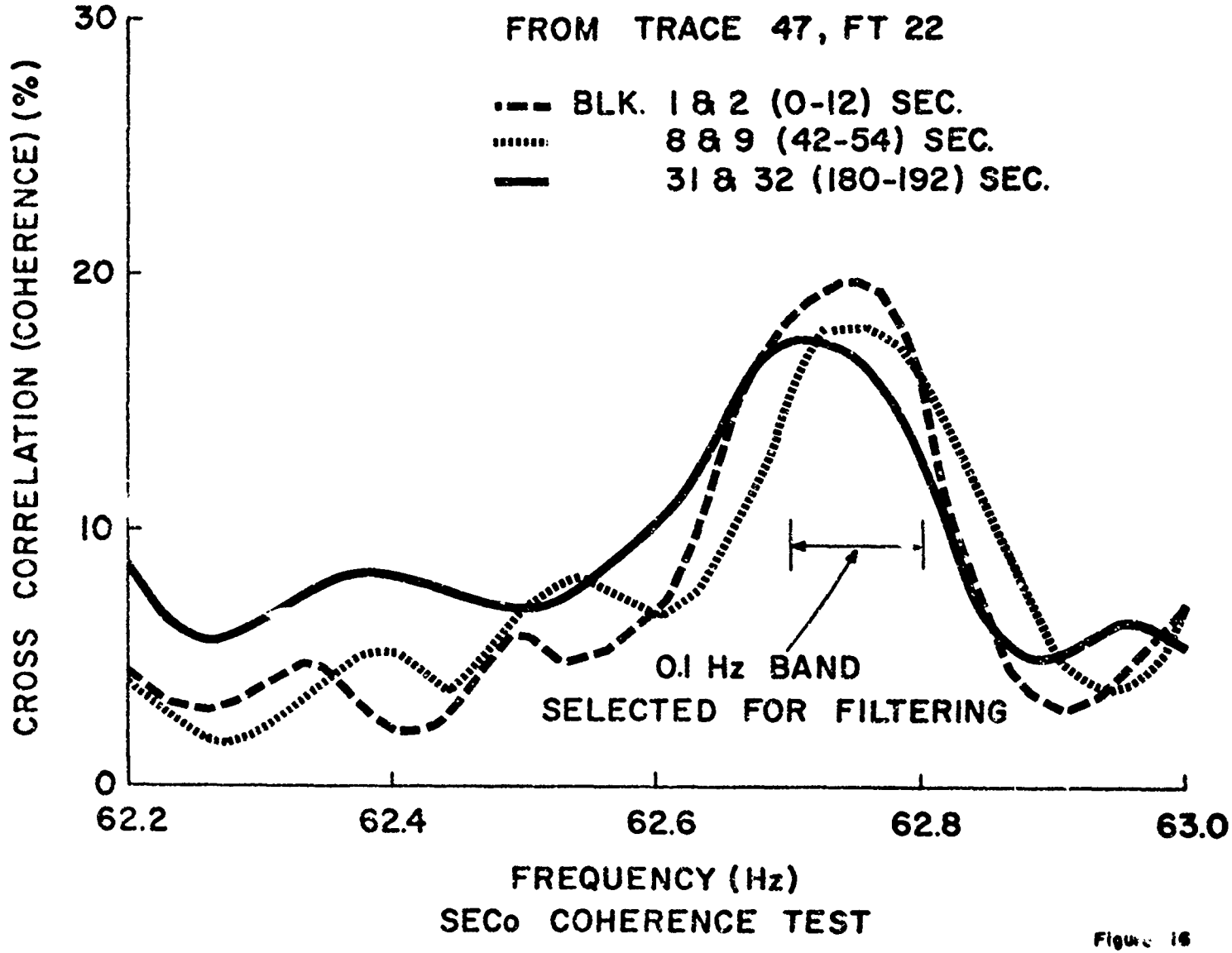
SOURCE FREQUENCY DETERMINATION
FROM TRACE 47, FT 22
BLK. 1 & 2 (0-12) SEC.
8 & 9 (42-54) SEC.
31 & 32 (180-192) SEC.
CROSS CORRELATION (COHERENCE) (%)
30
20
10
0
0.1 Hz BAND
SELECTED FOR FILTERING
62.2
62.4
62.6
62.8
63.0
FREQUENCY (Hz)
SECo COHERENCE TEST

Figure 16

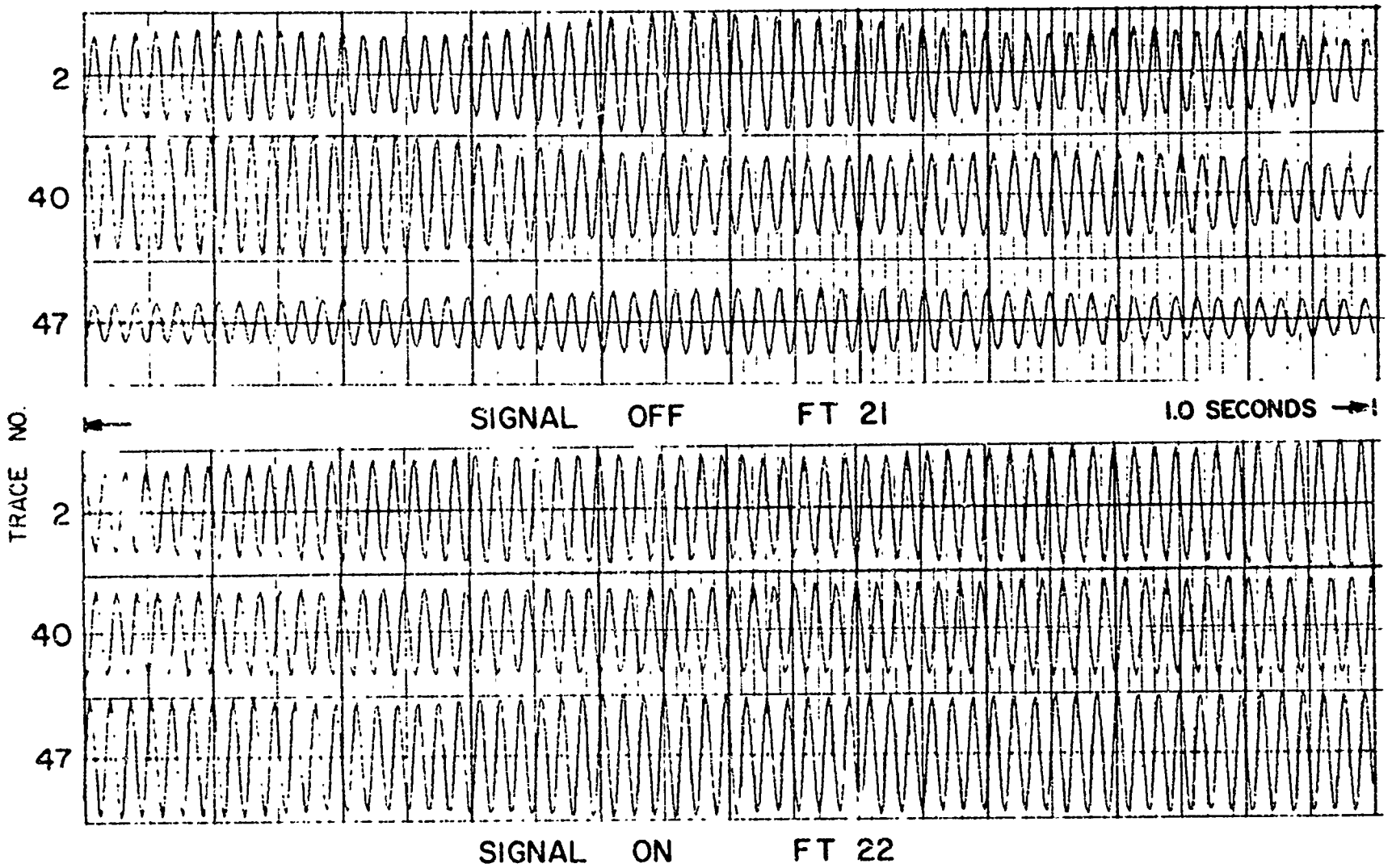

TRACE REPRODUCTION - FILTERED DATA (62.70-62.80 Hz)

SECo COHERENCE TEST

Figure 17

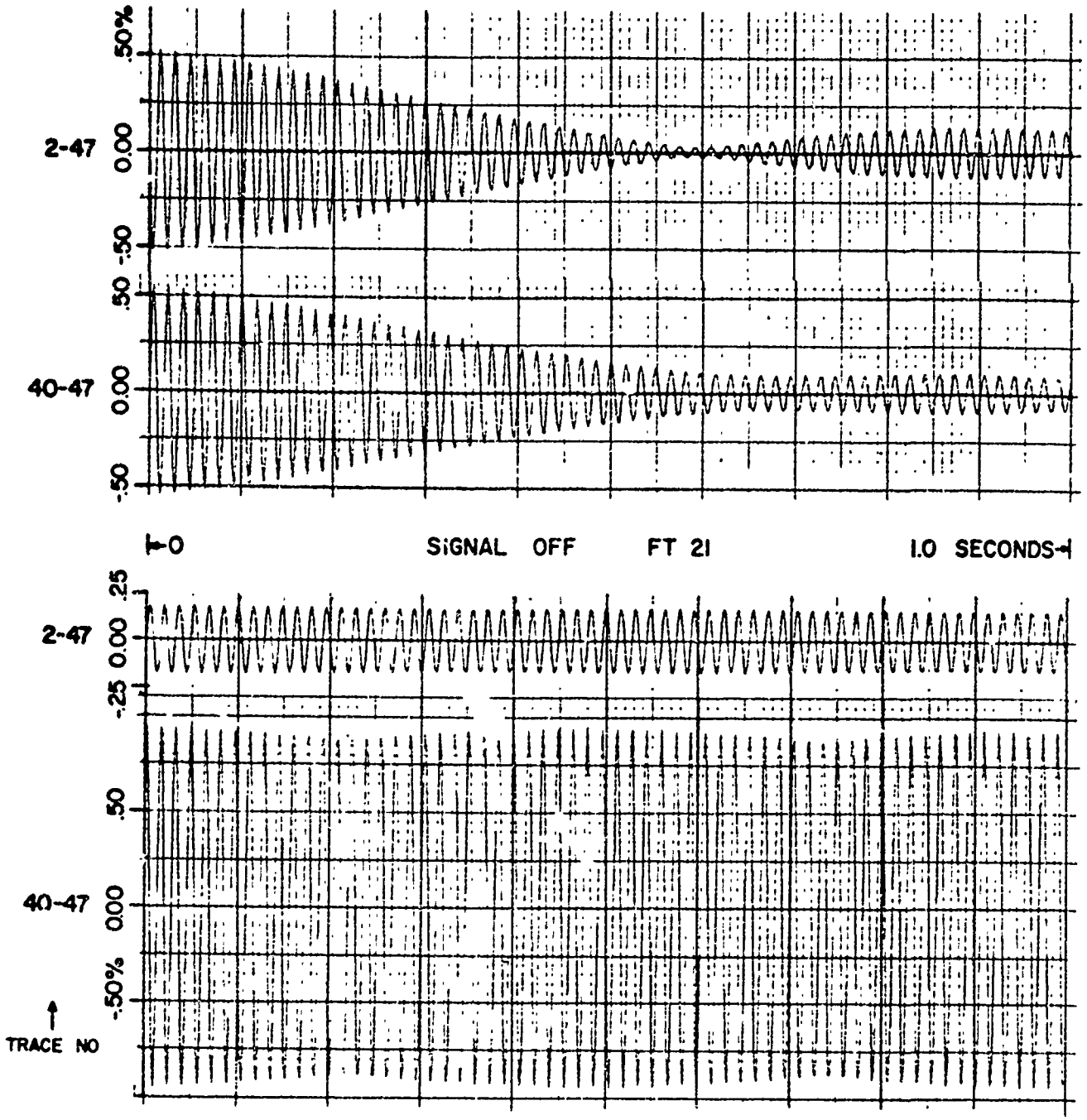

CROSS CORRELATION

SECo COHERENCE TEST

Figure 18

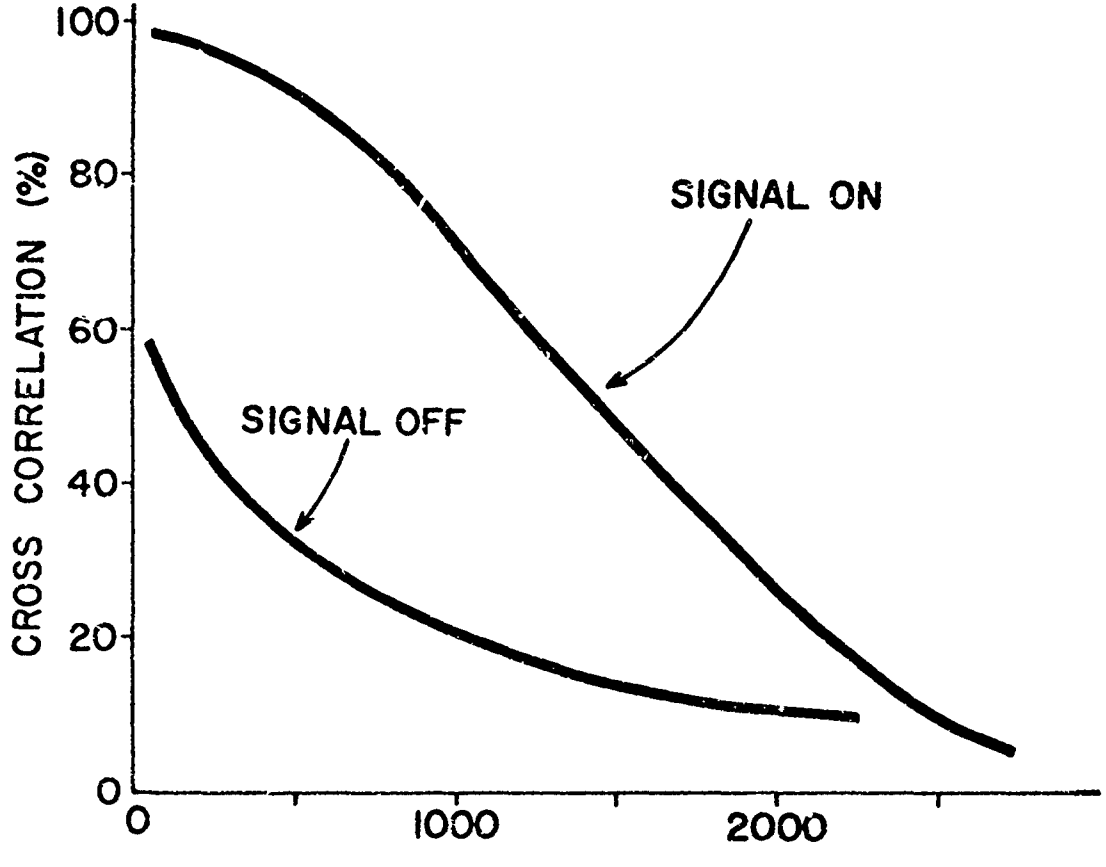

SIGNAL & NOISE COHERENCE
48 ELEMENT SECo ARRAY

Figure 19

BAY OF BISCAY SIGNAL AND NOISE COHERENCE - 48 Element SECo Array

Source Receiver Separation- 15 Miles

Field Tape # 03,04 (on, off)

o- - - - - - - - - - o Optimized Pairs, On

o———————o Standard Pairs, On

x- - - - - - - - - - - x Signal Off

Fig. 20

BAY OF BISCAY SIGNAL AND NOISE COHERENCE - 48 Element SECo Array

Source Receiver Separation- 15 Miles
Field Tape # 05, 06 (On, Off)
Optimized Pairs, On
Standard Pairs, On
Signal Off

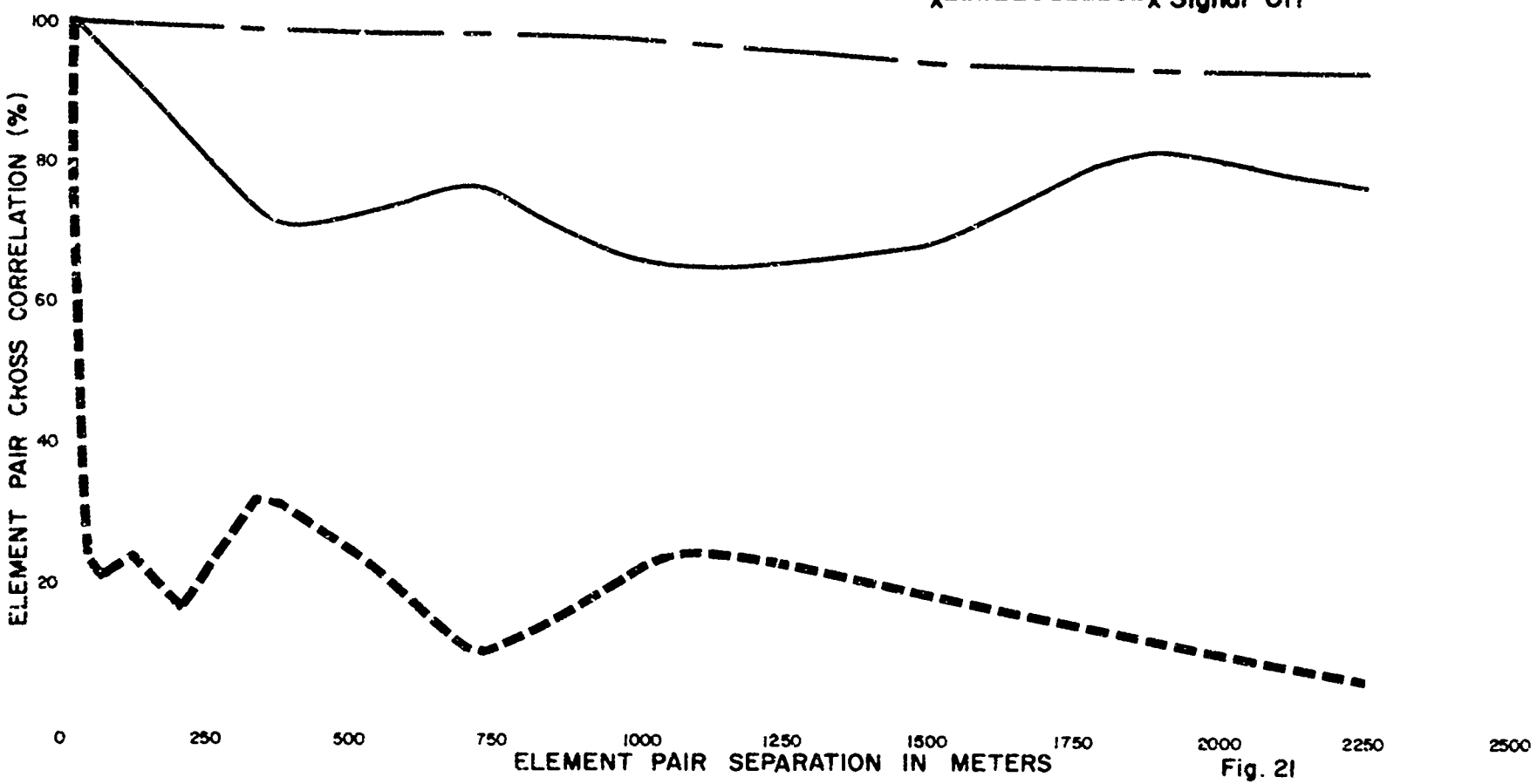

Fig. 21

BAY OF BISCAY SIGNAL AND NOISE COHERENCE - 48 Element SECo Array

Source Receiver Separation- 30 Miles

Field Tape # 20, 21 (On, Off)

o- - - - - - - - o Optimized Pairs, On

o———————o Standard Pairs, On

x- - - - - - - - - - - x Signal Off

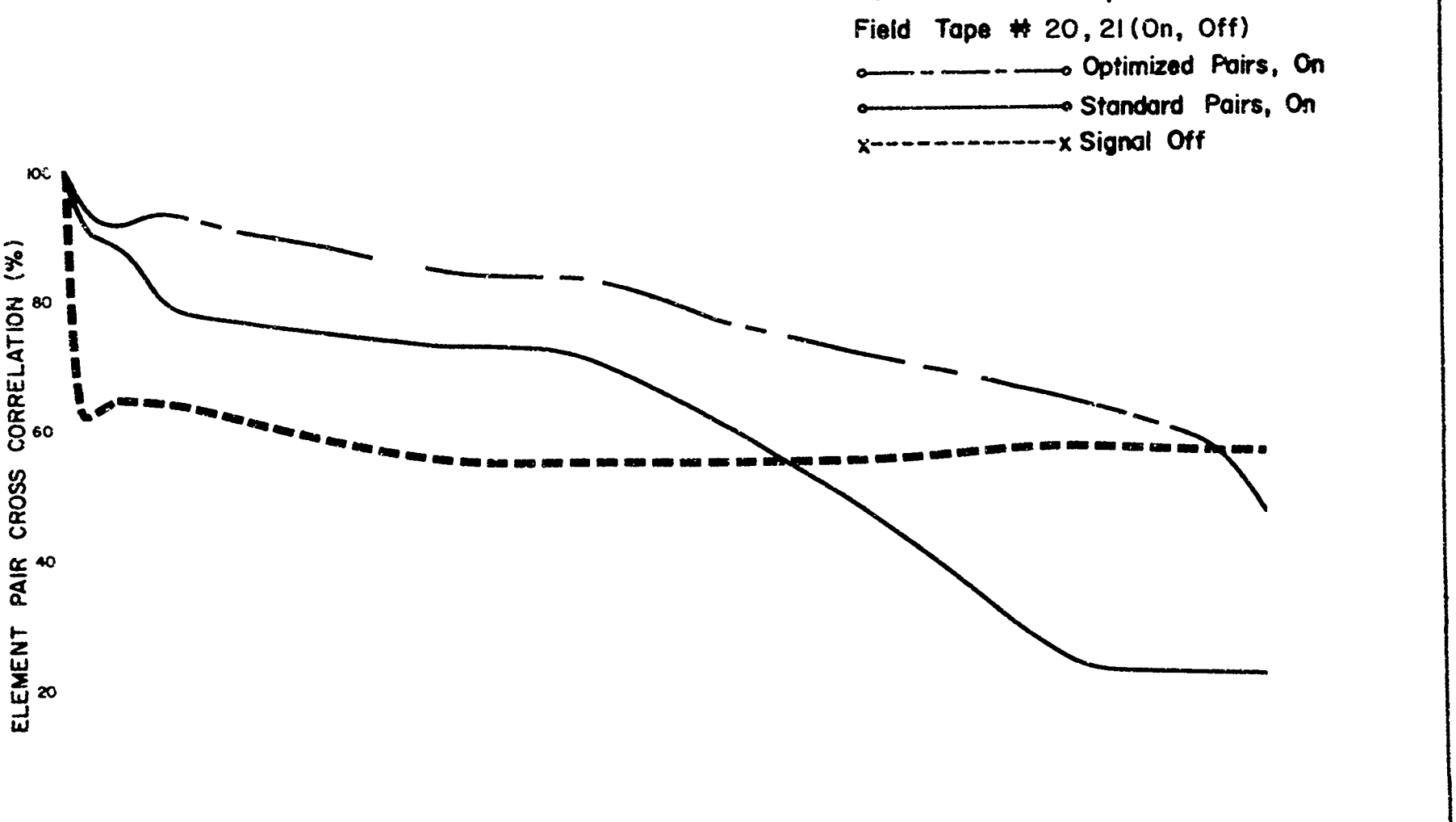

Fig. 22

BAY OF BISCAY SIGNAL AND NOISE COHERENCE - 48 Element SECo Array

Source Receiver Separation- 30 Miles
Field Tape # 22,23 (ON, OFF)
o— - — - —o Optimized Pairs, On
o————————o Standard Pairs, On
x----------x Signal Off

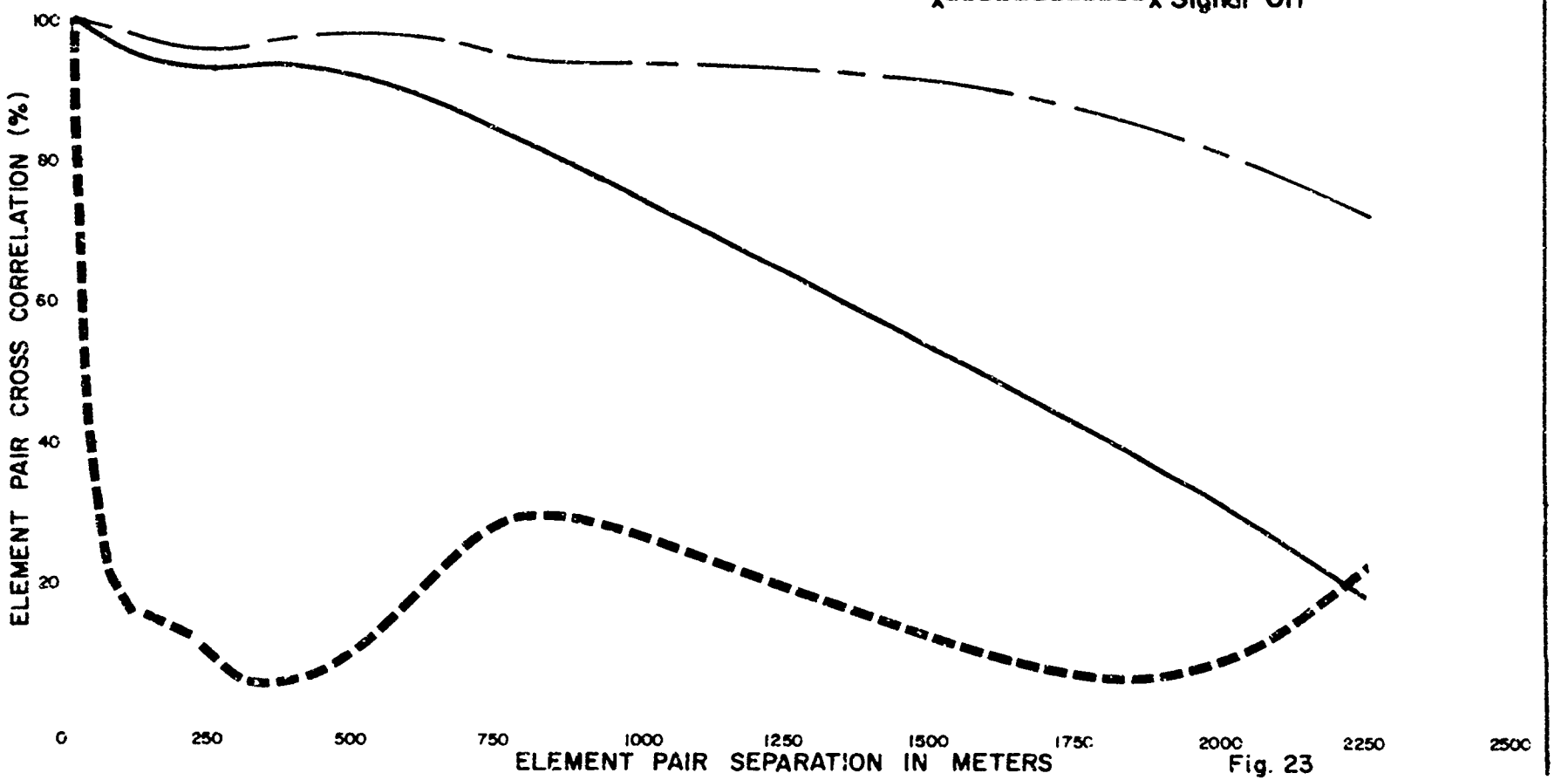

Fig. 23

BAY OF BISCAY SIGNAL AND NOISE COHERENCE - 48 Element SECo Array

Source Receiver Separation- 30 Miles
Field Tape # 24 (On Only)
o— - — - —o Optimized Pairs, On
o————————o Standard Pairs, On
x----------x Signal Off

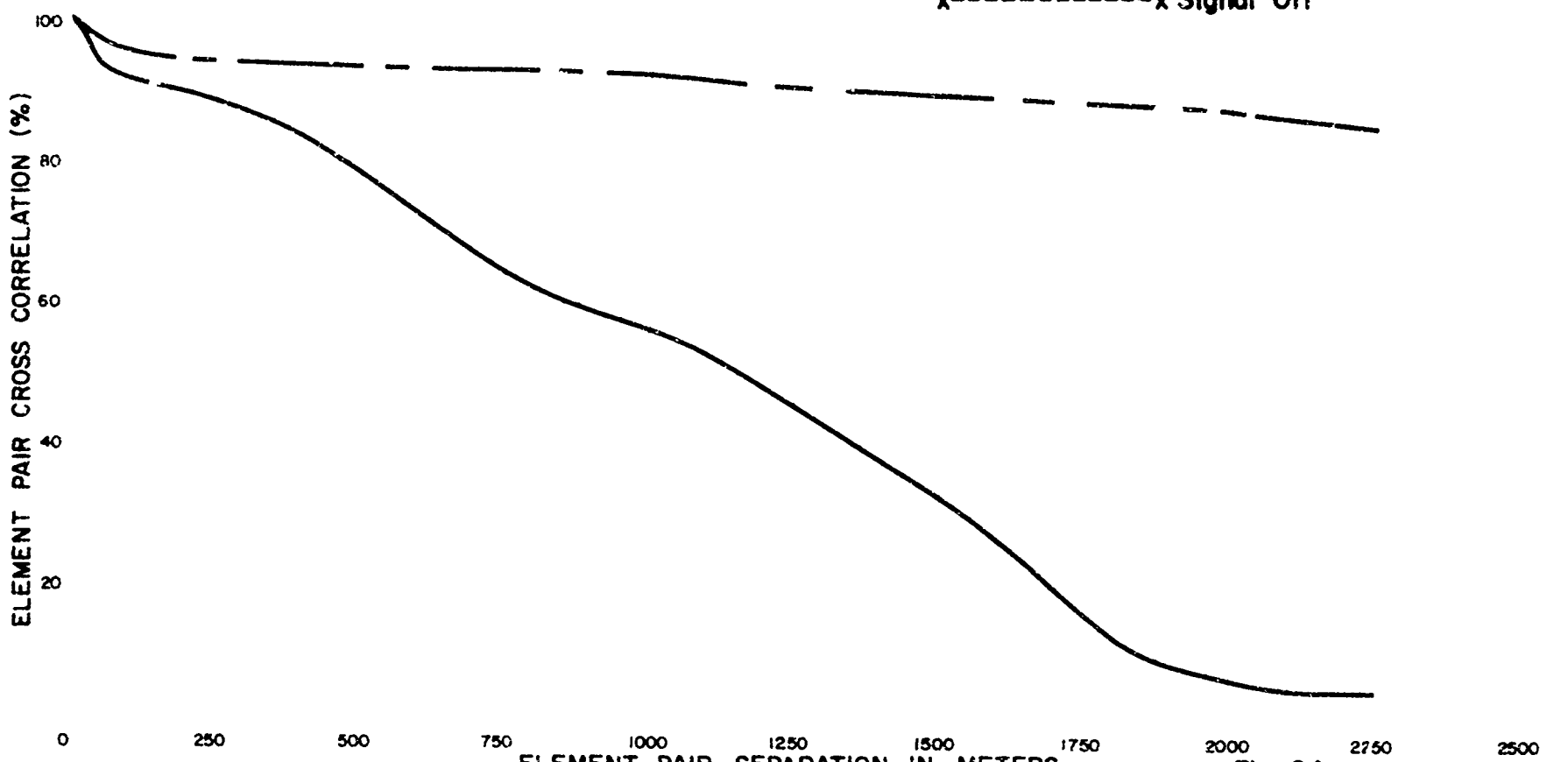

Fig. 24

BAY OF BISCAY SIGNAL AND NOISE COHERENCE - 48 Element SECo Array

Source Receiver Separation- 30 Miles

Field Tape # 66,69 (On, Off)

o- - - - - - - - o Optimized Pairs, On

o———————o Standard Pairs, On

x- - - - - - - - - - - x Signal Off

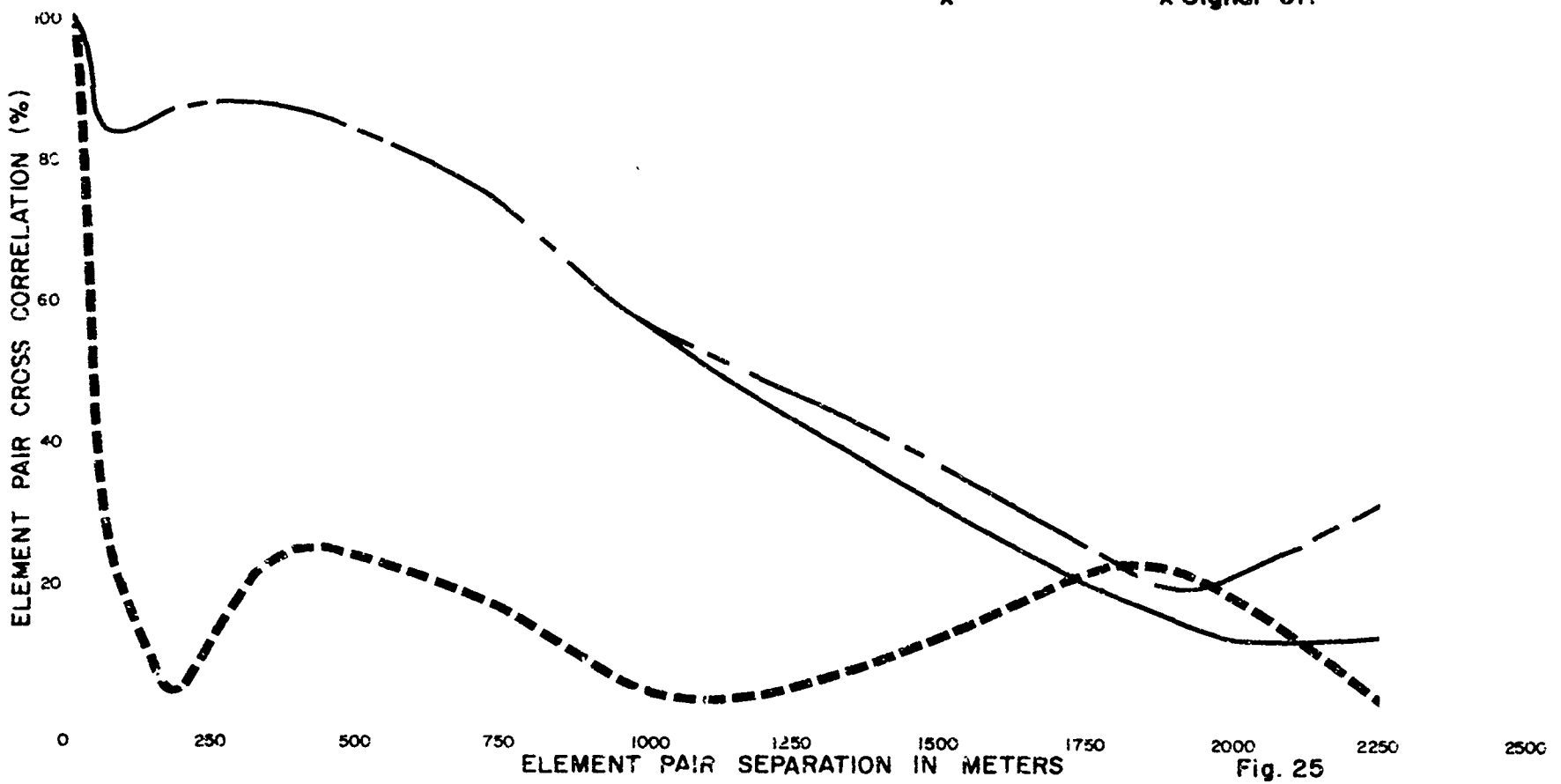

Fig. 25

BAY OF BISCAY SIGNAL AND NOISE COHERENCE - 48 Element SECo Array

Source Receiver Separation- 30 Miles

Field Tape # 67, 70 (On, Off)

Optimized Pairs, On

Standard Pairs, On

Signal Off

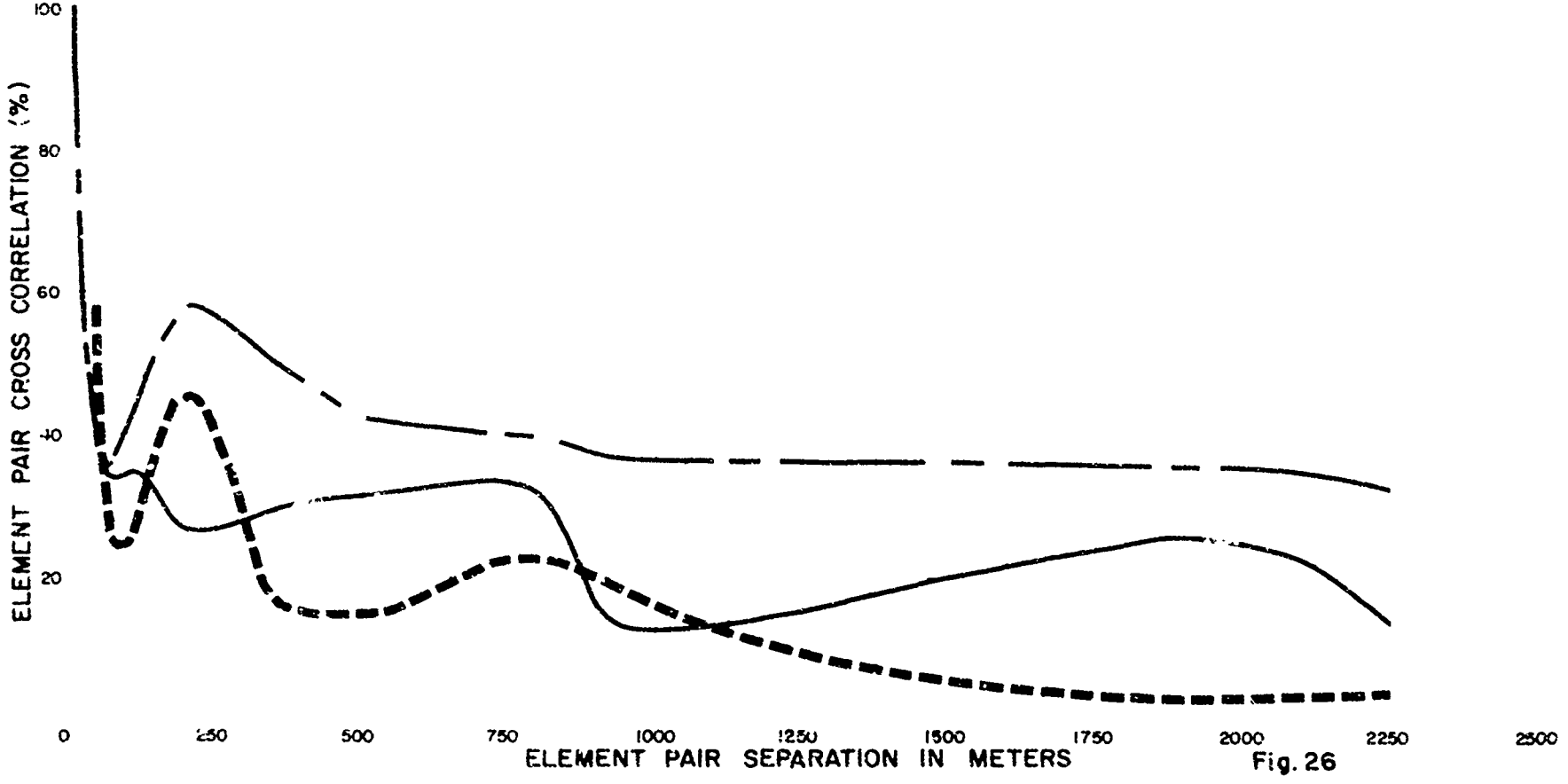

Fig. 26

BAY OF BISCAY SIGNAL AND NOISE COHERENCE - 48 Element SECo Array

Source Receiver Separation- 45 Miles

Field Tape # 32, 33 (On, Off)

o- - - - - - - - o Optimized Pairs, On

o———————o Standard Pairs, On

x---------x Signal Off

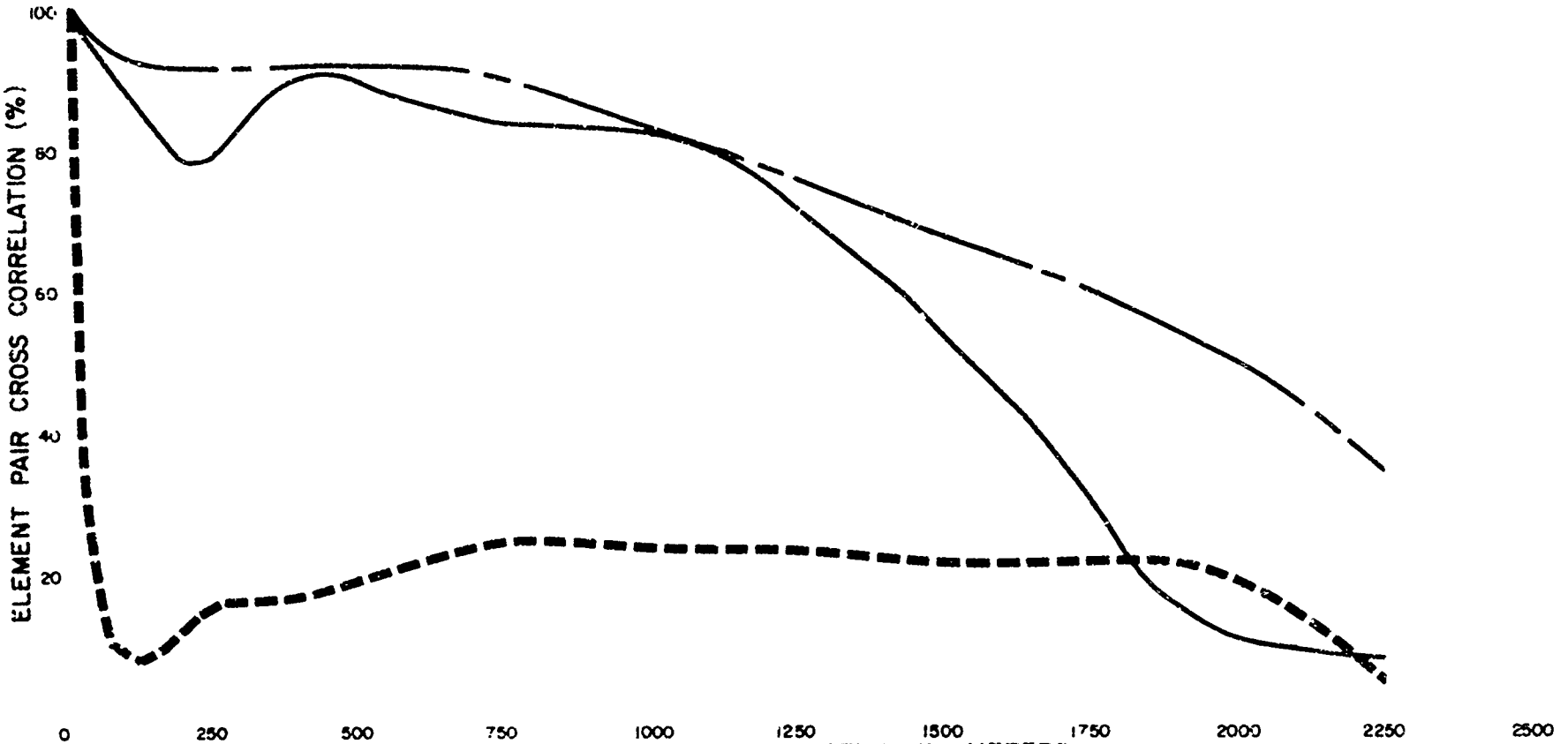

Fig. 27

BAY OF BISCAY SIGNAL AND NOISE COHERENCE - 48 Element SECo Array

Source Receiver Separation- 60 Miles

Field Tape # 44, 46 (ON, OFF)

o——— - ——— - ———o Optimized Pairs, On

o——————————o Standard Pairs, On

x----------x Signal Off

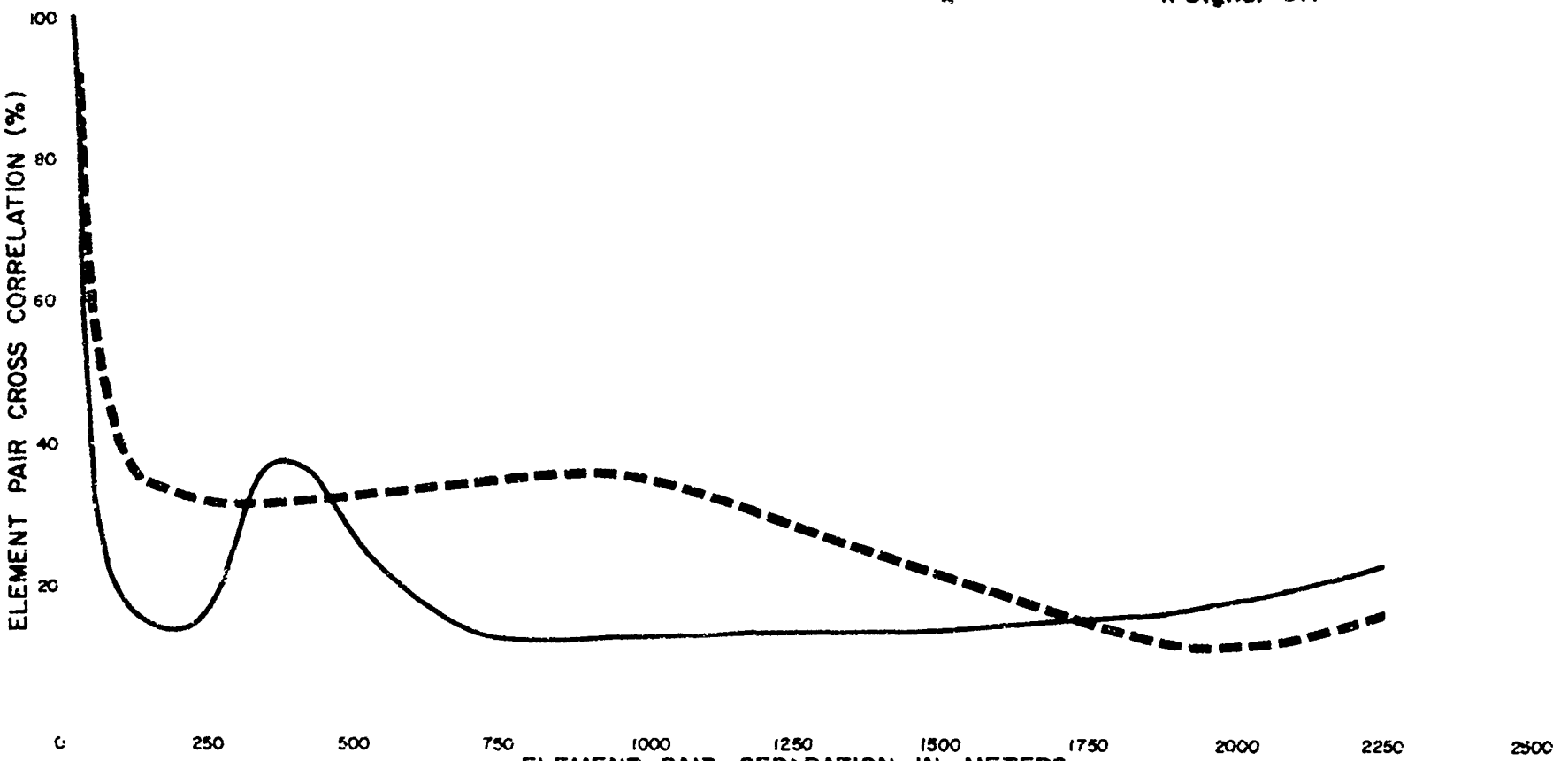

Fig. 28

BAY OF BISCAY SIGNAL AND NOISE COHERENCE - 48 Element SECo Array

Source Receiver Separation- 60 Miles

Field Tape # 47, 49 (ON, OFF)

o- - - - - - - - o Optimized Pairs, On

o———————— o Standard Pairs, On

x---------- x Signal Off

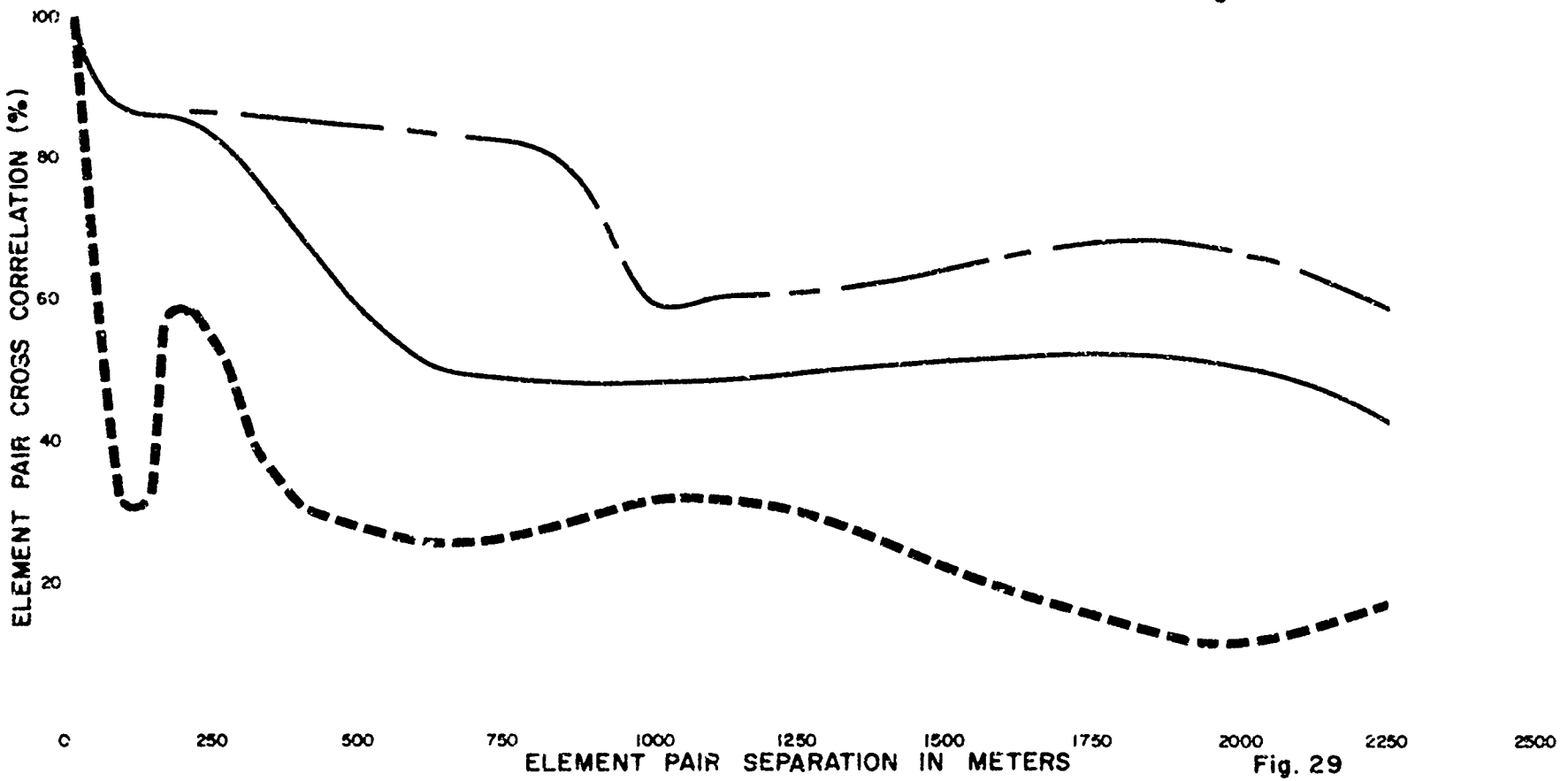

Fig. 29

BAY OF BISCAY SIGNAL AND NOISE COHERENCE - 48 Element SECo Array

Source Receiver Separation- 60 Miles
Field Tape # 50, 51 (ON, OFF)
o——— - ———o Optimized Pairs, On
o———·———o Standard Pairs, On
x----------x Signal Off

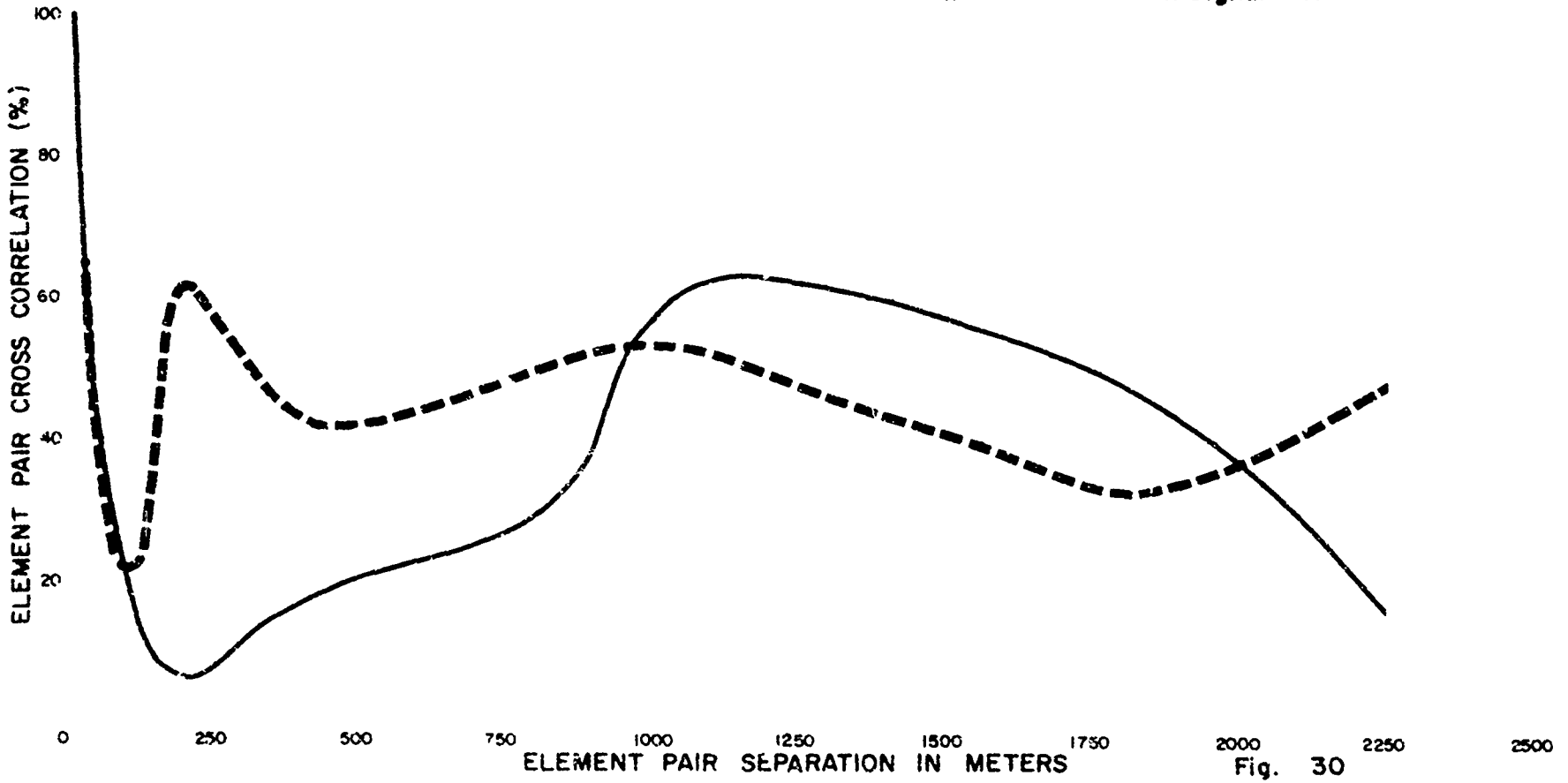

Fig. 30

BAY OF BISCAY – SIGNAL COHERENCE VARIABILITY - OPTIMIZED PAIRS

30 Mile Source - Receiver Separation

Time Lag: FT 20 - FT 24; 32 Minutes
FT 20 - FT 69; 43 Hours
FT 66 - FT 69; 30 Minutes

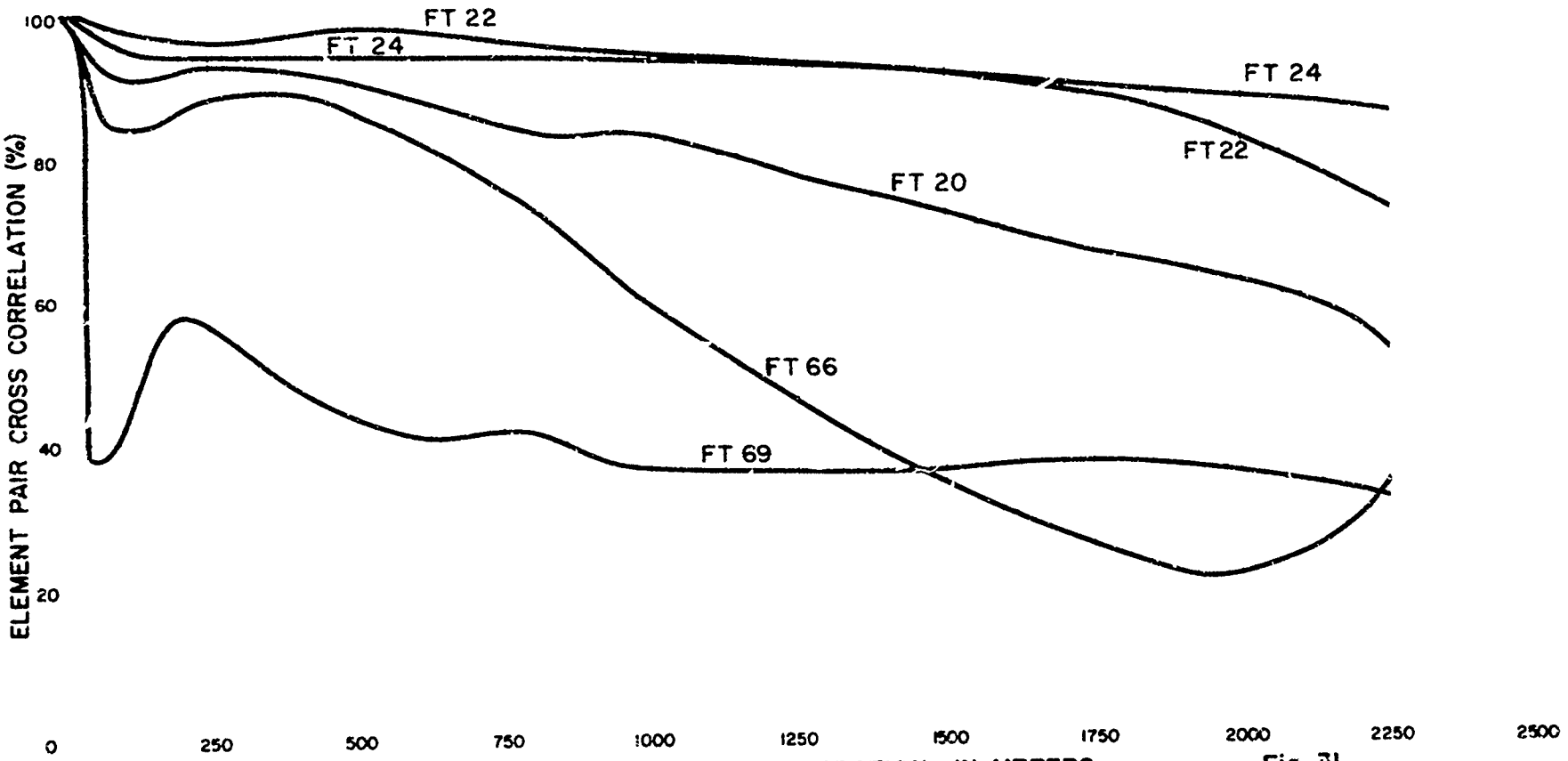

Fig. 31

BAY OF BISCAY — NOISE COHERENCE VARIABILITY

30 Mile Source-Receiver Separation
Time Lag: FT 21 - FT 23; 10 Minutes
FT 69 - FT 70; No Delay
FT 21 - FT 69; 42 Hours

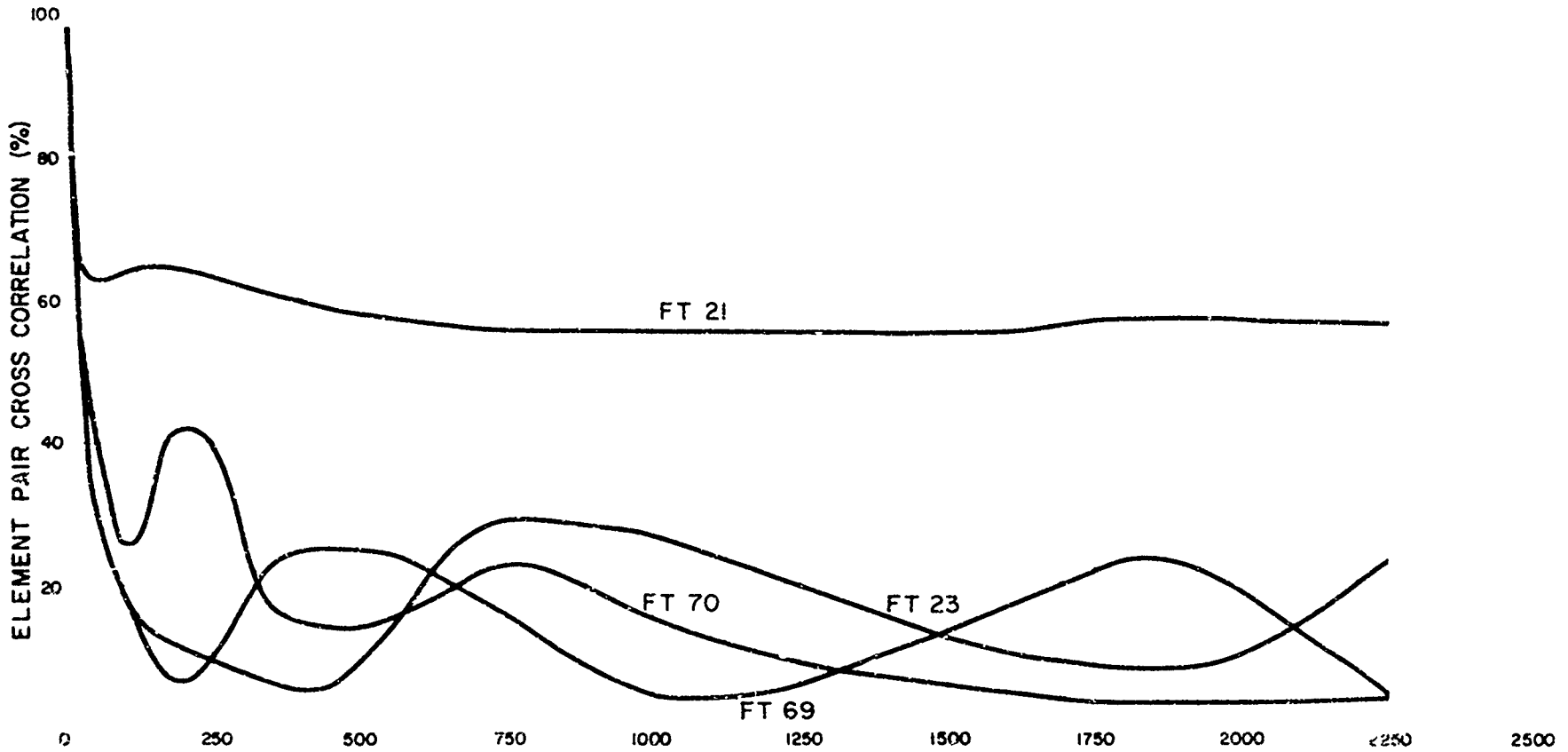

Fig. 32

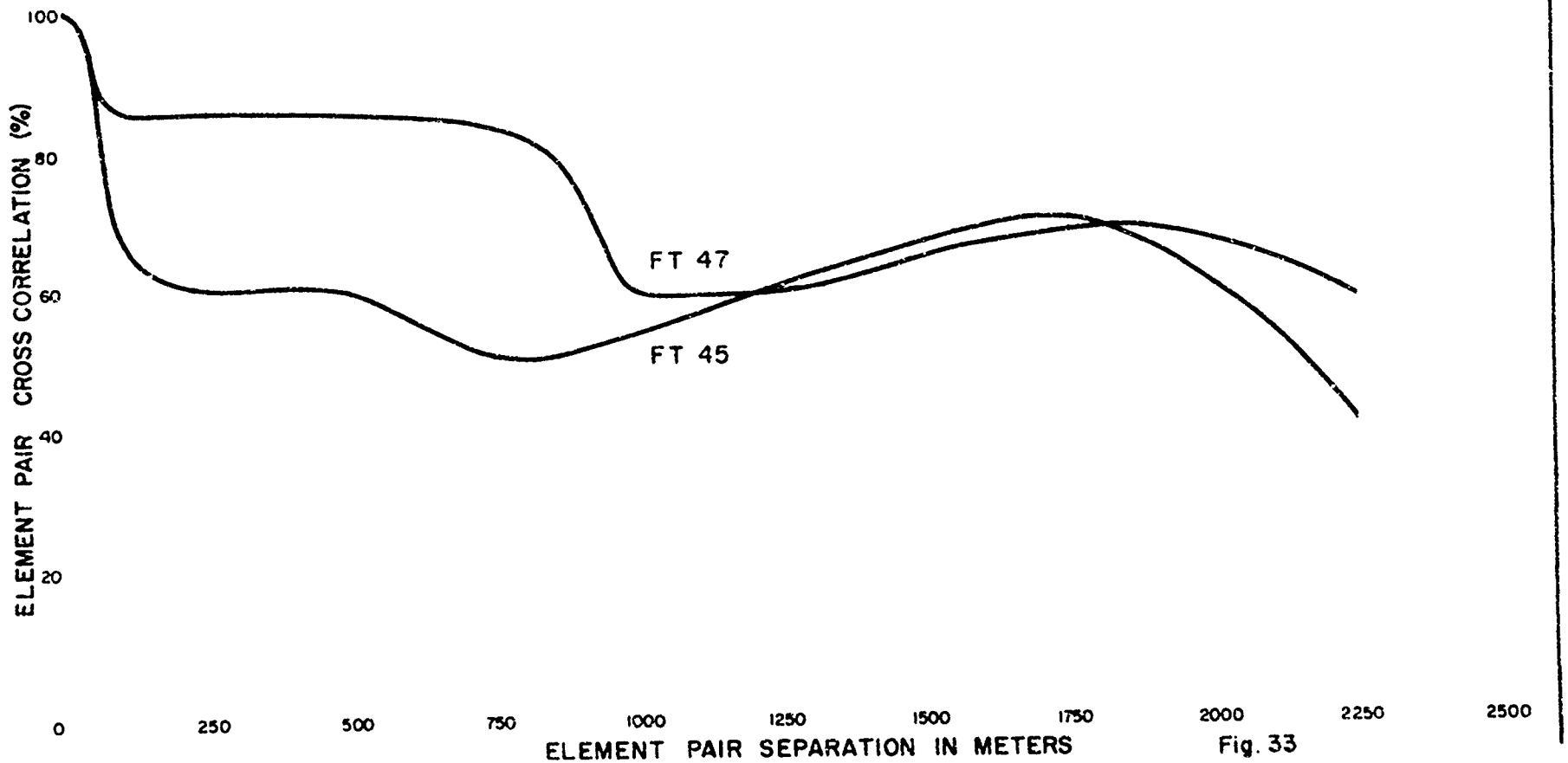
BAY OF BISCAY – SIGNAL COHERENCE VARIABILITY - OPTIMIZED PAIRS
60 Mile Source - Receiver Separation
FT 45 – FT 47
Time Lag: 8 Minutes
ELEMENT PAIR CROSS CORRELATION (%)
100
80
60
40
20
0
FT 47
FT 45
250
500
750
1000
1250
1500
1750
2000
2250
2500
ELEMENT PAIR SEPARATION IN METERS

Fig. 33

BAY OF BISCAY – NOISE COHERENCE VARIABILITY

60 Mile Source-Receiver Separation
Time Lag: FT 44-FT 46; 7 Minutes
FT 49-FT 51; 7 Minutes
FT 44-FT 51; 71 Minutes

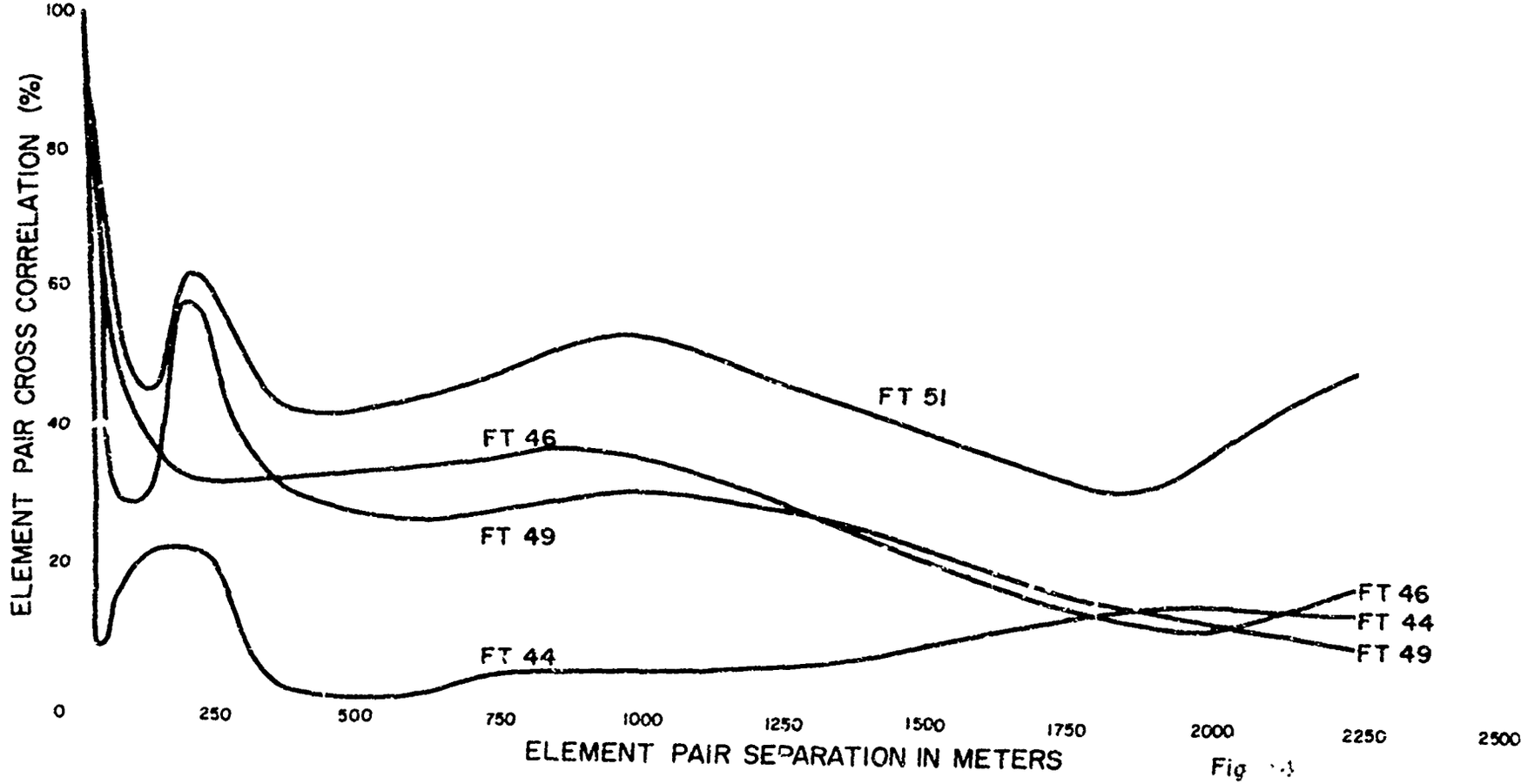

Fig

PROGRAM FUNCTION	PROGRAM NAME	DATA FLOW
Reformat	SUBEDIT	Field Tape
Frequency Domain Transform (FFT)	FOURI	Demultiplexed Traces
Talpey Correlation	TALPEYL	FFT Data

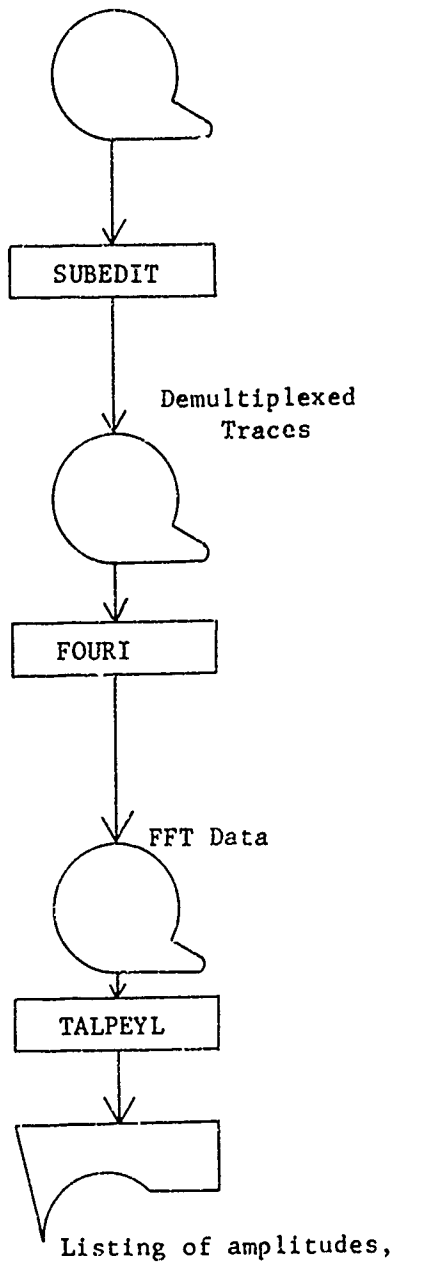

DATA FLOW
TALPEY AMPLITUDE & PHASE CORRELATION

Figure 35

BAY OF BISCAY - TALPEY AMPLITUDE CORRELATION

Signal On (S + N), FT 24

Signal Off (Noise Only), FT 25

< > Average of 8 amplitude values from 3 minutes of data

Fig. 44

BAY OF BISCAY - TALPEY AMPLITUDE & PHASE CORRELATION

Signal On (S + N) - FT 24
Signal Off (Noise Only) FT 25
< > Average of 8 Amplitude & Phase values from 3 minutes of data.

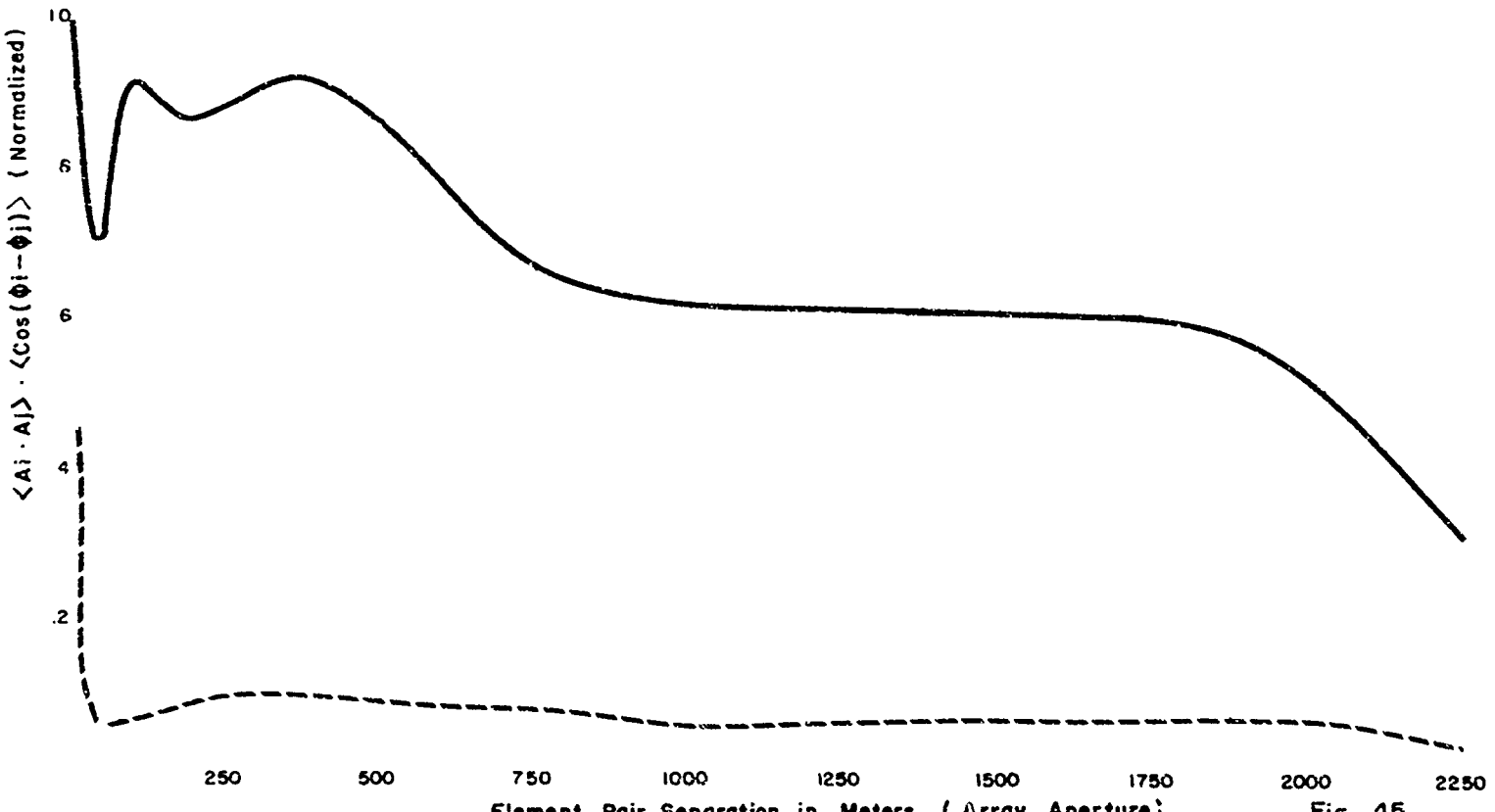

Fig. 45

BAY OF BISCAY - TALPEY AMPLITUDE CORRELATION

Signal On (S + N), FT 66

Signal Off (Noise Only), FT 69

< > Average of 8 amplitude values from 3 minutes of data

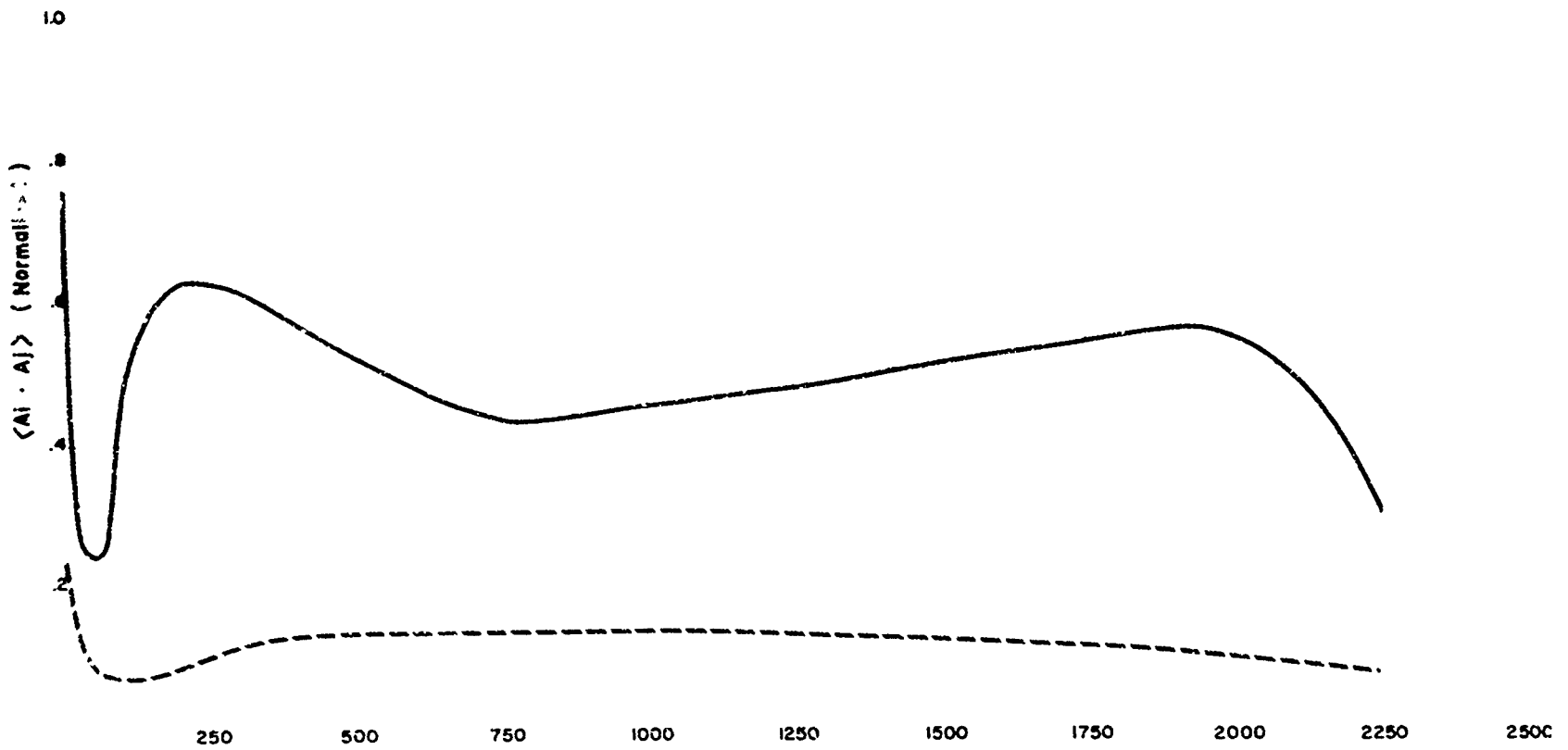

Fig. 46

BAY OF BISCAY - TALPEY AMPLITUDE & PHASE CORRELATION

Signal On (S + N) - FT 66

Signal Off (Noise Only) FT 69

< > Average of 8 Amplitude & Phase values from 3 minutes of data.

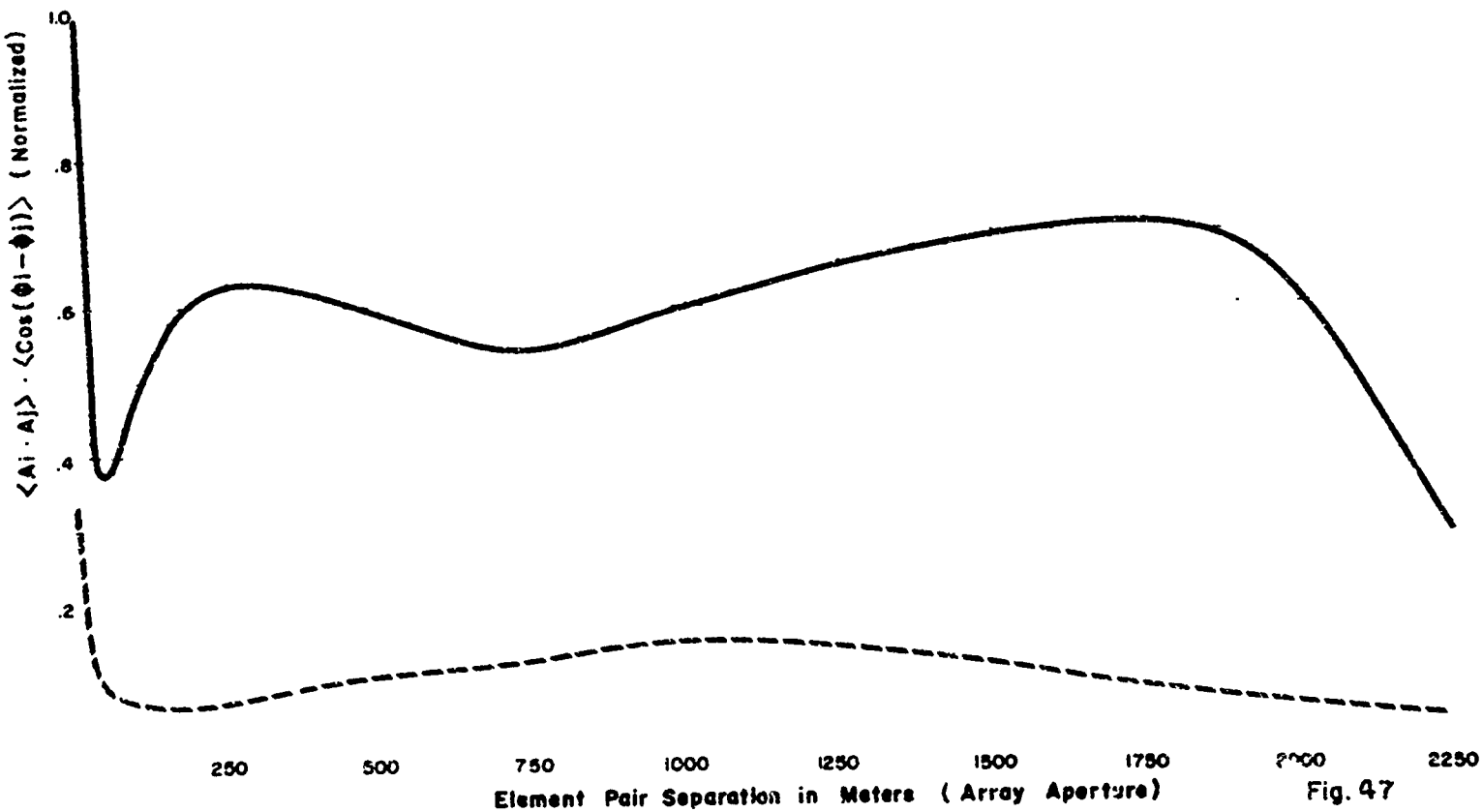

Fig. 47

BAY OF BISCAY - TALPEY AMPLITUDE CORRELATION

Signal On (S + N), FT 67

Signal Off (Noise Only), FT 70

< > Average of 8 amplitude values from 3 minutes of data

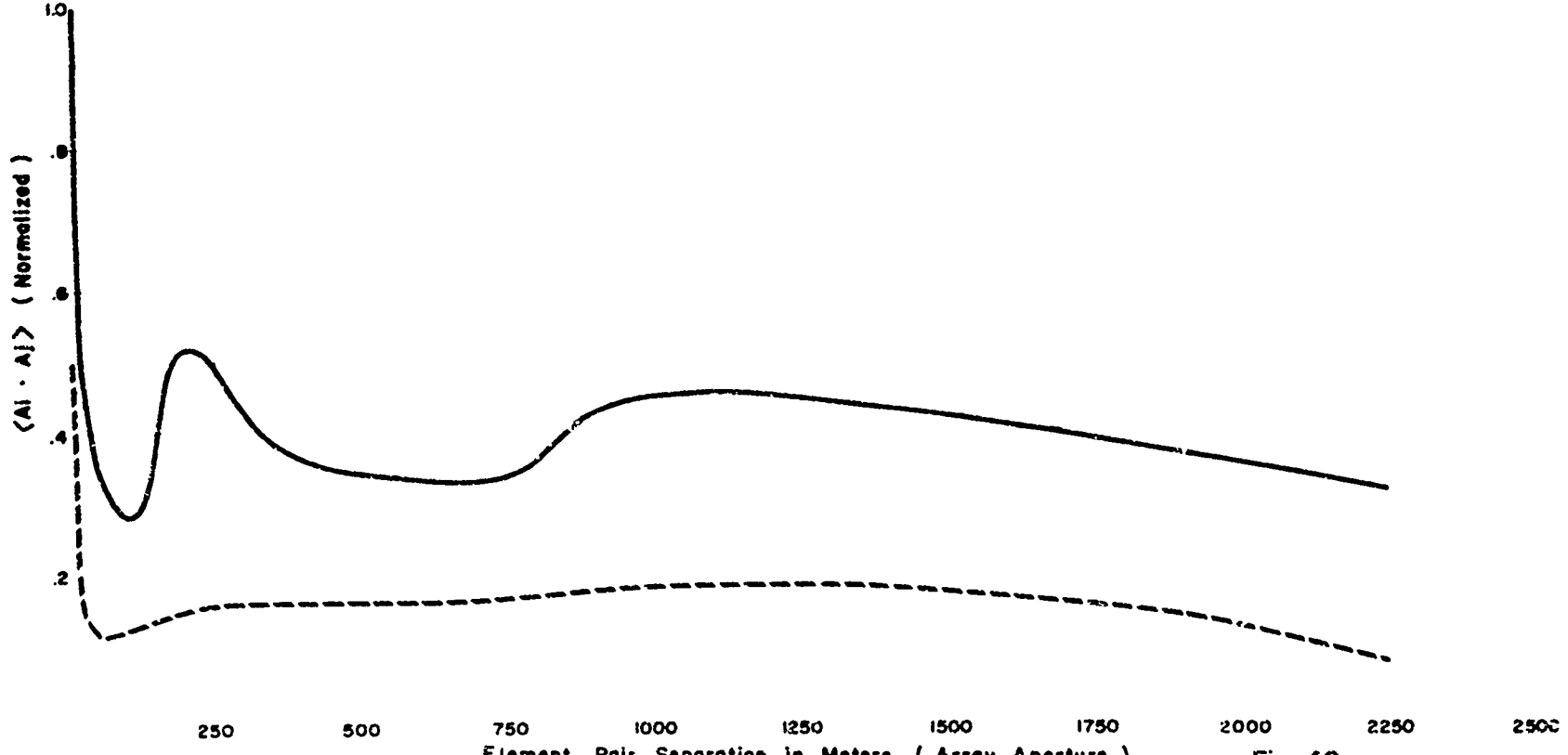

Fig. 48

BAY OF BISCAY - TALPEY AMPLITUDE & PHASE CORRELATION

Signal On (S + N) - FT 67
Signal Off (Noise Only) FT 70
< > Average of 8 Amplitude & Phase values from 3 minutes of data.

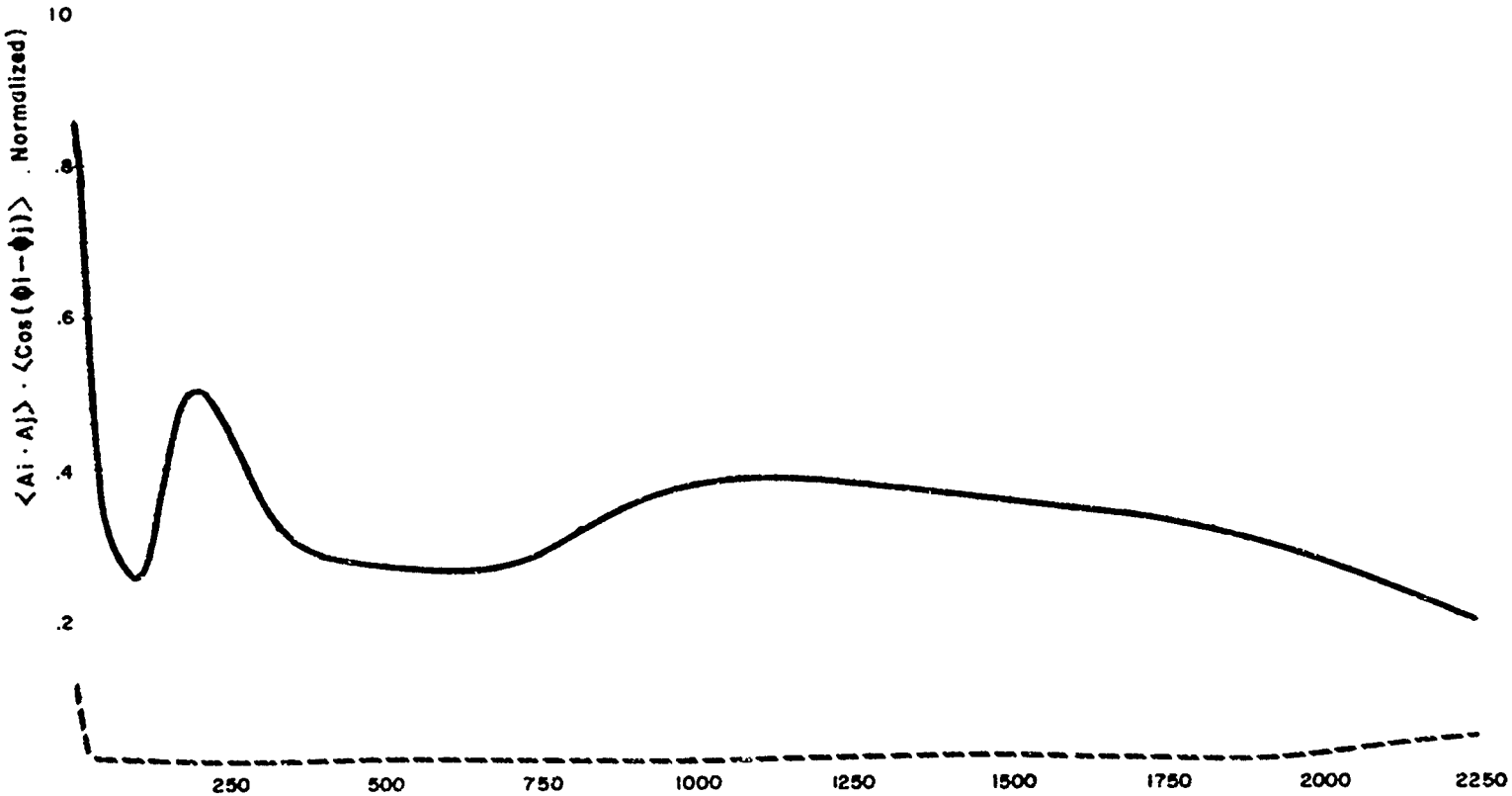

Fig. 49

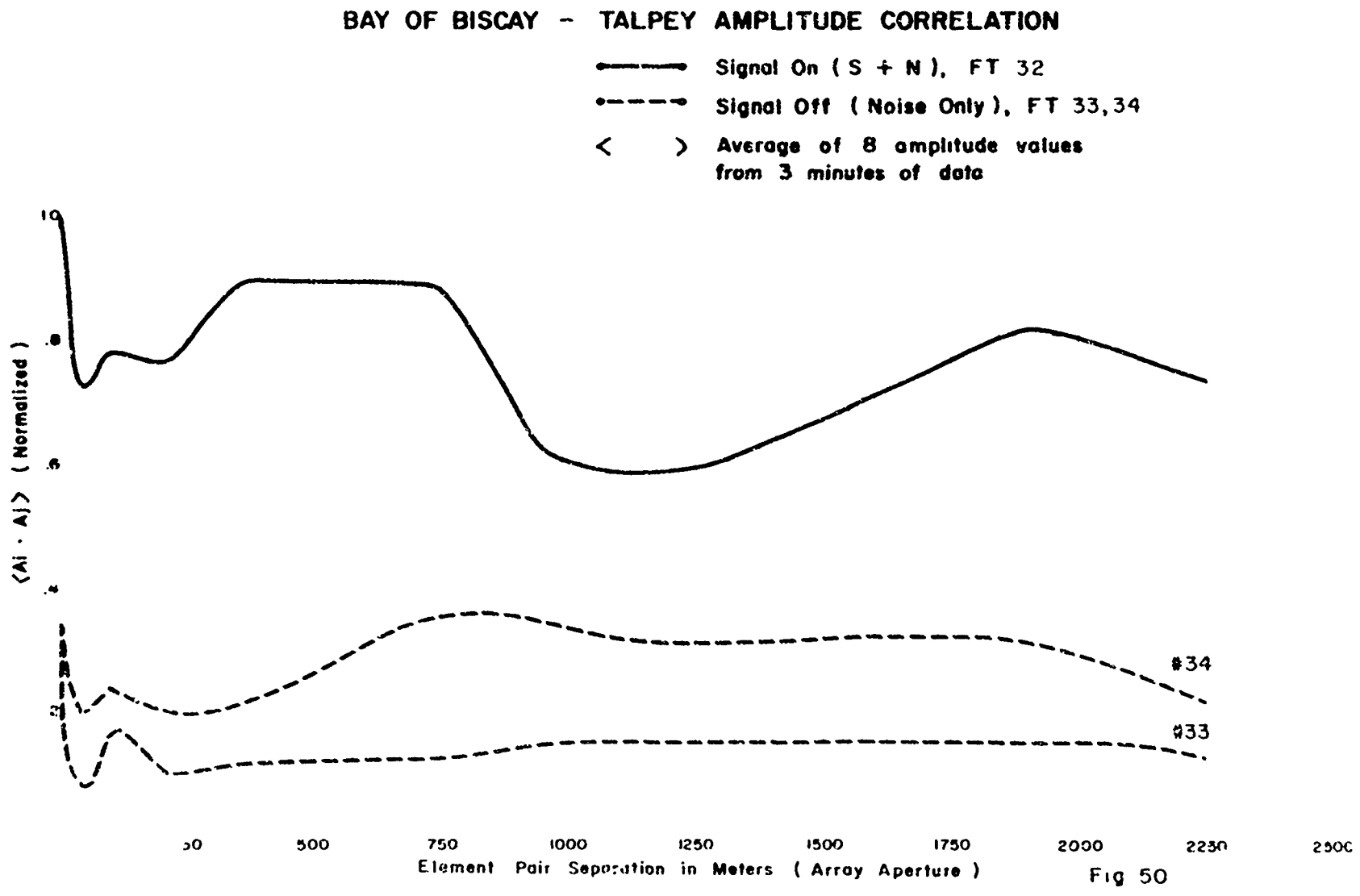
BAY OF BISCAY - TALPEY AMPLITUDE CORRELATION
Signal On (S + N), FT 32
Signal Off (Noise Only), FT 33,34
< > Average of 8 amplitude values from 3 minutes of data
1.0
.8
.6
.4
.2
⟨Ai · Aj⟩ (Normalized)
#34
#33
0
500
750
1000
1250
1500
1750
2000
2250
2500
Element Pair Separation in Meters (Array Aperture)

Fig 50

BAY OF BISCAY - TALPEY AMPLITUDE & PHASE CORRELATION

Signal On (S + N) - FT 32
Signal Off (Noise Only) FT 33, 34
< > Average of 8 Amplitude & Phase values from 3 minutes of data.

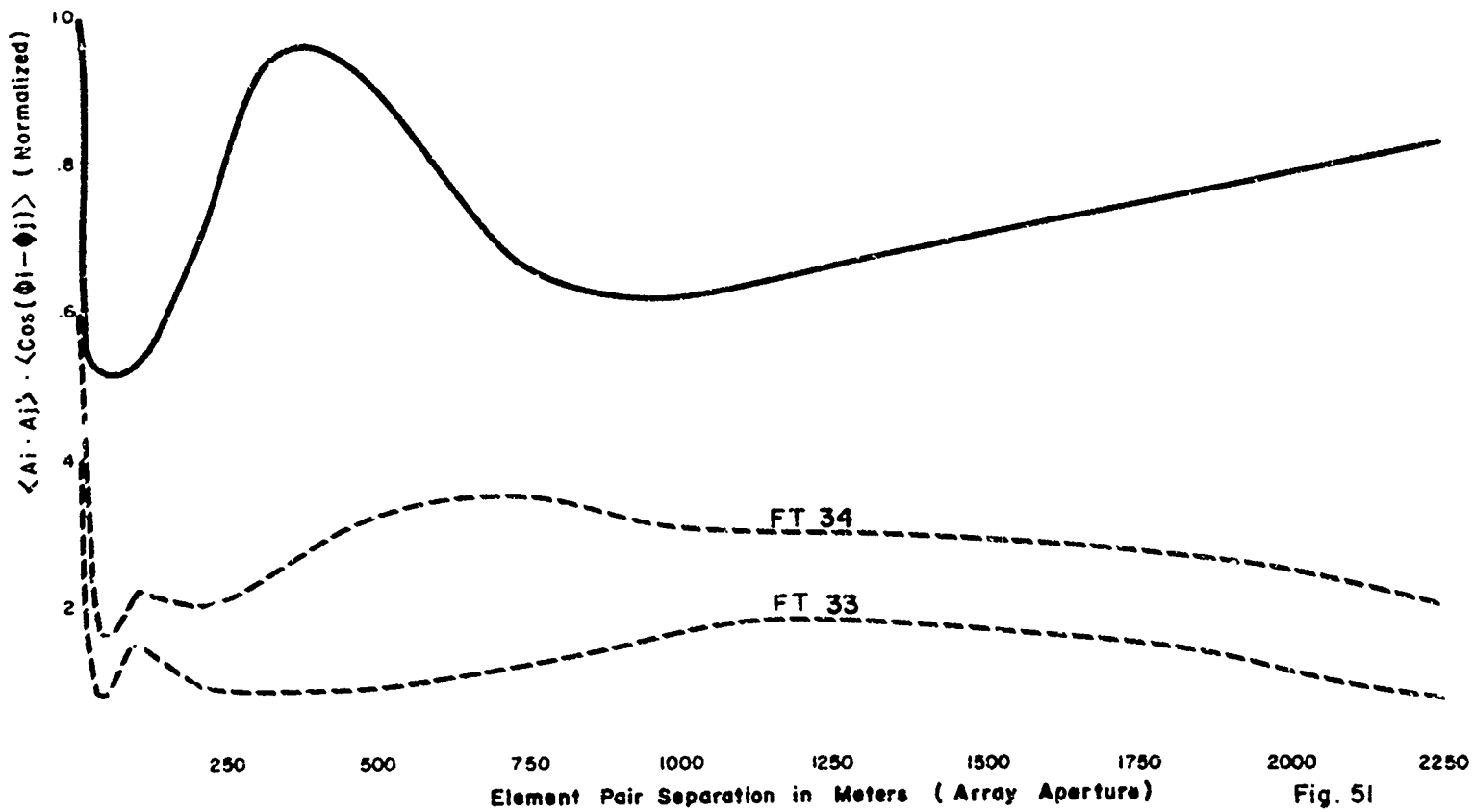

Fig. 51

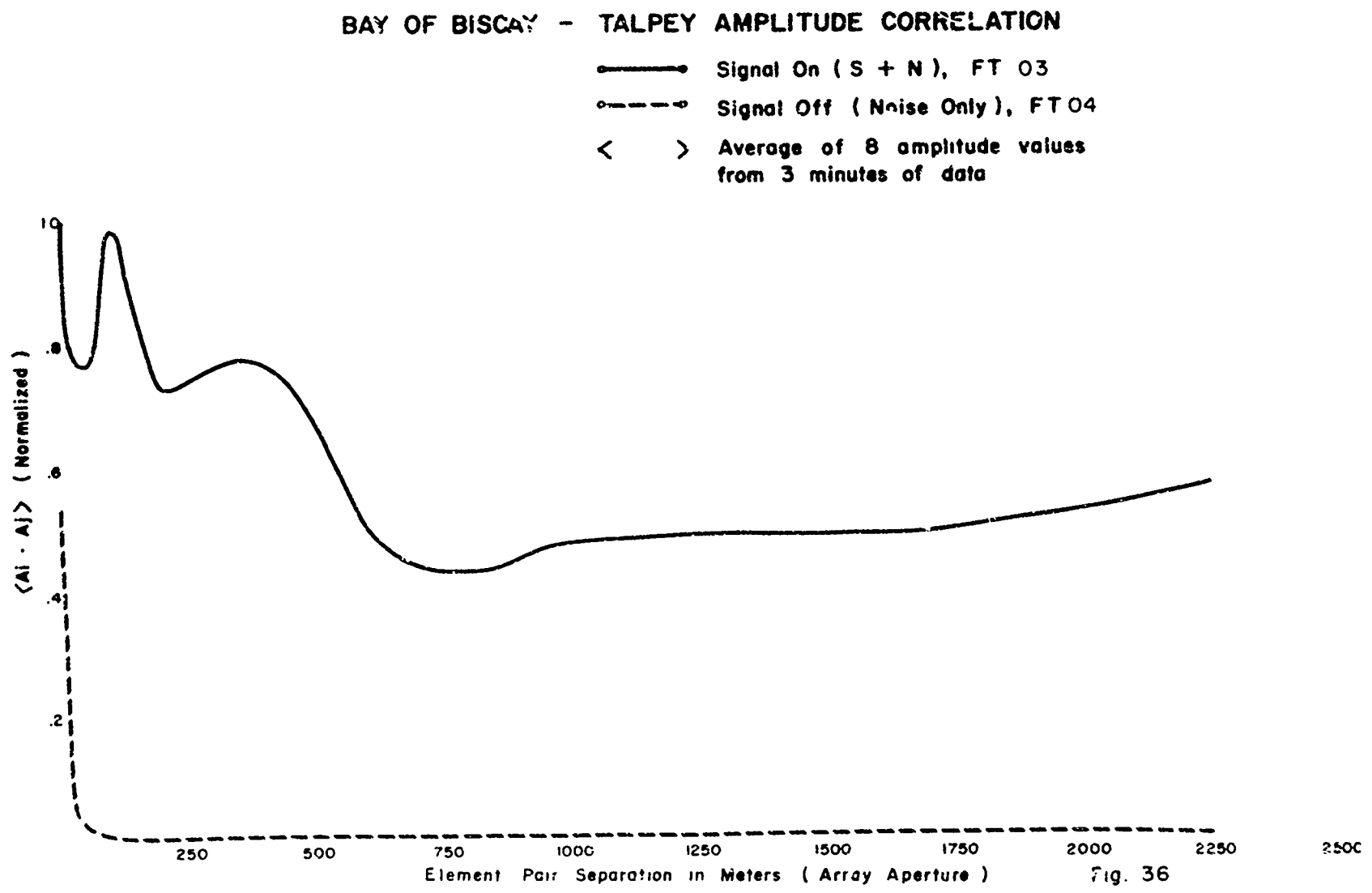
BAY OF BISCAY - TALPEY AMPLITUDE CORRELATION
Signal On (S + N), FT 03
Signal Off (Noise Only), FT 04
< > Average of 8 amplitude values from 3 minutes of data
<Ai · Aj> (Normalized)
1.0
.8
.6
.4
.2
250
500
750
1000
1250
1500
1750
2000
2250
2500
Element Pair Separation in Meters (Array Aperture)

Fig. 36

BAY OF BISCAY - TALPEY AMPLITUDE & PHASE CORRELATION

Signal On (S + N) - FT 03

Signal Off (Noise Only) FT 04

< > Average of 8 Amplitude & Phase values from 3 minutes of data.

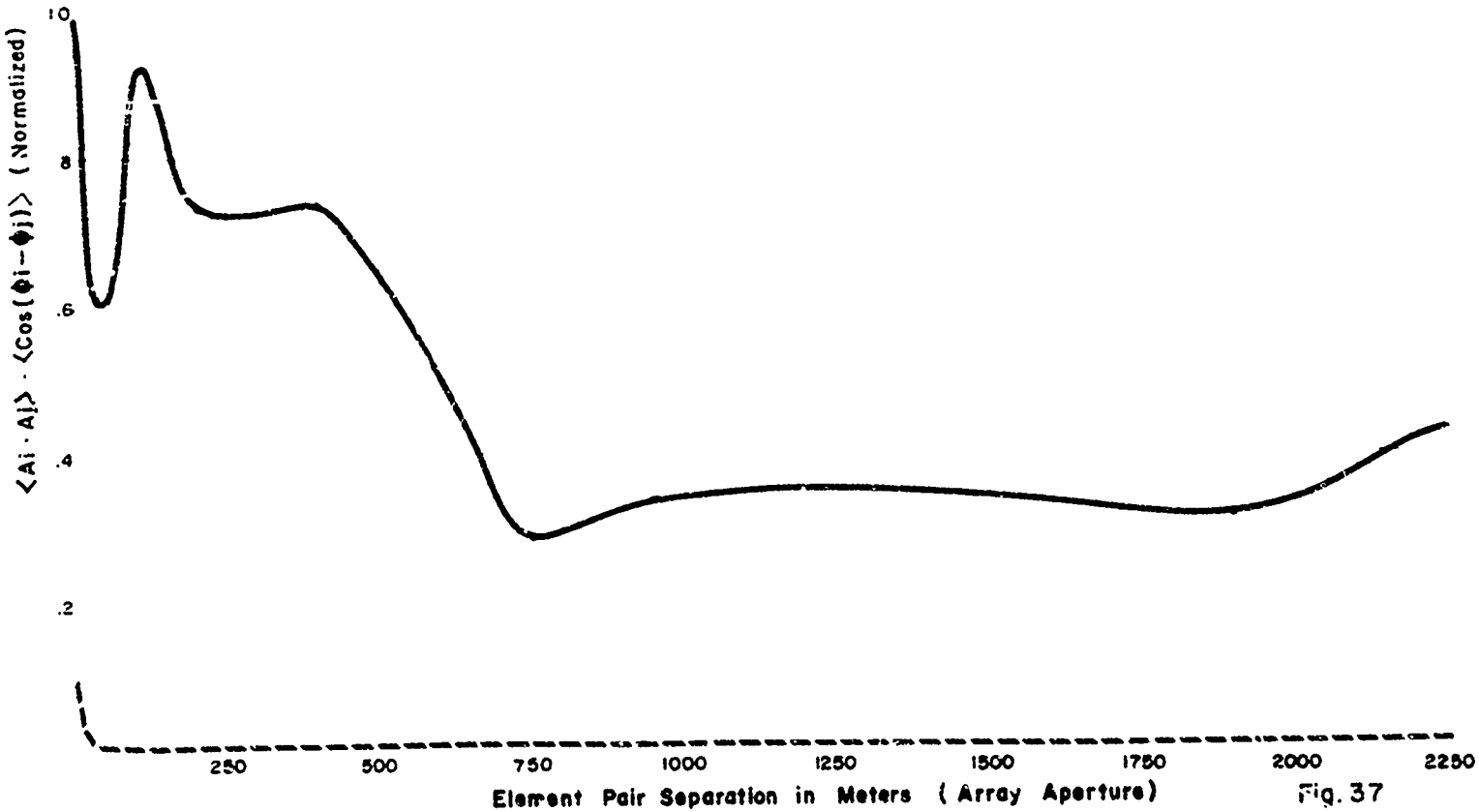

Fig. 37

BAY OF BISCAY - TALPEY AMPLITUDE CORRELATION

Signal On (S + N), FT 05

Signal Off (Noise Only), FT 06

< > Average of 8 amplitude values from 3 minutes of data

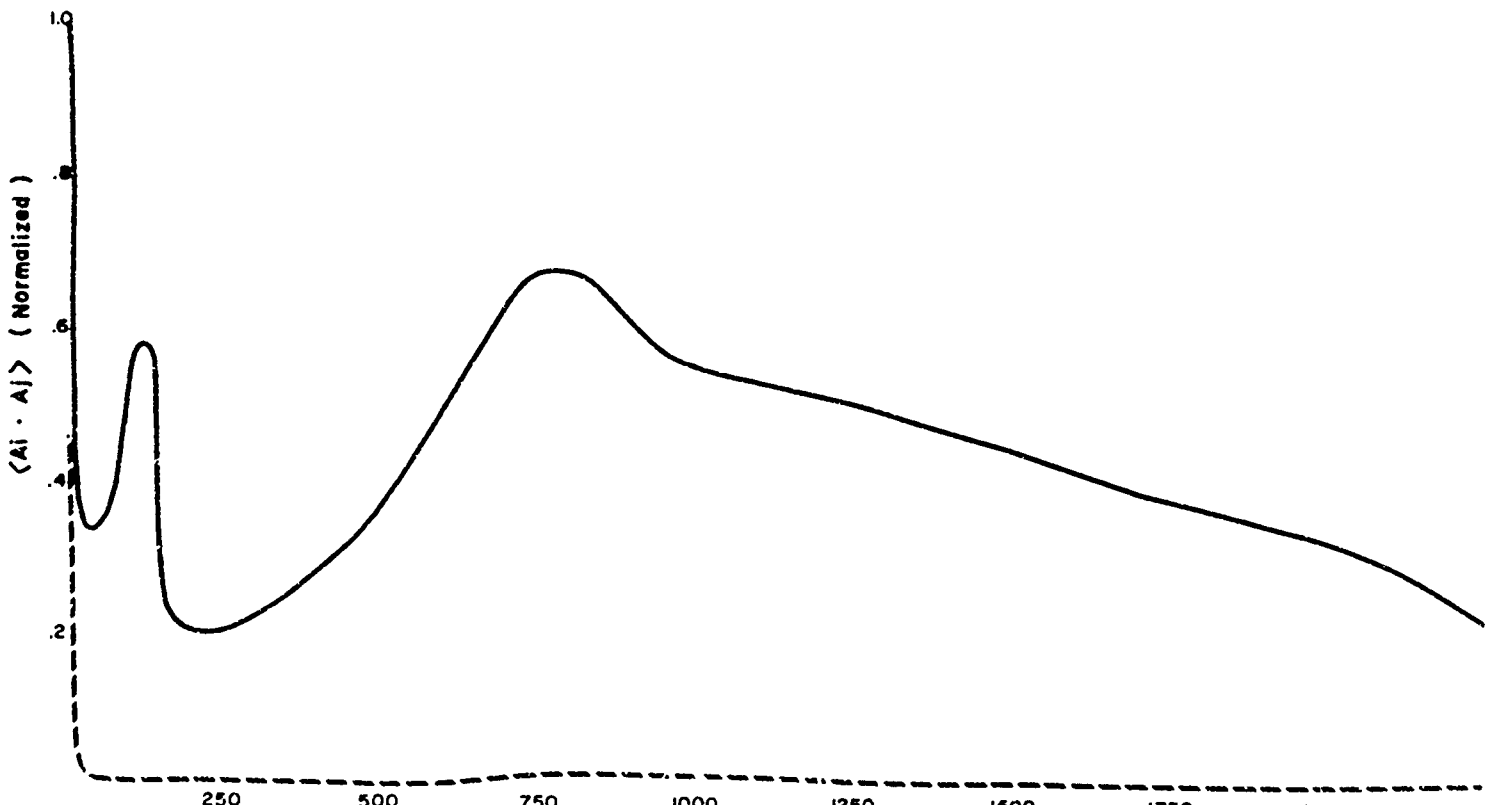

Fig. 38

BAY OF BISCAY - TALPEY AMPLITUDE & PHASE CORRELATION

Signal On (S + N) - FT 05

Signal Off (Noise Only) FT 06

< > Average of 8 Amplitude & Phase values from 3 minutes of data.

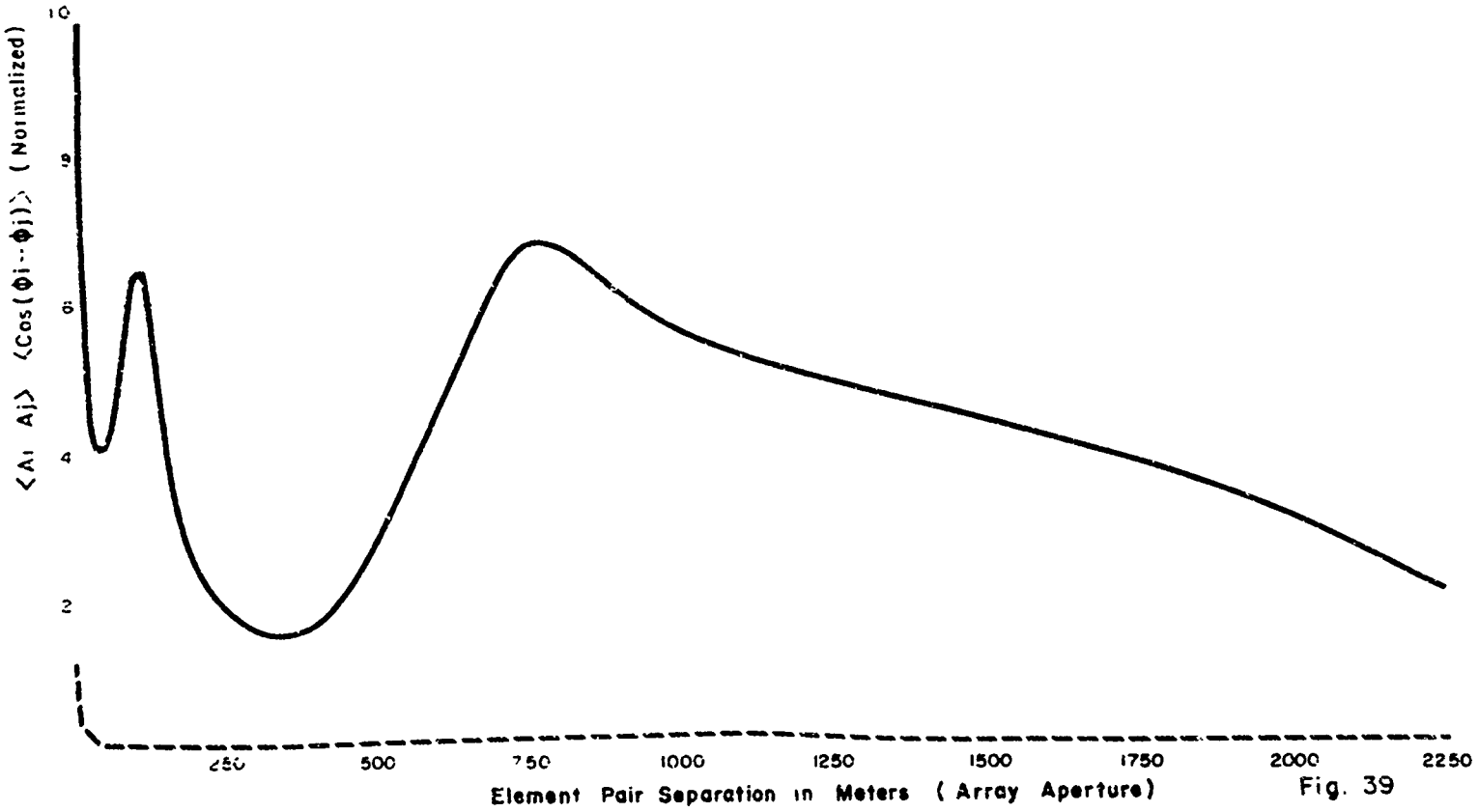

Fig. 39

BAY OF BISCAY - TALPEY AMPLITUDE CORRELATION

Signal On (S + N), FT 20

Signal Off (Noise Only), FT 21

< > Average of 8 amplitude values from 3 minutes of data

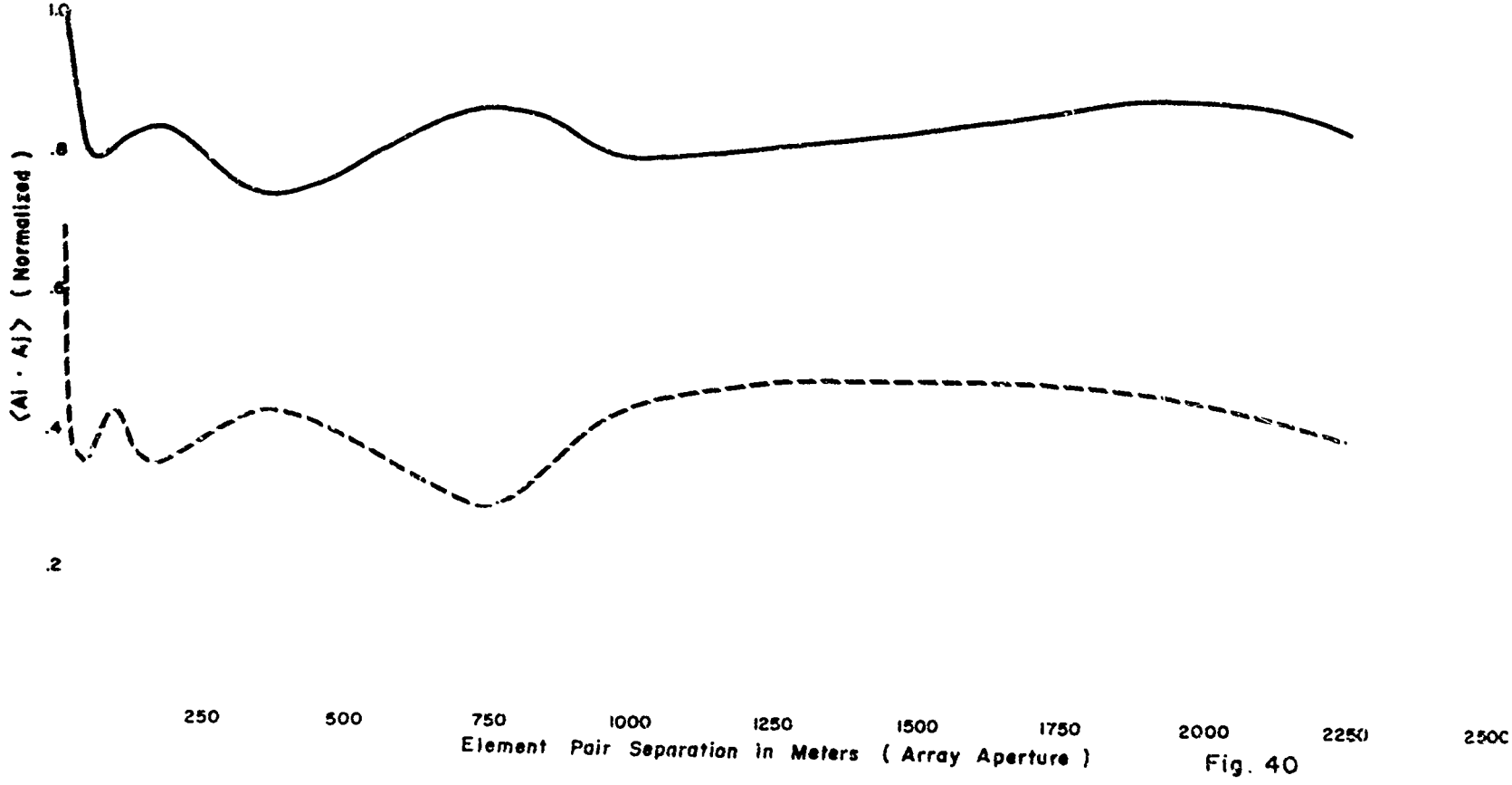

Fig. 40

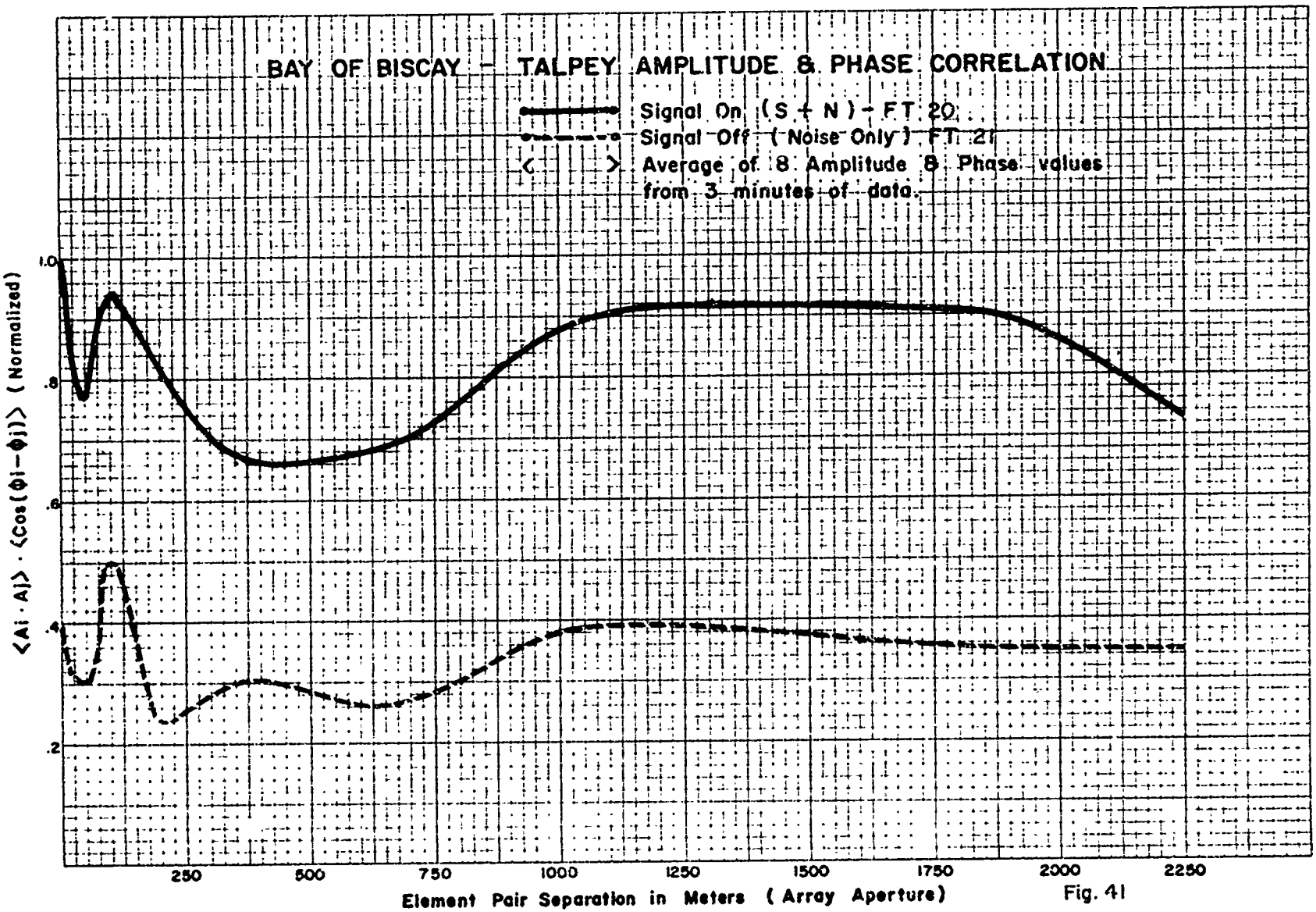
BAY OF BISCAY – TALPEY AMPLITUDE & PHASE CORRELATION
Signal On (S + N) – FT 20
Signal Off (Noise Only) FT 21
< > Average of 8 Amplitude & Phase values from 3 minutes of data.
<Ai · Aj> · <Cos(φi – φj)> (Normalized)
1.0
.8
.6
.4
.2
250
500
750
1000
1250
1500
1750
2000
2250
Element Pair Separation in Meters (Array Aperture)

Fig. 41

BAY OF BISCAY - TALPEY AMPLITUDE CORRELATION

Signal On (S + N), FT 22

Signal Off (Noise Only), FT 23

< > Average of 8 amplitude values from 3 minutes of data

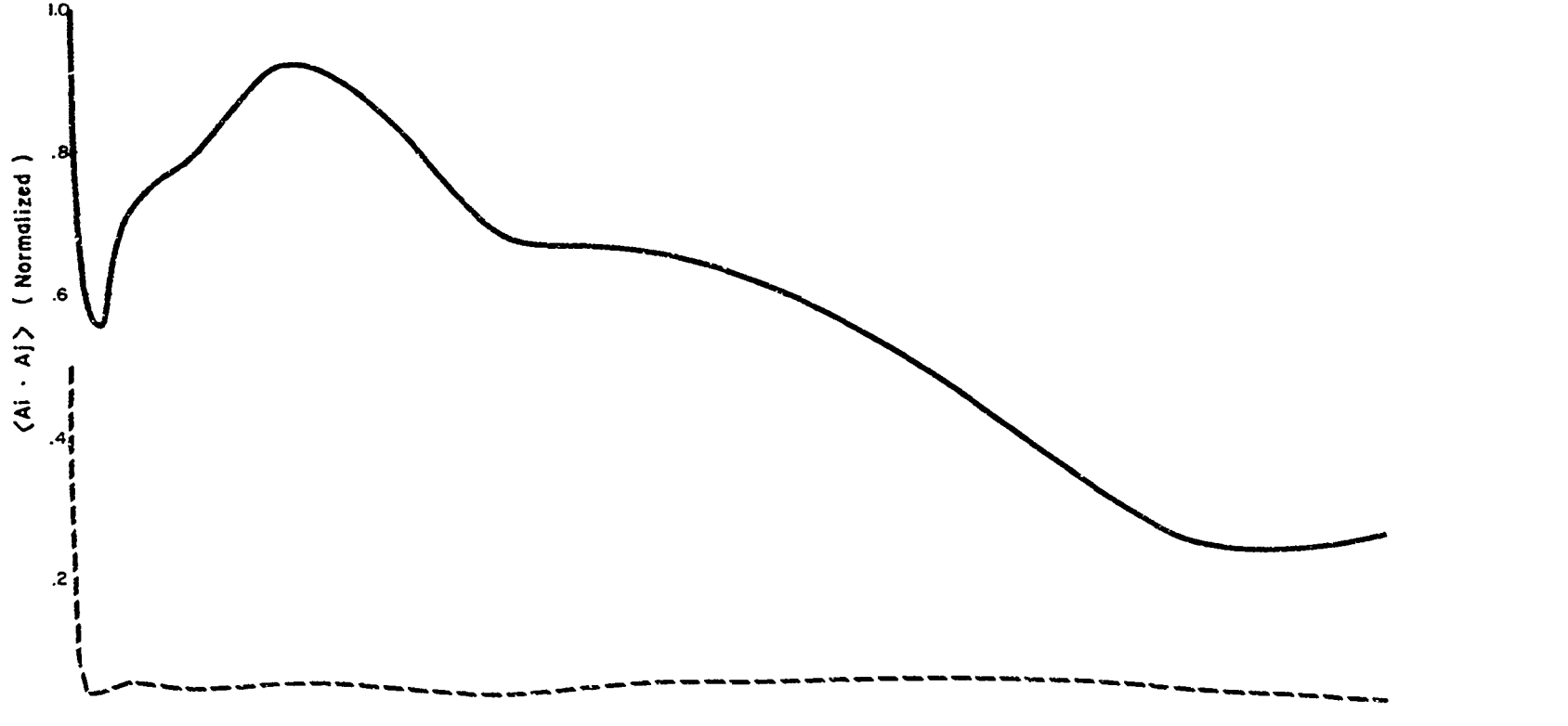

Fig. 42

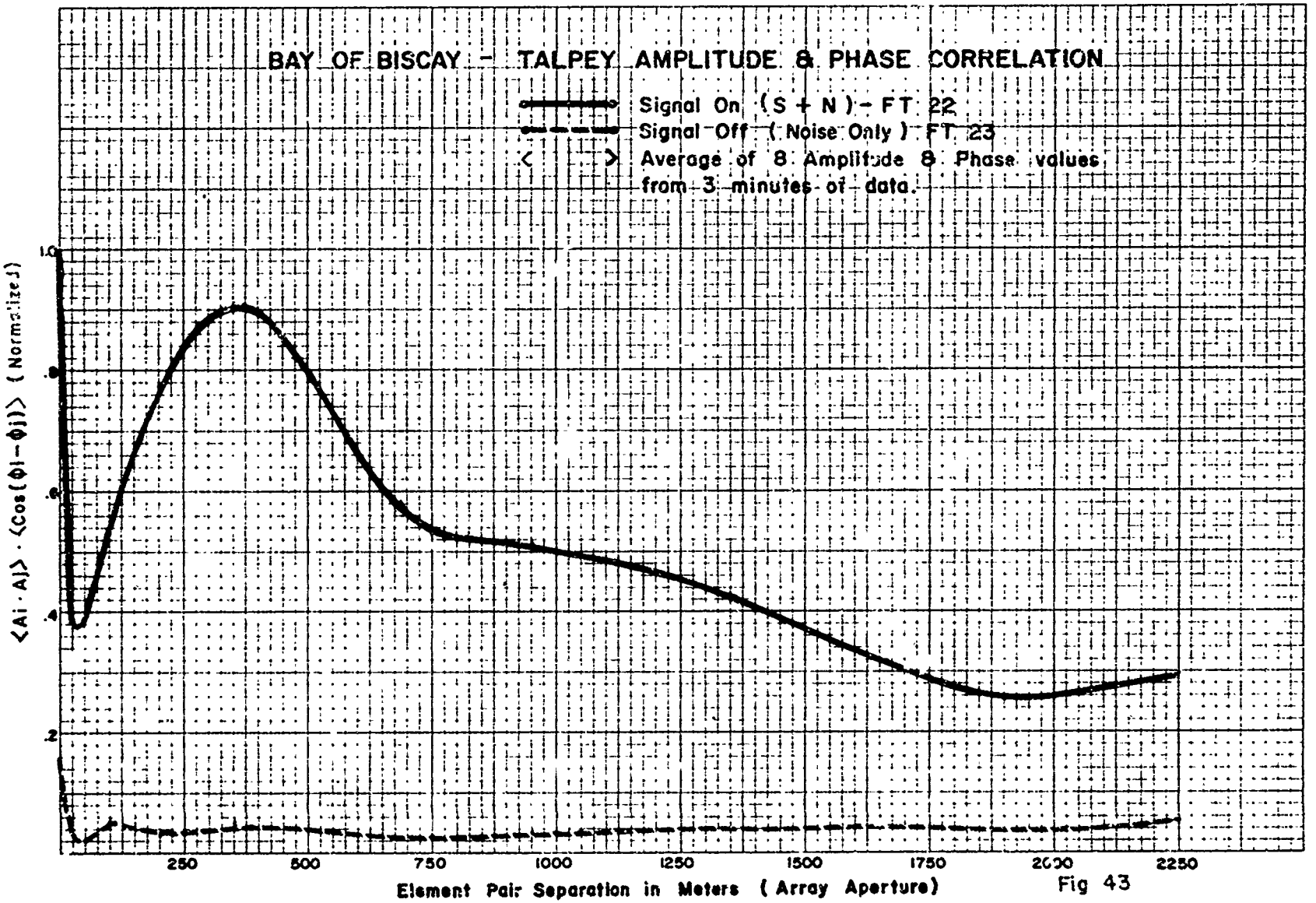
BAY OF BISCAY - TALPEY AMPLITUDE & PHASE CORRELATION
Signal On (S + N) - FT 22
Signal Off (Noise Only) FT 23
< > Average of 8 Amplitude & Phase values from 3 minutes of data.
<Ai · Aj> · <Cos(Φi − Φj)> (Normalized)
1.0
.8
.6
.4
.2
250
500
750
1000
1250
1500
1750
2000
2250
Element Pair Separation in Meters (Array Aperture)

Fig 43

BAY OF BISCAY - TALPEY AMPLITUDE CORRELATION

Signal On (S + N), FT 44

Signal Off (Noise Only), FT 45,46

< > Average of 8 amplitude values from 3 minutes of data

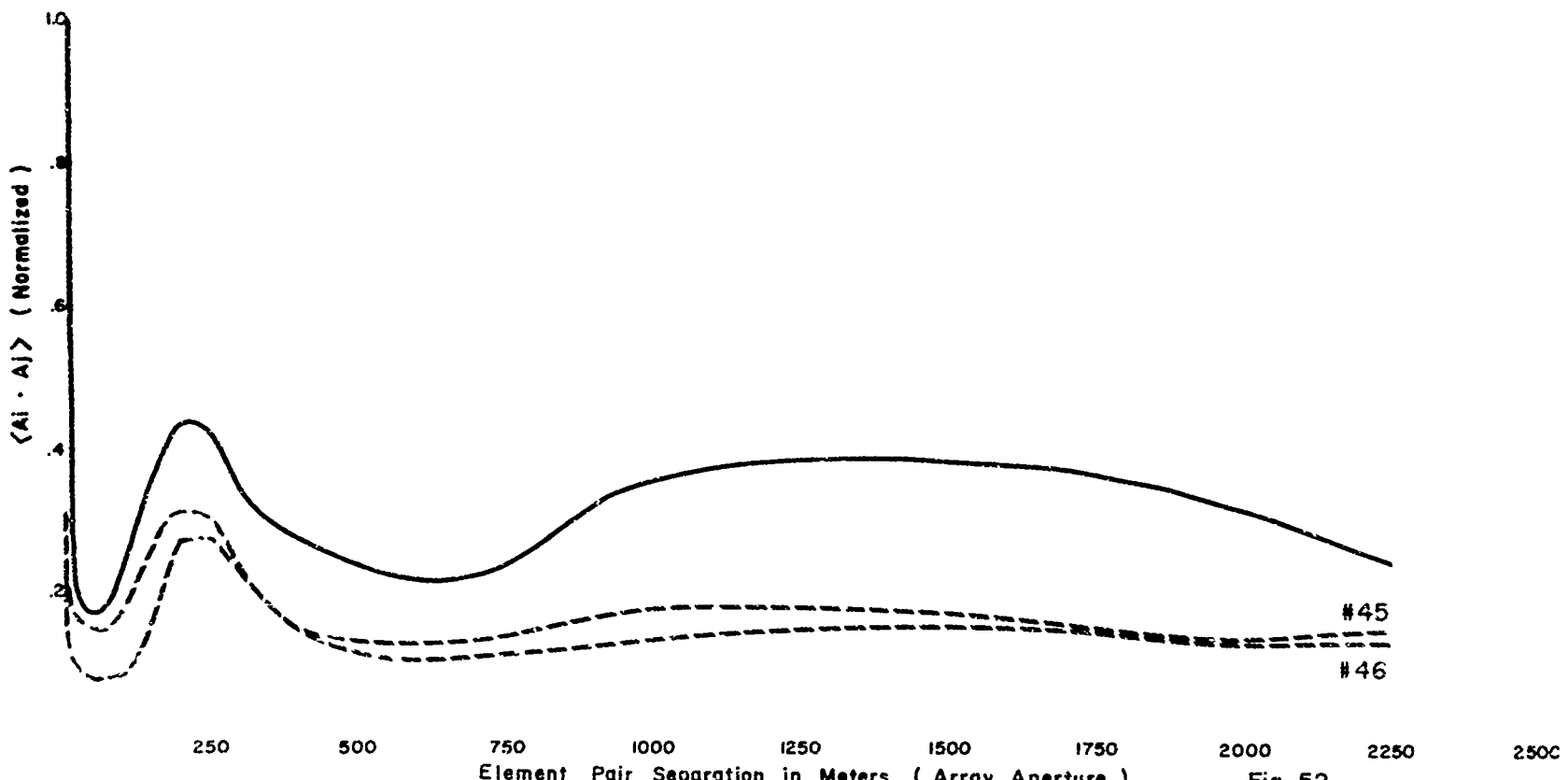

Fig. 52

BAY OF BISCAY - TALPEY AMPLITUDE & PHASE CORRELATION

Signal On (S + N) - FT 44
Signal Off (Noise Only) FT 45, 46
< > Average of 8 Amplitude & Phase values from 3 minutes of data.

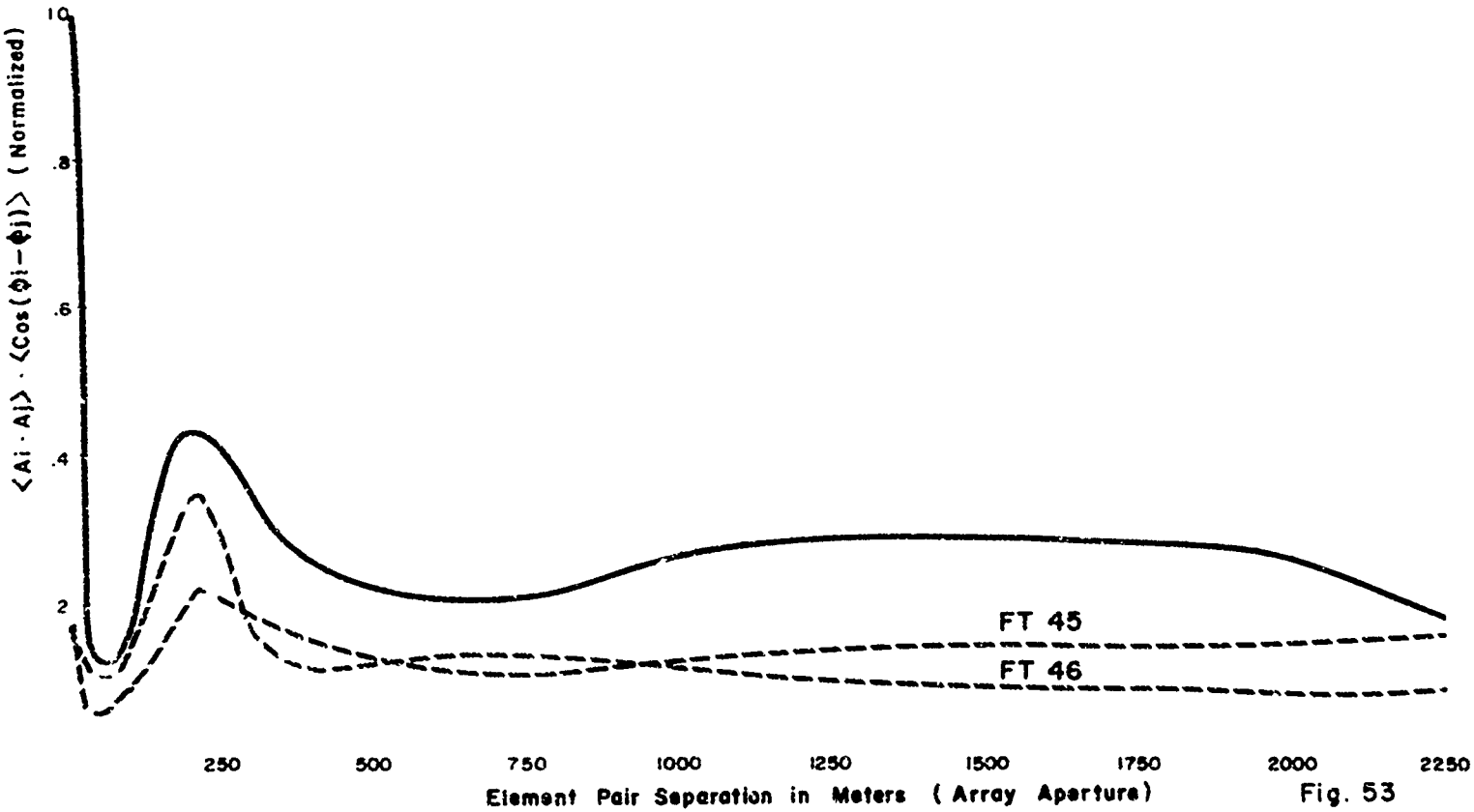

Fig. 53

BAY OF BISCAY - TALPEY AMPLITUDE CORRELATION

Signal On (S + N), FT 47

Signal Off (Noise Only), FT 48, 49

< > Average of 8 amplitude values from 3 minutes of data

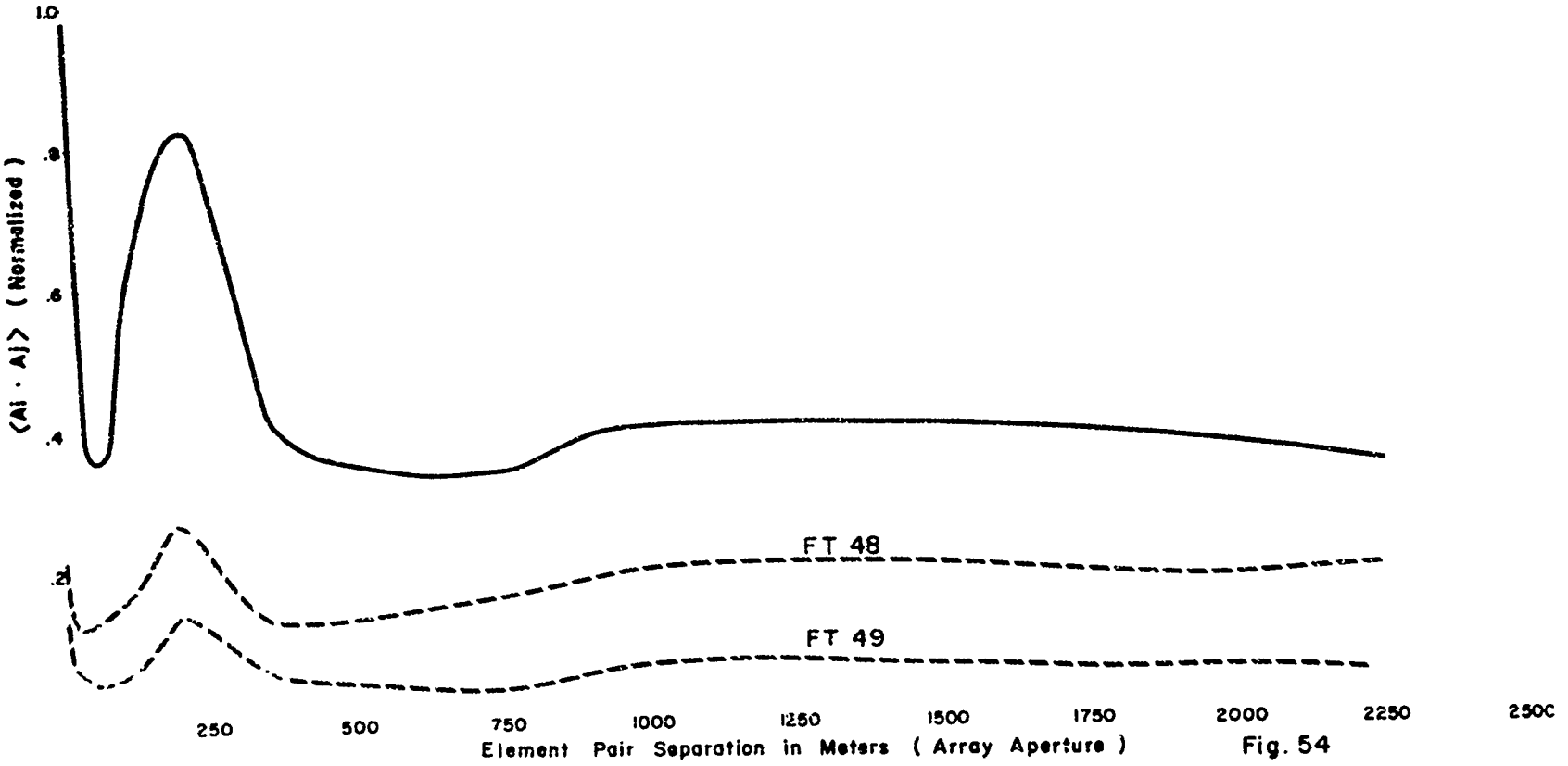

Fig. 54

BAY OF BISCAY - TALPEY AMPLITUDE & PHASE CORRELATION

Signal On (S + N) - FT 47
Signal Off (Noise Only) FT 48, 49
< > Average of 8 Amplitude & Phase values from 3 minutes of data.

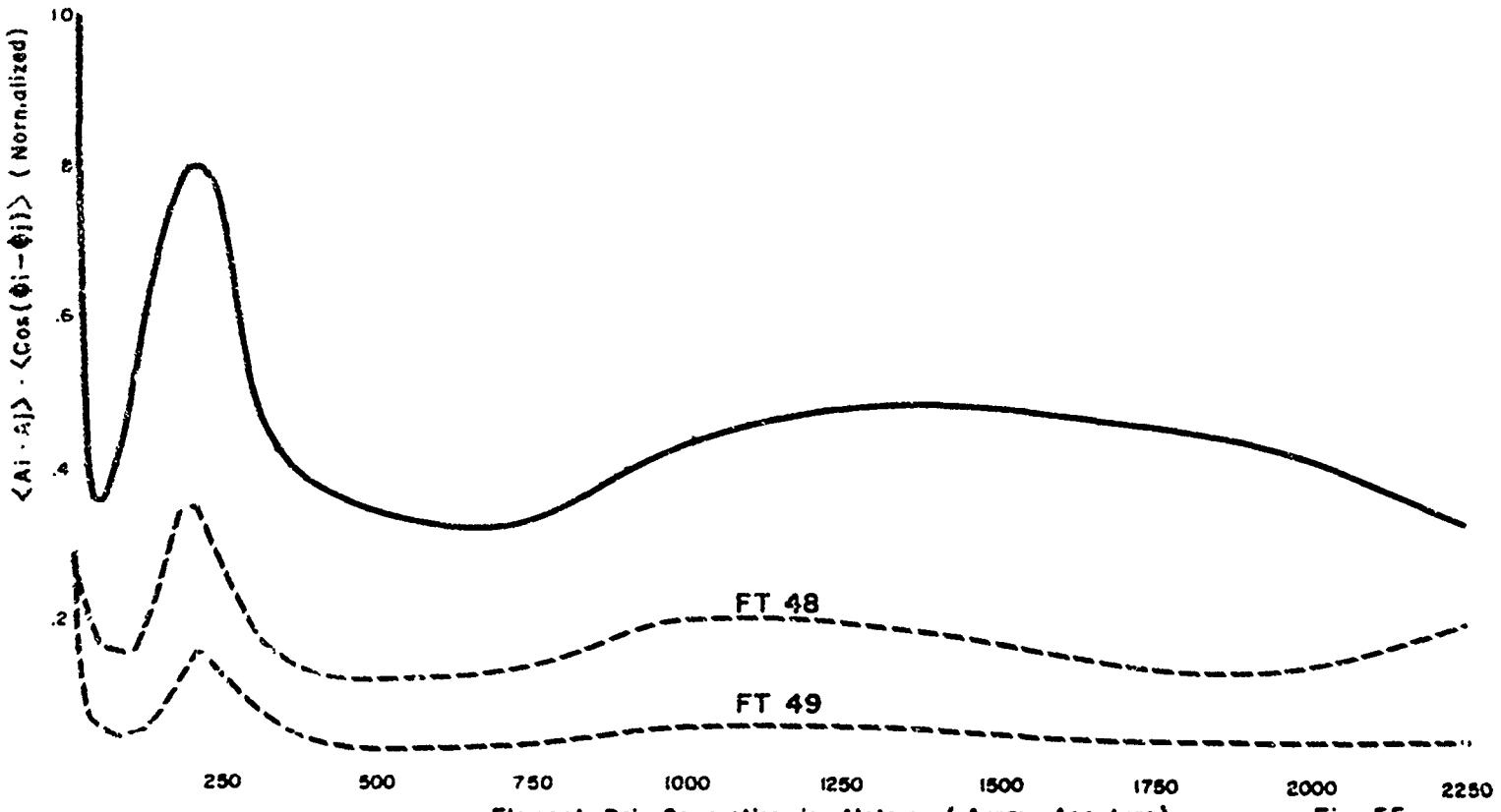

Fig. 55

BAY OF BISCAY - TALPEY AMPLITUDE CORRELATION

Signal On (S + N), FT 50

Signal Off (Noise Only), FT 51

< > Average of 8 amplitude values from 3 minutes of data

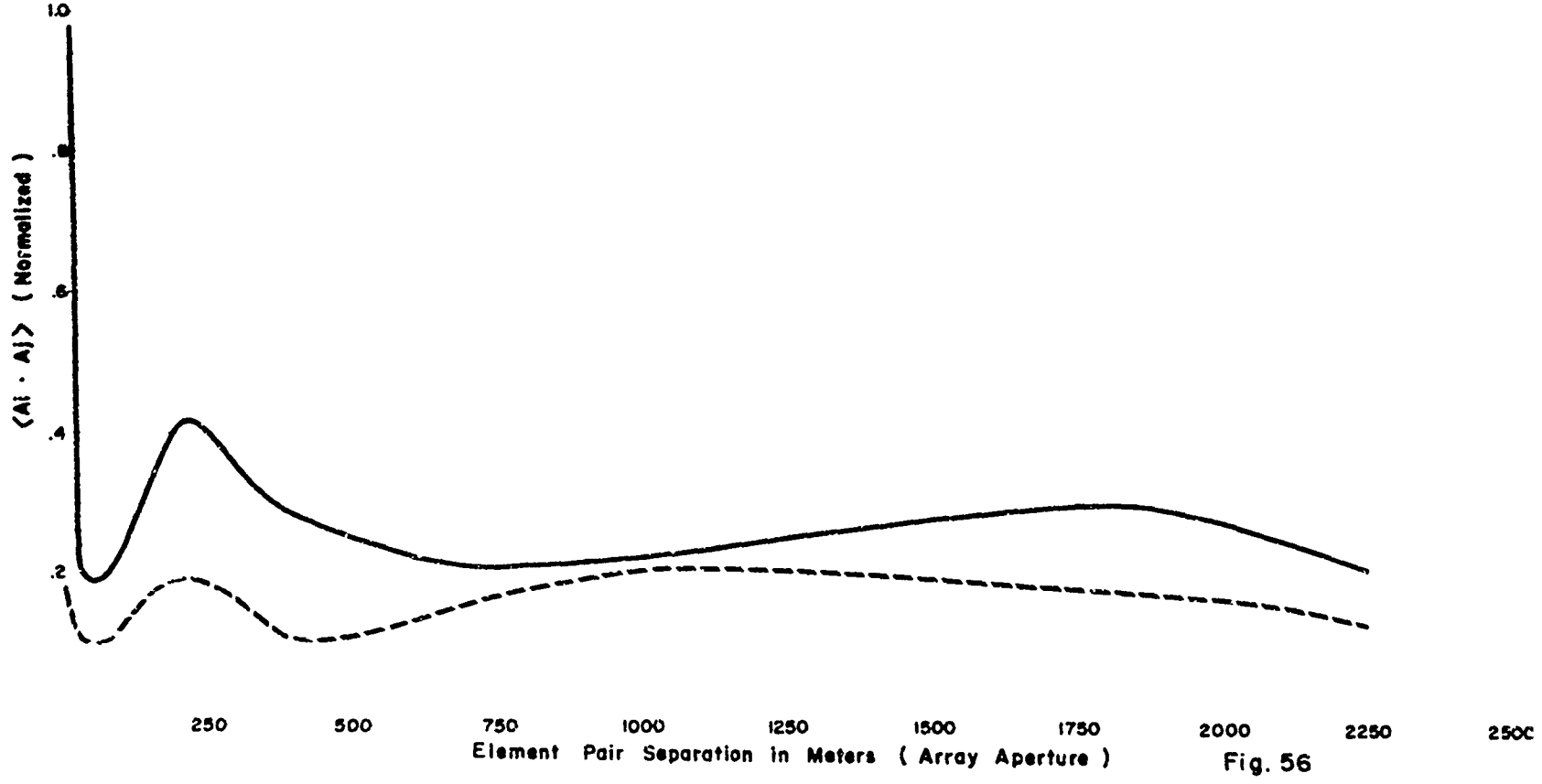

Fig. 56

BAY OF BISCAY - TALPEY AMPLITUDE & PHASE CORRELATION

Signal On (S + N) - FT 50

Signal Off (Noise Only) FT 51

< > Average of 8 Amplitude & Phase values from 3 minutes of data.

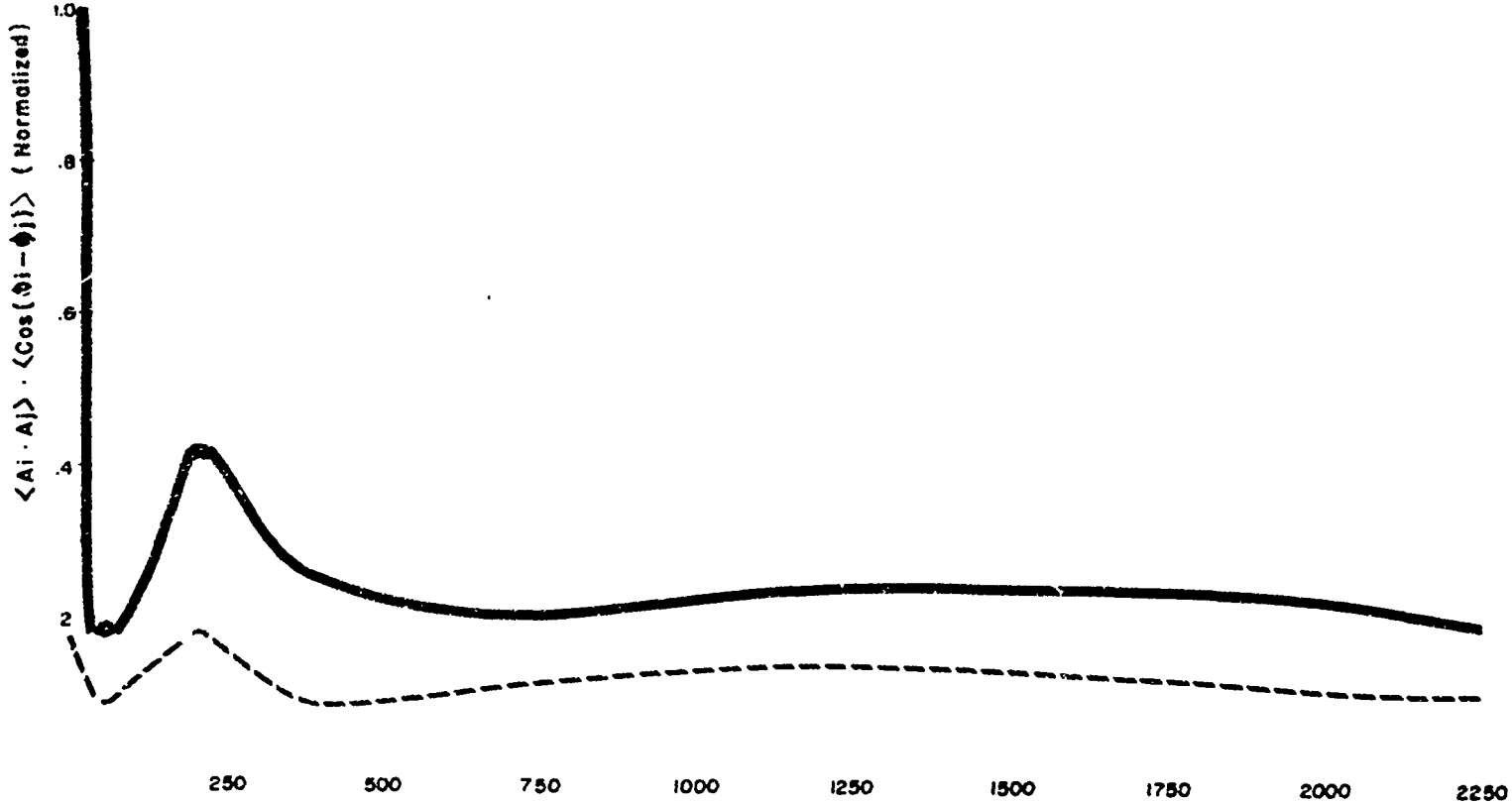

Fig. 57

BAY OF BISCAY – TALPEY PHASE CORRELATION

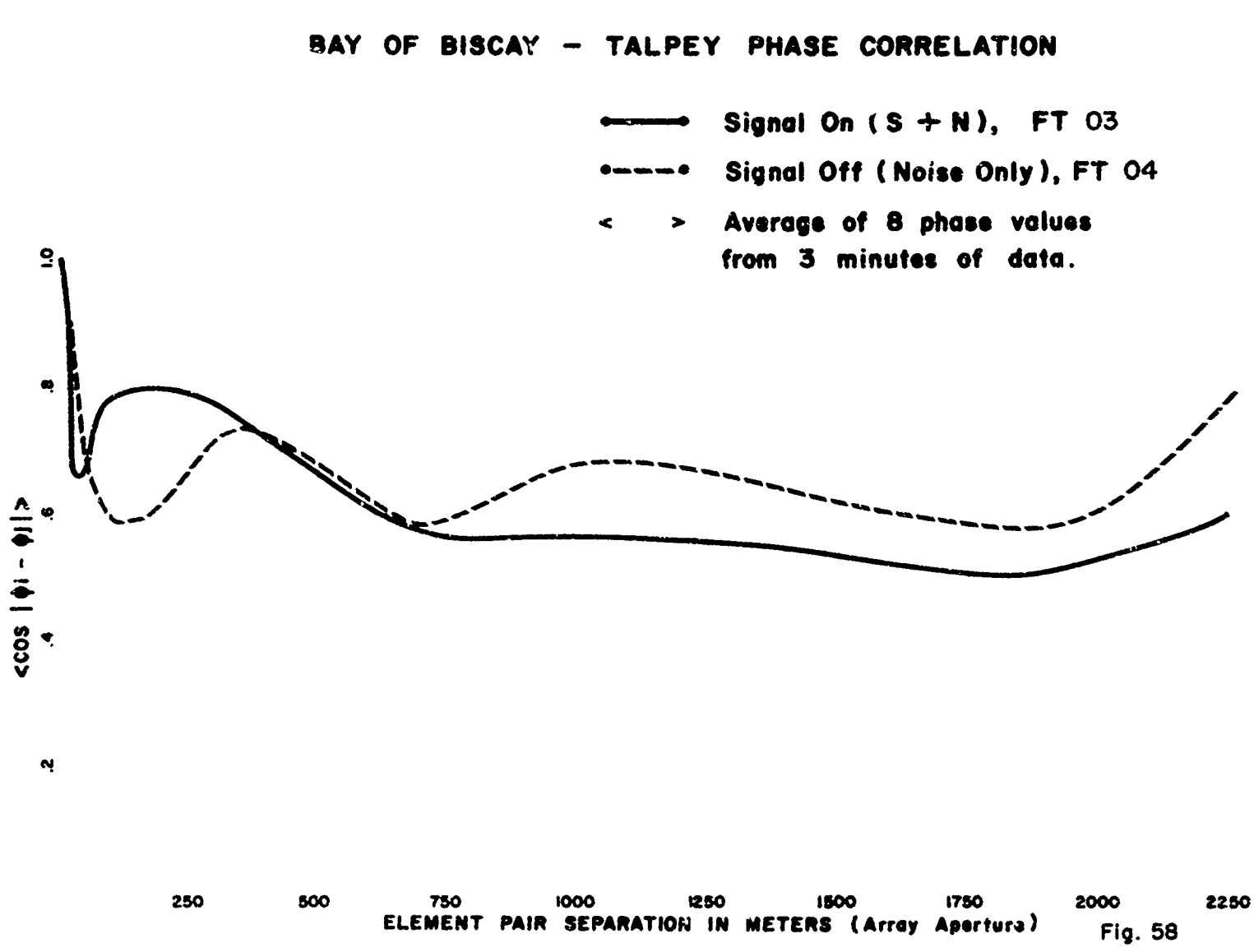

Fig. 58

BAY OF BISCAY – TALPEY PHASE CORRELATION

Signal On (S + N), FT 05

Signal Off (Noise Only), FT 06

< > Average of 8 phase values from 3 minutes of data.

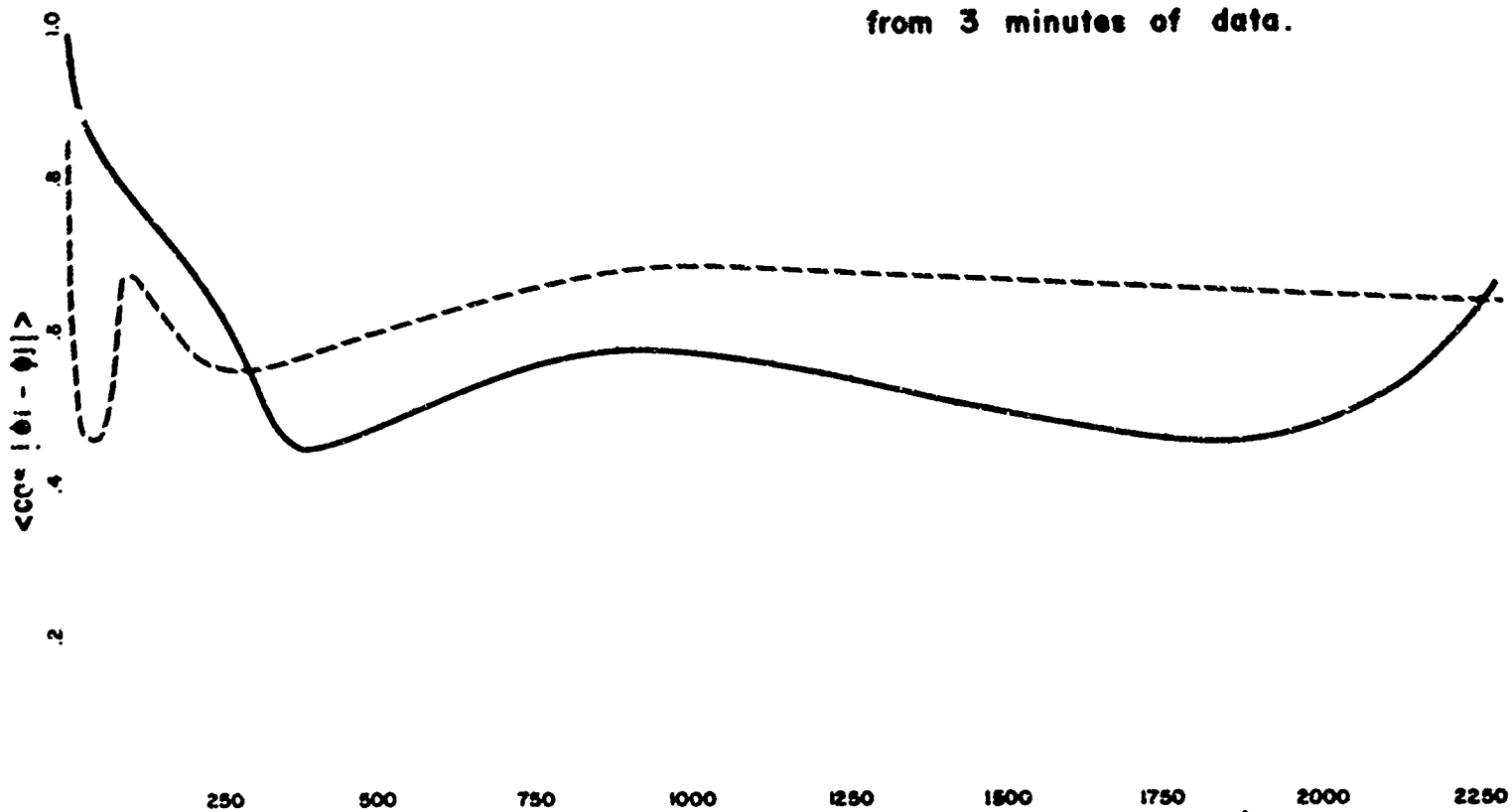

Fig. 59

BAY OF BISCAY – TALPEY PHASE CORRELATION

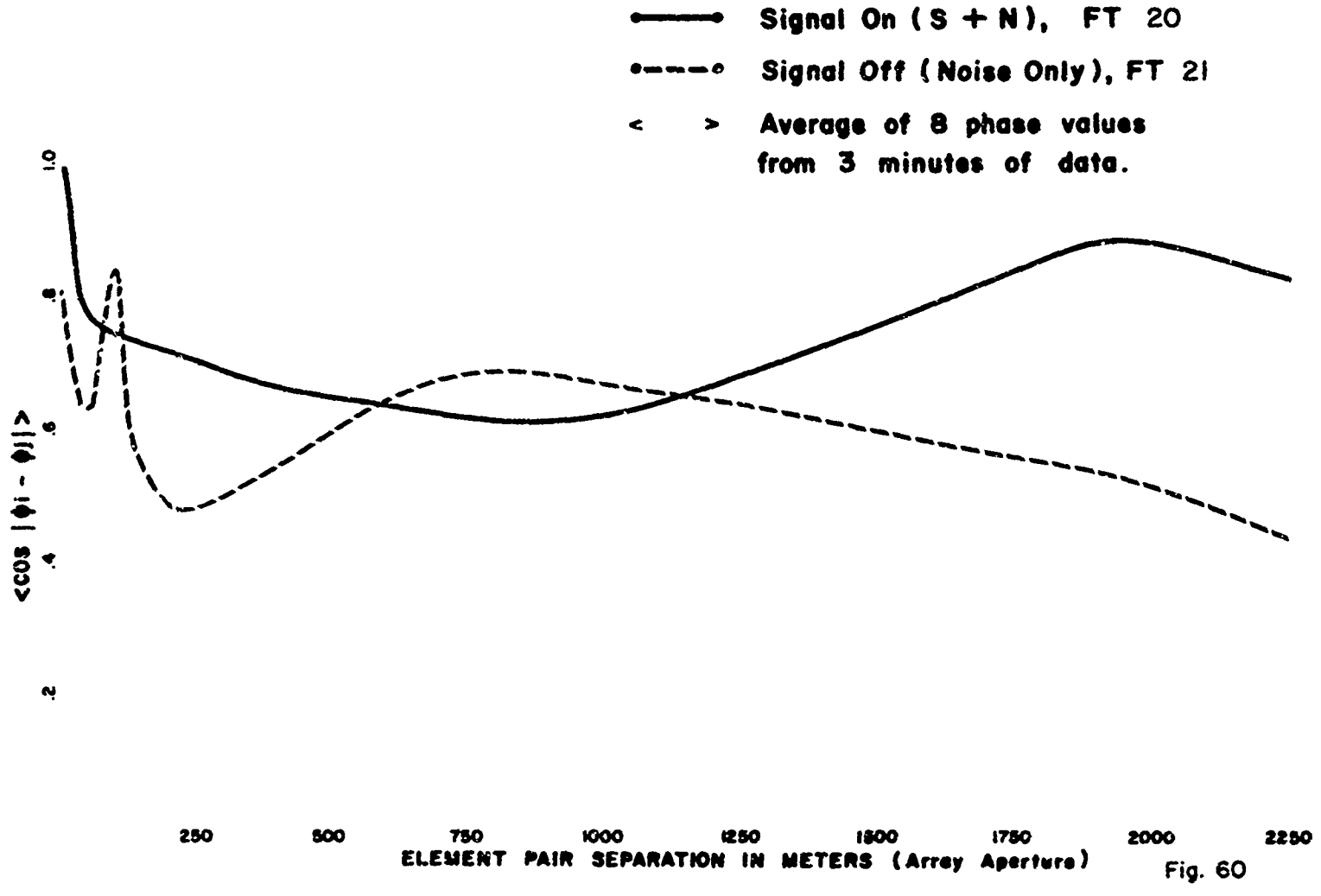

Fig. 60

BAY OF BISCAY – TALPEY PHASE CORRELATION

Signal On (S + N), FT 22

Signal Off (Noise Only), FT 23

< > Average of 3 phase values from 3 minutes of data.

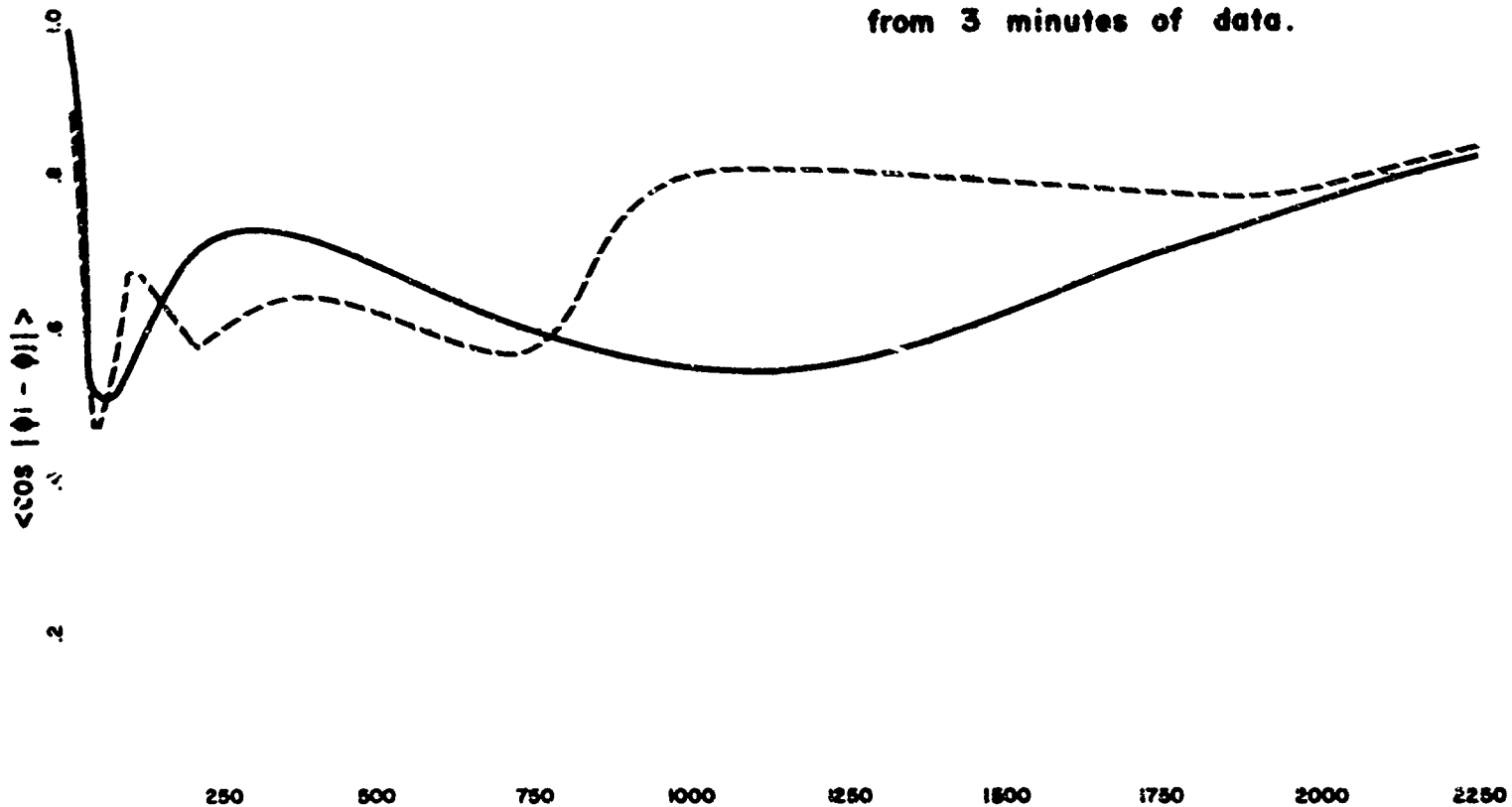

Fig. 61

BAY OF BISCAY – TALPEY PHASE CORRELATION

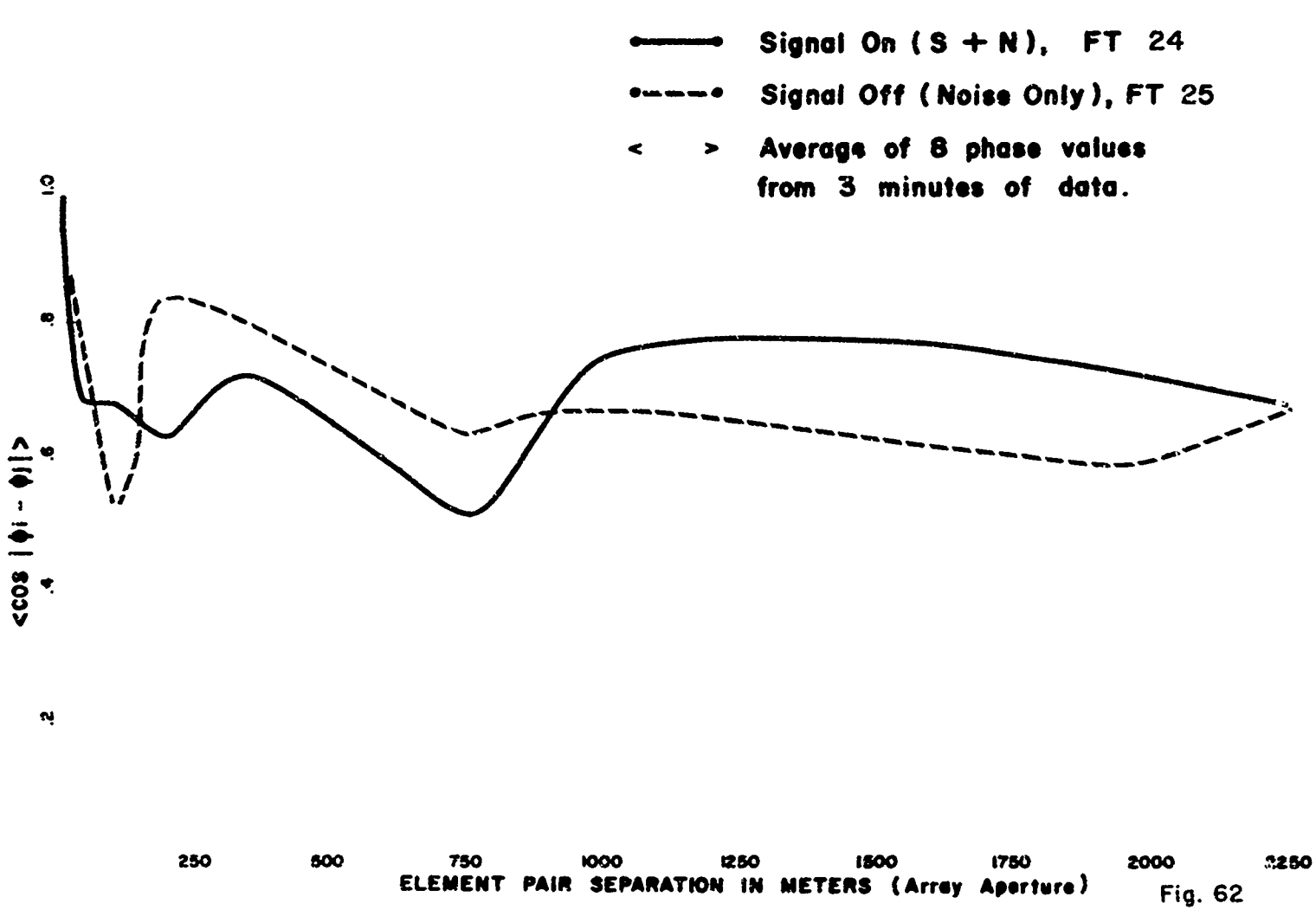

Fig. 62

BAY OF BISCAY – TALPEY PHASE CORRELATION

Signal On (S + N), FT 66

Signal Off (Noise Only), FT 69

< > Average of 8 phase values from 3 minutes of data.

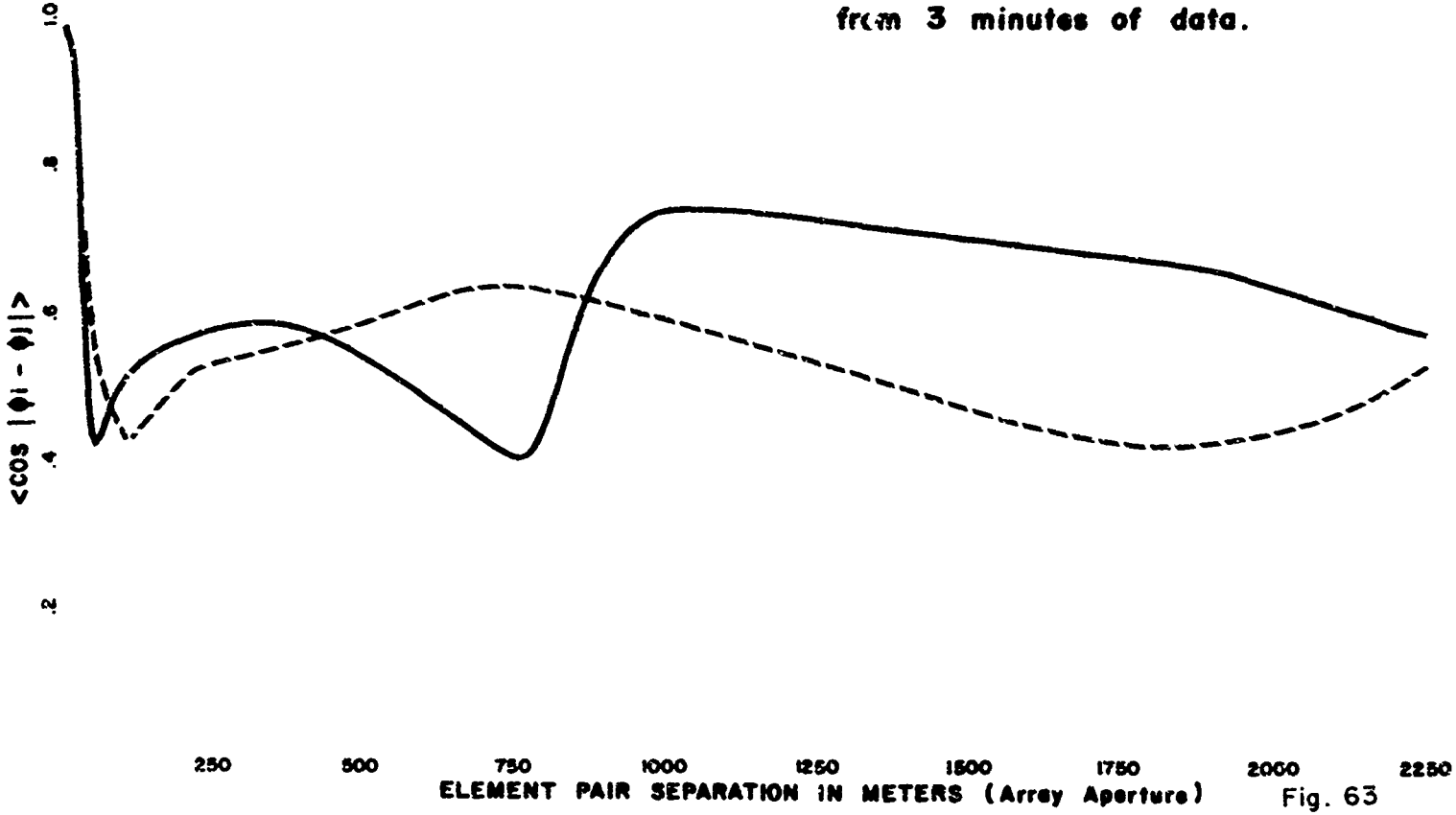

Fig. 63

BAY OF BISCAY – TALPEY PHASE CORRELATION

Signal On (S + N), FT 67

Signal Off (Noise Only), FT 70

< > Average of 8 phase values from 3 minutes of data.

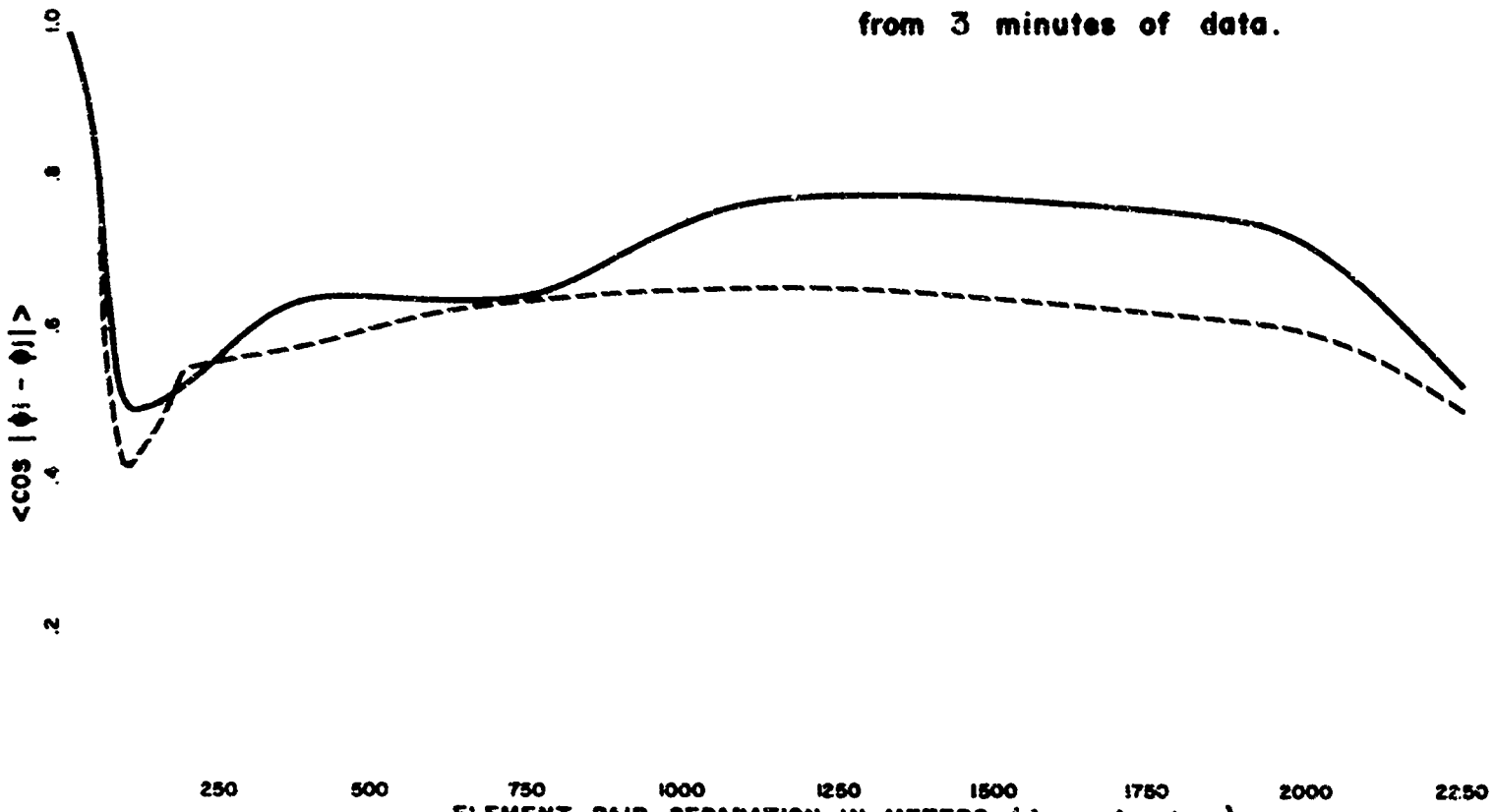

Fig. 64

BAY OF BISCAY – TALPEY PHASE CORRELATION

Signal On (S + N), FT 32

Signal Off (Noise Only), FT 33

< > Average of 8 phase values from 3 minutes of data.

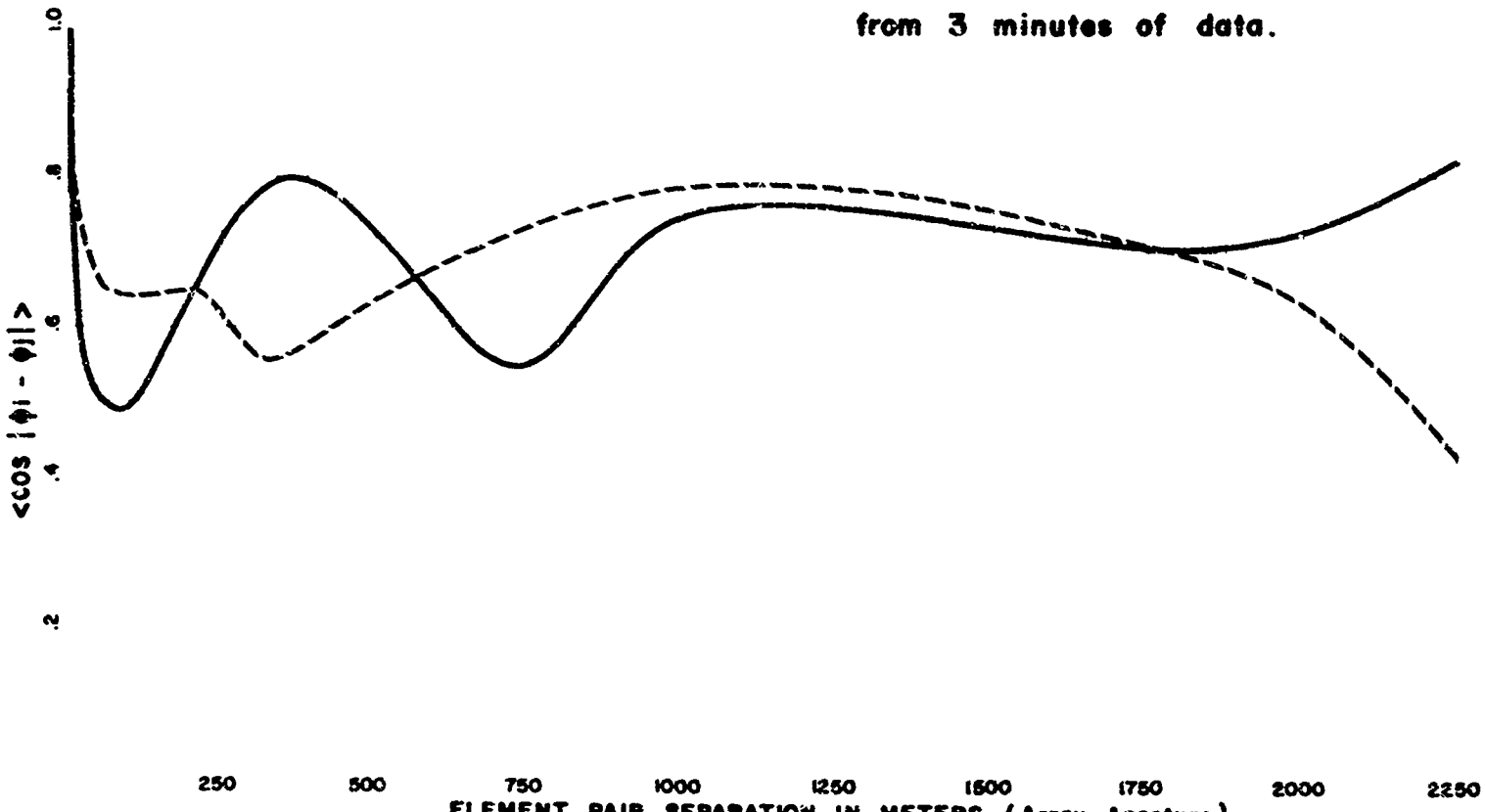

Fig. 65

BAY OF BISCAY – TALPEY PHASE CORRELATION

Signal On (S + N), FT 44

Signal Off (Noise Only), FT 45

< > Average of 8 phase values from 3 minutes of data.

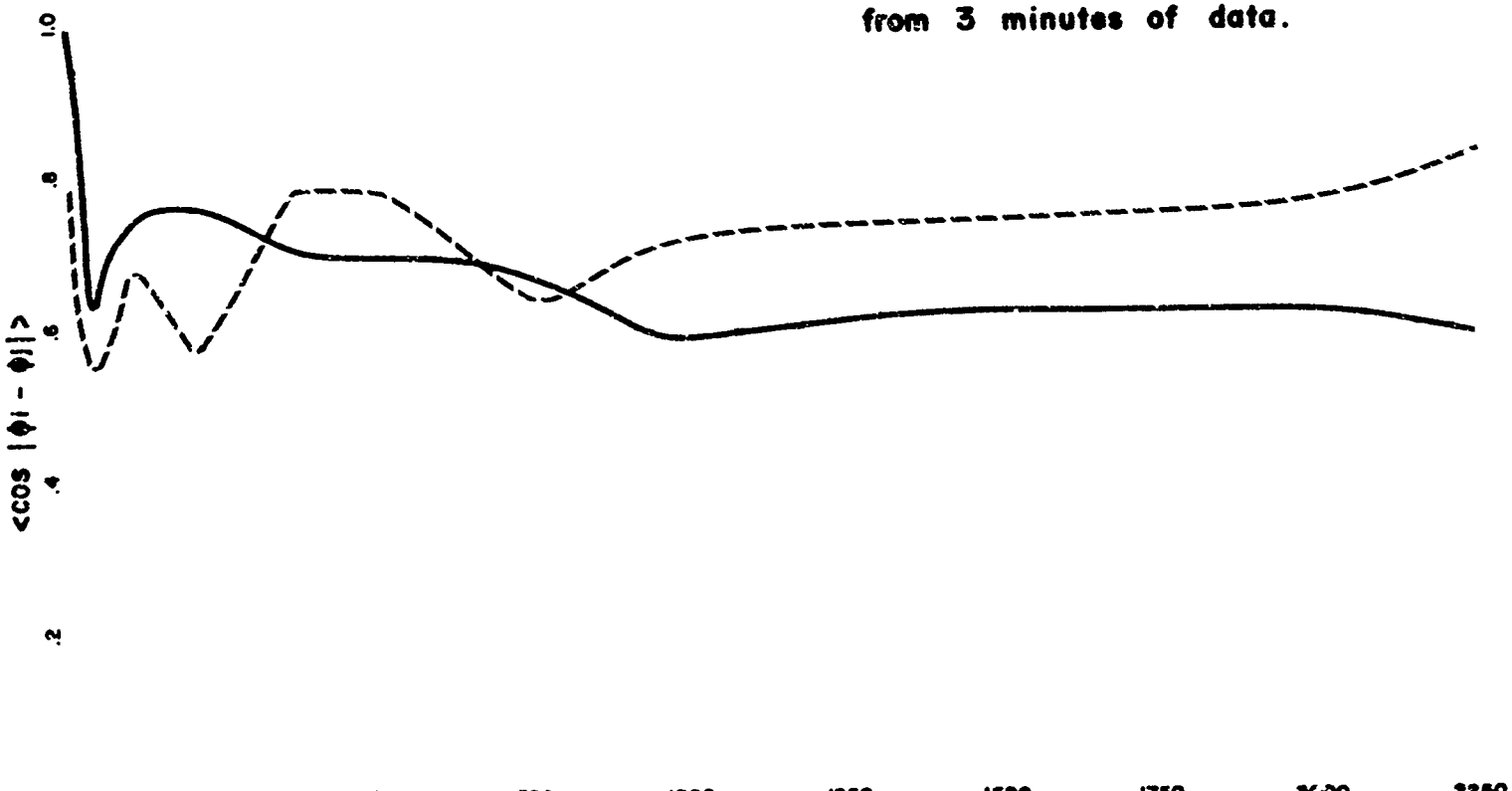

Fig. 66

BAY OF BISCAY – TALPEY PHASE CORRELATION

——— Signal On (S + N), FT 47

•–––• Signal Off (Noise Only), FT 48

< > Average of 8 phase values from 3 minutes of data.

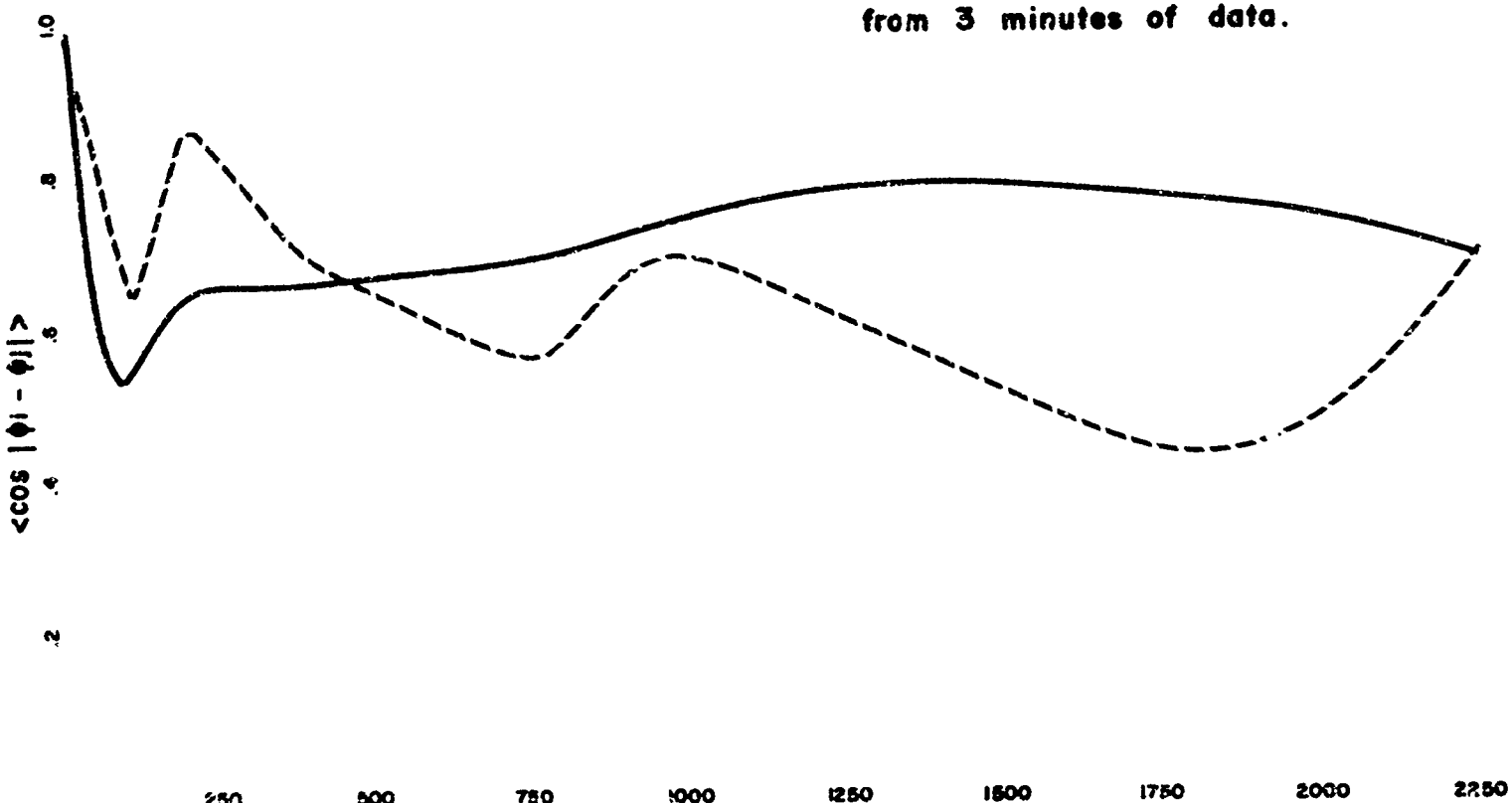

Fig. 67

BAY OF BISCAY – TALPEY PHASE CORRELATION

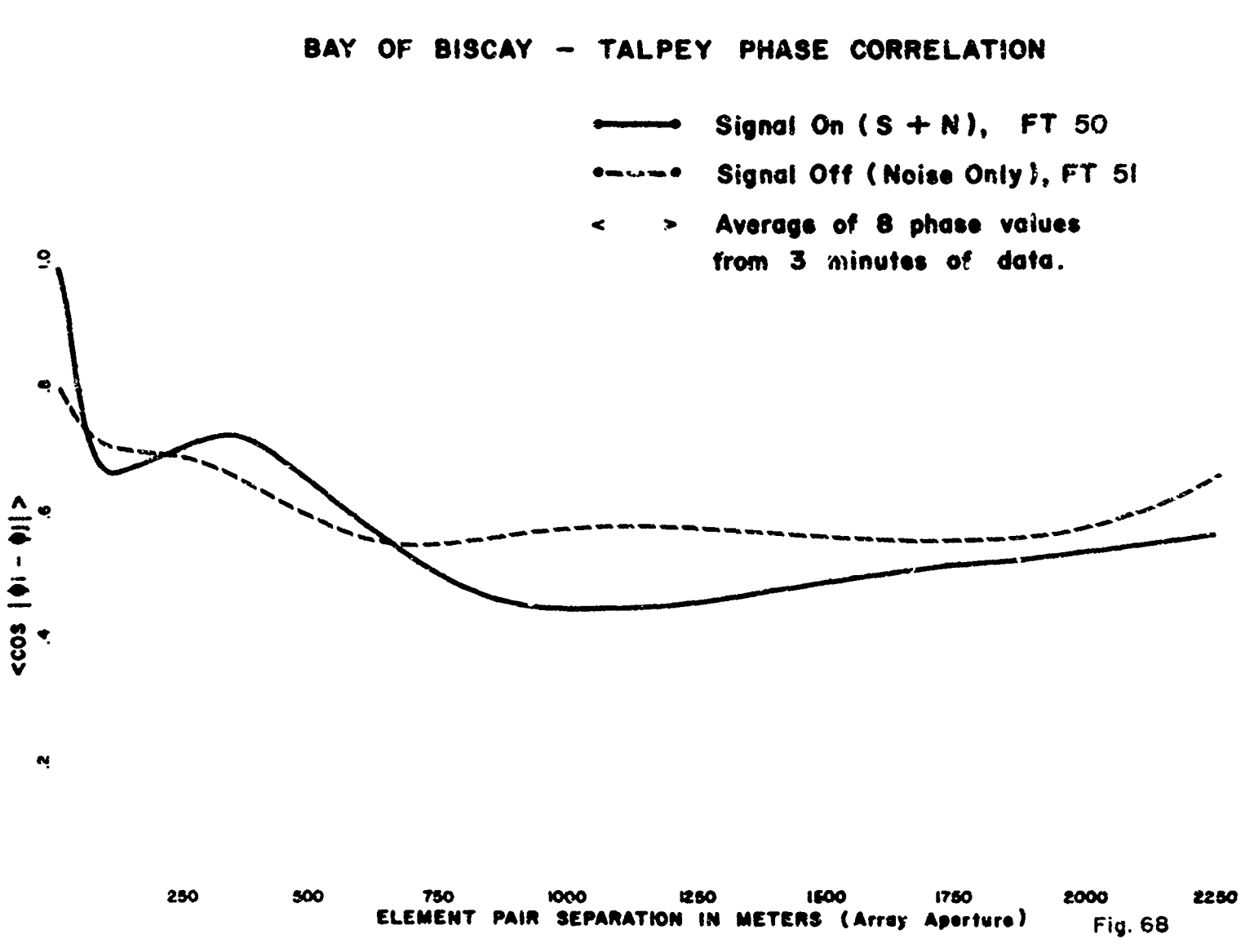

Fig. 68

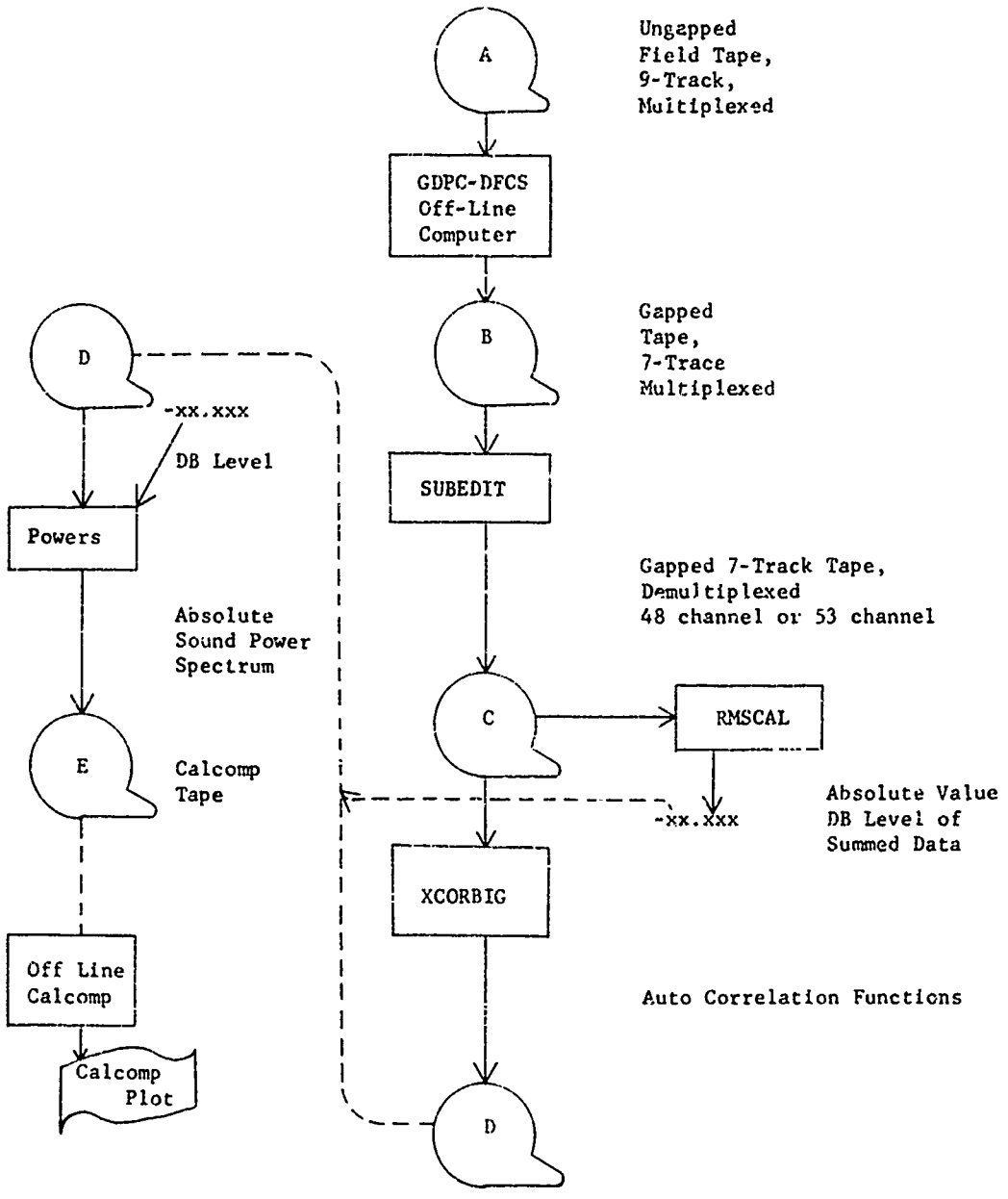

DATA FLOW-POWER SPECTRUM

Figure 69

PROGRAMS

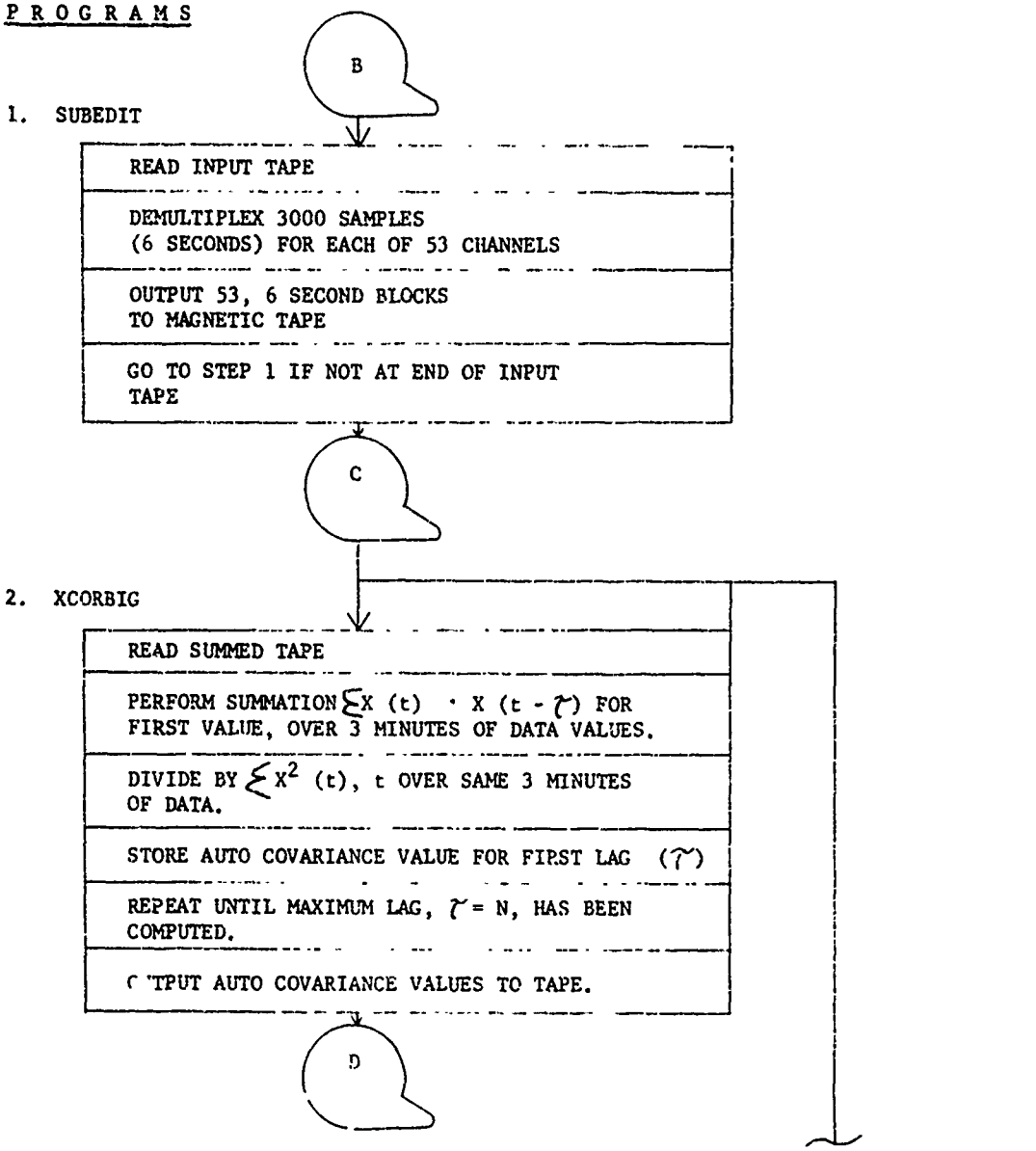

Figure 70
(1 of 2)

POWER SPECTRUM
PROGRAM FLOW

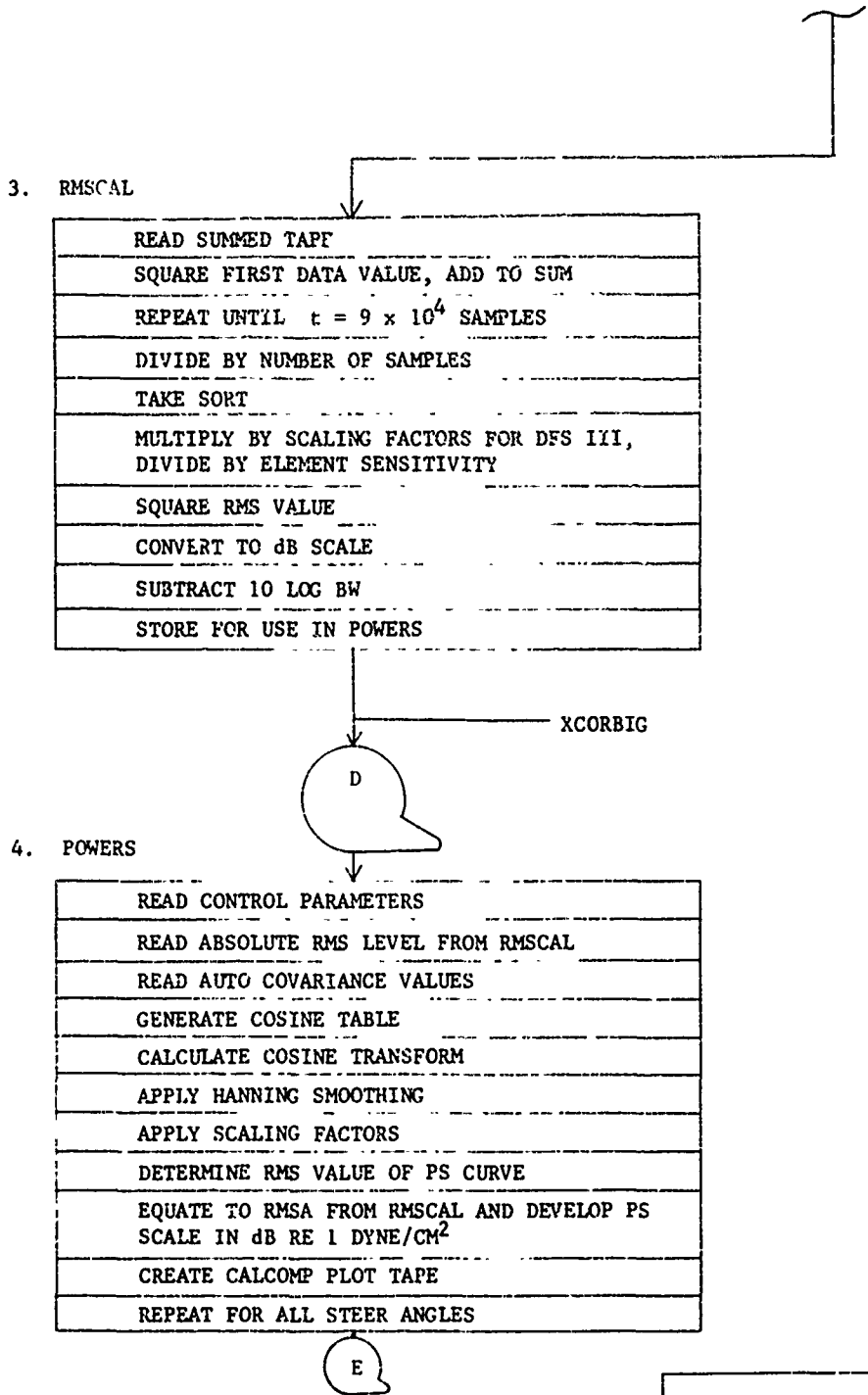

Figure 70
(2 of 2)

POWER SPECTRUM
PROGRAM FLOW

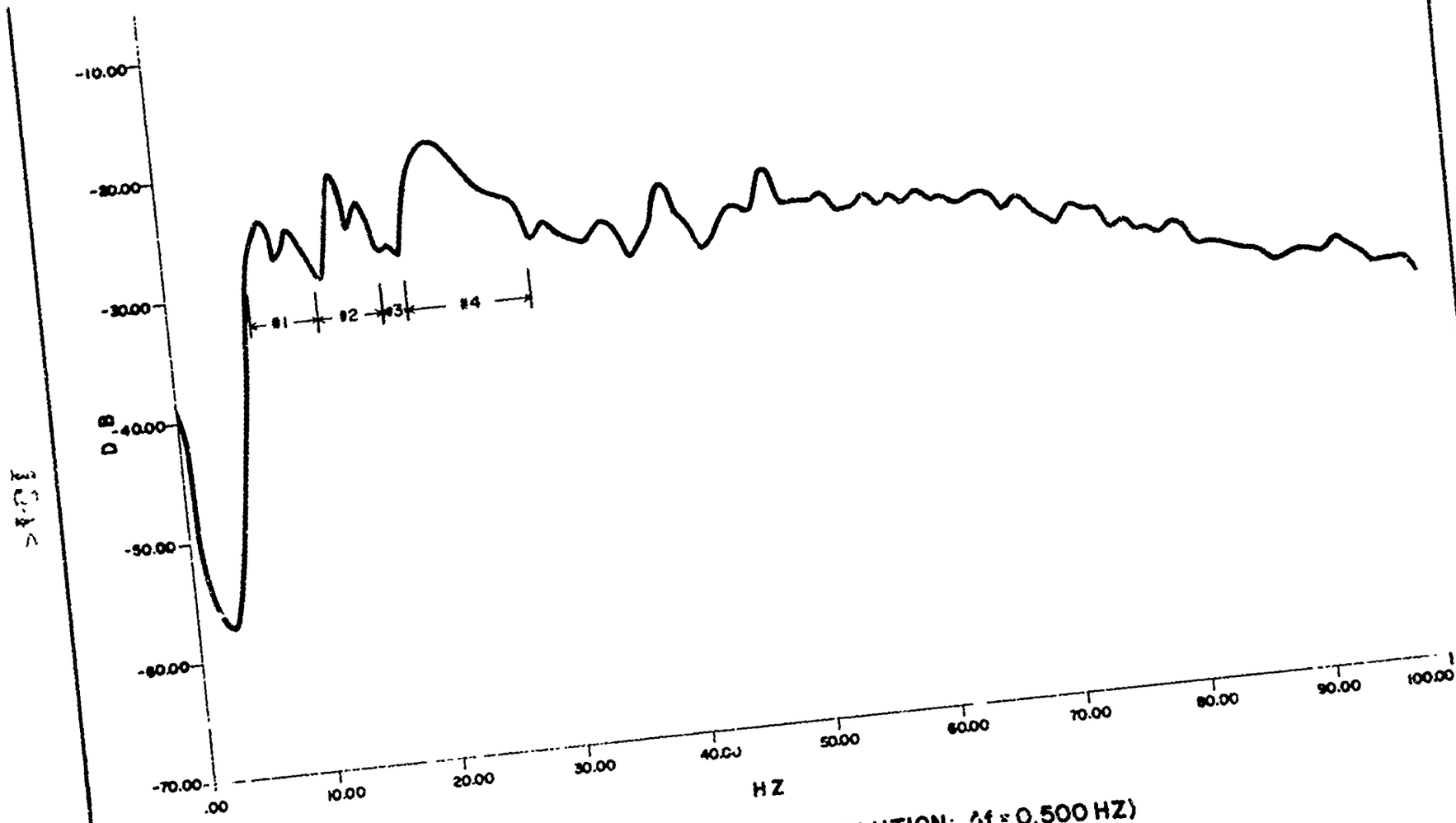

SECo POWER SPECTRUM (RESOLUTION: $\Delta f \approx 0.500$ HZ)

Figure 71

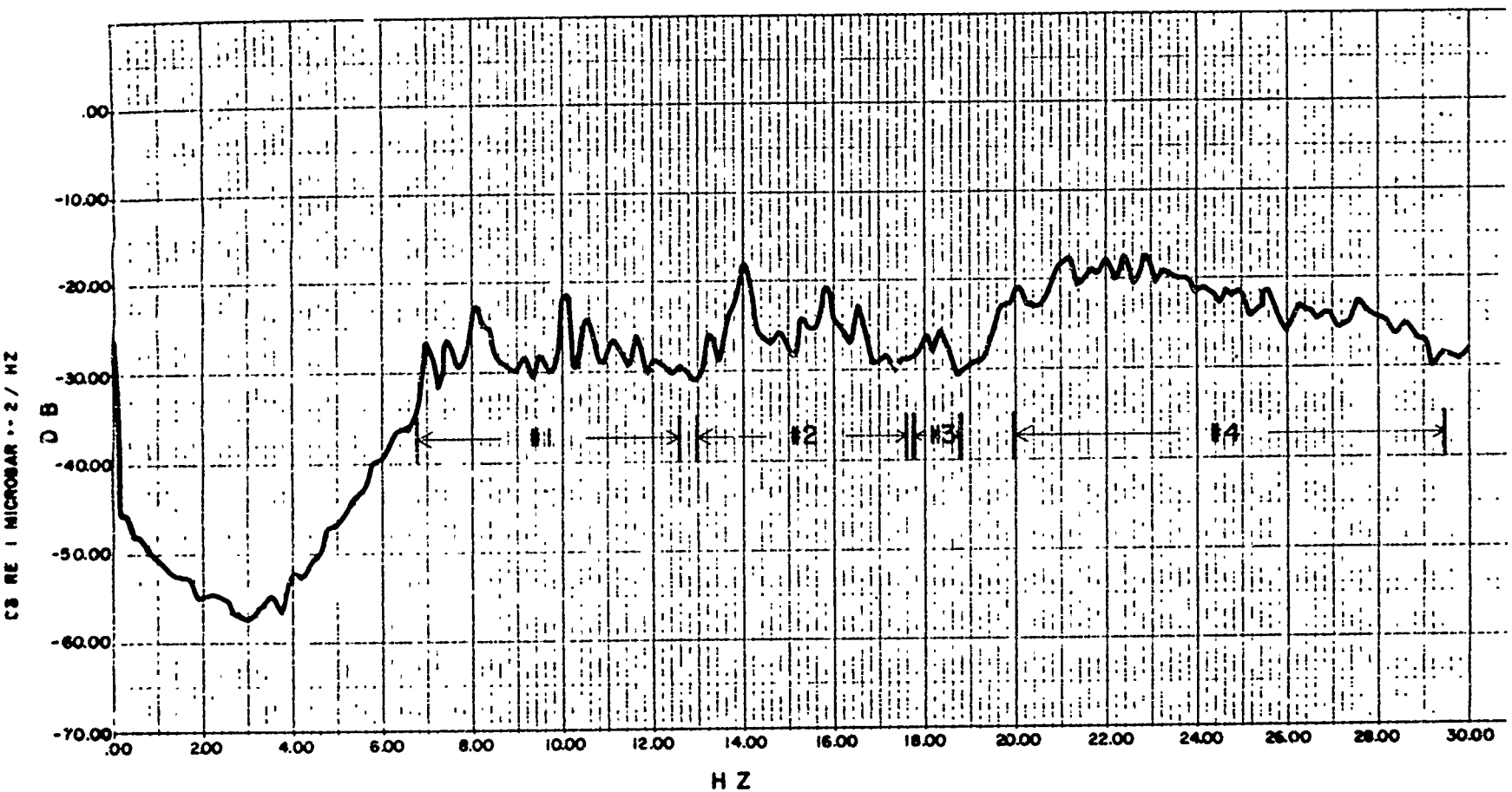

SECo HIGH RESOLUTION POWER SPECTRUM ($\Delta f = 0.0833$ HZ)

Figure 72